Kristian Husmo Lyngved
Thomas Mickelborg
Anders Teigmoen

Active load management in microgrids

A case study of Rye microgrid

Bachelor's project

NTNU
Norwegian University of Science and Technology
Faculty of Engineering
Department of Energy and Process Engineering

NTNU
Kunnskap for en bedre verden

TrønderEnergi®

NORWEGIAN UNIVERSITY OF SCIENCE AND TECHNOLOGY

DEPARTMENT OF ENERGY AND PROCESS ENGINEERING

BACHELOR'S THESIS

Active load management in microgrids

A case study of Rye microgrid

SPRING 2019

Kristian Husmo Lyngved

Thomas Mickelborg

Anders Teigmoen

NTNU TrønderEnergi REMOTE

Bachelor's thesis

Project title	**Date of issue**
Active load management in microgrids	08.11.2018
A case study of Rye microgrid	
	Deadline
Oppgavens tittel	24.05.2019
Aktiv laststyring av mikronett	
Case-studie av Rye mikronett	**Number of pages / appendices**
	94 / 18
Group participants	**Supervisors**
Kristian Husmo Lyngved	Håvard Karoliussen / Robert Bock
Thomas Mickelborg	Associate Professor, NTNU / Postdoc, NTNU
Anders Teigmoen	Havard.karoliussen@ntnu.no / Robert.bock@ntnu.no
	922 95 082 / 734 12 734
Field of study	**Project number**
Renewable Energy, Engineer	FEN1903
Industry partner	**Contact at industry partner**
TrønderEnergi AS	Anniken Auke Borgen
	Business developer, TrønderEnergi AS
	Anniken.Borgen@tronderenergi.no
	992 43 936

Free for publishing | X |

Temporarily tied | |

Free for publishing after | |

Abstract

Norway has a large coastal area with many islands that are provided with electricity from expensive sub-sea cables and long transmission lines. In stead of renewing existing infrastructure in remote areas, it could be cost efficient to implement local power production from renewable energy sources.

This thesis is a case study that considers one of four demos in Project REMOTE. The demo is located at Rye in the municipality of Trondheim, Norway. The project is partially EU funded and aims to demonstrate the technical and economical feasibility of fuel cell-based hydrogen energy storage systems in microgrids. The energy storage system (ESS) in the demo is a hybrid solution, consisting of a lithium-ion battery and hydrogen energy storage. The project is divided into two phases of operation. During the first, the system remains connected to the main grid, while during the second phase the goal is an off-grid system that requires less than 5 % connection to the main grid, annually.

The main objective for this thesis is to investigate the possibility of downsizing the battery capacity of a planned 550 kWh battery at Rye microgrid. This is examined by implementing active load management (ALM) as a mean to utilize renewable power production more efficiently.

In order to achieve this objective, a four stage strategy was completed. The first stage consisted of creating a model of the microgrid. This included simulations of the solar energy production, loss calculations and a complete Simulink model. Secondly, a site survey of the microgrid, consisting of two farm sites, was performed to achieve knowledge of the flexibility potential. The third stage included developing an ALM algorithm in MATLAB. The algorithm performs energy conservation as the highest priority in order to decrease the load demand. Shifting flexible loads to hours with sufficient energy production is the second priority. The third priority is to shift remaining flexible loads to hours with the lowest consumption to increase the load factor of the system. The fourth and last stage consisted of analyzing the microgrid performance by investigating four different cases.

Each case has its own objective. Case 1 acts as a reference case where no ALM is performed. Case 2 applies a statistical method to define flexible loads, before ALM is performed. It is investigated if this method of classification can be regarded as valid. Case 3 is the most optimistic case, as it utilizes ALM on all the loads classified as flexible or power-shiftable. Case 4 is the most conservative case, as it only uses ALM on the most predictable of the flexible or power-shiftable loads. The flexibility potential, energy storage system performance and load factor is investigated for each case. This includes the amount of energy needed from the main grid, energy needed from hydrogen storage, throttled energy and battery lifetime expectancy.

The statistical method applied in Case 2 is found to be an inaccurate method of classifying flexible loads and is not recommended for further use. The amount of shifted load in Case 3 is 11.7 % of the load demand for 2018. This is the most optimistic outcome, but is thought to give a good representation of what is realistic. Case 4, on the other hand, is the most conservative with 1.9 % shifted load for 2018. This is thought to be a minimum of what is theoretically achievable.

Results from the performance analysis reveal that the battery capacity can be downsized after implementing active load management. The potential battery capacities are 500 kWh, 110 kWh and 530 kWh for Cases 2, 3 and 4, respectively. These results are based on not exceeding the amount of energy needed from the main grid, compared to Case 1. Case 3 was the only case that achieved the goal of less than 5 % energy from the main grid, with a battery capacity down to 320 kWh. A downsize in battery capacity results in an increase in the number of battery cycles and, as a consequence, reduce the battery lifetime. An economical evaluation is necessary to asses if a possible downsize is beneficial, although, this is outside the scope of this thesis.

The findings in this thesis are only theoretical. In order to implement ALM in a real system, it is imperative to have metering on component level as a mean to identify the usage pattern of flexible loads and enable their flexibility potential. A reliable forecasting system regarding loads and energy production is also an essential component. In addition, the consumers must be willing to adapt in order to reach the maximum effect of ALM.

Preface

This bachelor thesis was completed in the spring of 2019 at the Department of Energy and Process Engineering in the bachelor-program at The Norwegian University of Science and Technology (NTNU). The project is equivalent to 20 ECT credits, and concludes the study course for a bachelor's degree in Renewable Energy.

During this process we have gained knowledge and insight regarding cooperation and project planning, in addition to valuable experience in utilizing different software tools and the subjects regarding this thesis.
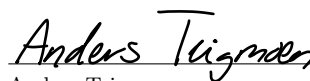
Trondheim, May 24th 2019

Kristian Husmo Lyngved   Thomas Mickelborg   Anders Teigmoen

Nomenclature

η	Efficiency [%]
P_0	No-load losses [W]
P_k	Load losses [W]
U_p	Primary voltage [V]
U_s	Secondary voltage [V]
a	Ratio of transformation [-]
E_{Acc}	Accumulated energy [kWh]
E_{Cap}	Battery capacity [kWh]
I	Current [A]
I_p	Primary current [A]
I_s	Secondary current [A]
l	Length [m]
Q_1	First quartile [-]
Q_3	Third quartile [-]
Q_{inter}	Interquartile range [-]
R	Resistance [Ω]
r	Specific resistance [Ω/m]
S	Apparent power [VA]
S_n	Nominal apparent power [VA]
U	Voltage [V]

Abbreviations

ALM	Active Load Management
AC	Alternating Current
DSM	Demand Side Management
DC	Direct Current
DG	Distributed Generator
ESS	Energy Storage System
G2P	Gas to Power
LF	Load Factor
MPP	Maximum Power Point
MPPT	Maximum Power Point Tracking
Meteo	Meteorological
NOC	Number Of Cycles
NS	Norwegian: Nettstasjon, English: Substation
PV	Photovoltaic
PCS	Power Conversion System
P2G	Power to Gas
P2P	Power to Power
PLC	Programmable Logical Controller
PEM	Proton Exchange Membrane
RES	Renewable Energy Sources
SN	Standard Norge
SOC	State Of Charge
SOH	State Of Health
STC	Standard Test Conditions

Contents

List of Figures

List of Tables

Chapter 1

Introduction

Norway has a large coastal area with many islands that are provided with electricity from expensive sub-sea cables and long transmission lines. In remote areas, it could be cost efficient to implement local power production from renewable energy sources, instead of renewing existing infrastructure. Local power production at these locations could ensure better security regarding power delivery. It could also act as a backup-solution in case of power outage.[1] According to Statnett, which is the system operator of the Norwegian power system, the investment cost for the power system in the following years will be approximately 35 - 45 billion NOK. [2]

As many of the islands and remote areas have a low number of inhabitants, a microgrid solution could be a cost efficient way to meet their power need without investing in new cables and transmission lines. Other power consumers such as aquaculture and remote cabin areas could also be applicable for implementation of microgrids. It would act as a substitute for new infrastructure and/or fossil fuel based generators. [3]

Another aspect is the transfer of electrical energy over vast distances. This is linked to power losses, which can be seen both as an economical and environmental problem. As microgrids consist of distributed energy resources, e.g. PV, battery, fuel-cell etc., close to the loads, these losses can be minimized. [4]

In October 2014 the European Council agreed on a new 2030 Framework for climate and energy, in order to achieve its decarbonisation goals for 2050, in a cost efficient manner. The aim is for EU to be a global leader in renewable energy technologies and achieve that 32 % of its total energy consumption originates from renewables.[5]

As the demand for renewable energy increases, so does the need for energy storage. This is due to the intermittent power production from renewable energy sources (RES) and energy storage systems' (ESS) ability to distribute energy when it is needed. The goal for this thesis is to investigate the possibility of downsizing the energy storage system at Rye microgrid by performing active load management as a mean to utilize the power production more efficiently.

1.1 Contributors

Table 1.1.1 presents the external contributors for this thesis. The people listed have contributed with their respective fields of valuable competences.

Table 1.1.1: List of external contributors for this thesis.

Name	Position	Company
Anniken Auke Borgen	Business developer	TrønderEnergi AS
Bernhard Kvaal	Senior project manager	TrønderEnergi AS
Hanne Sæle	Research Scientist	SINTEF Energy
Merkebu Zeneba Degafa	Research Scientist	SINTEF Energy
Eirik Lockertsen	Managing director	Solbes AS
Lars Hoem	Farm owner	-

TrønderEnergi

TrønderEnergi AS is responsible for production and distribution of electrical energy in Southern Trøndelag. TrønderEnergi is owned by 24 municipalities in Trøndelag county, KLP and Nordmøre Energiverk AS. It generates annual sales of approximately 1.5 billion NOK and employs approximately 400 staff members. TrønderEnergi strives to create value through environmentally friendly production and distribution of energy for the benefit of the local region. [6]

TrønderEnergi is the principal contributor for this thesis. As one of the stakeholders in the project, TrønderEnergi have an interest in learning about the feasibility of microgrids in remote areas, and if active load management can contribute to a more cost efficient and stable system.

SINTEF

SINTEF is a multidiciplinary research organisation with expertise in a broad array of applied sciences. SINTEF employs approximately 2 000 staff members and generated annual sales of roughly 4.5 billion NOK in 2016. [7]

SINTEF provided the necessary data to complete Case 3 in this thesis. This data consisted of load profiles for relevant household appliances and statistics on probability of start-time of the respective appliance.

Solbes

Solbes is a Norwegian firm stationed in Trondheim that specializes in consulting, design and assembly of PV systems.[8]

Managing director at Solbes, Eirik Lockertsen, provided guidance in performing simulations regarding solar power production with the PVsyst software.

1.2   Project Remote

Project REMOTE (**R**emote area **E**nergy supply with **M**ultiple **O**ptions for integrated hydrogen based **TE**chnologies) is a partially EU funded project that investigates the possibility of a renewable energy system running a microgrid by applying hydrogen energy storage. The project consists of four demos and are budgeted at 64.5 million NOK, in which EU contributes with 47.6 million NOK.[9] The demos are all situated at secluded locations in Europe, where energy supply proves to be a challenge. A map displaying the locations of Project REMOTE's demos can be seen in figure 1.2.1. Similarly to the level of globalization of the demos, the stakeholders within the project are also widespread geographically. In addition to SINTEF and TrønderEnergi, there are 7 project partners from Italy, Denmark, France, Greece and Belgium, each with their respective fields of competences. [9]

REMOTE's objective for this project is to demonstrate the technical and economical feasibility of the fuel cell-based hydrogen energy storage solution.[10] As renewable energy sources are intermittent, a cost efficient, reliable and energy dense energy storage solution has to be a part of the system. This is imperative in the case of isolated microgrids. The experiences made from Project REMOTE will provide valuable insight towards a solution on this problem and enable the deployment of large scale hydrogen-based storage solutions. [11, 12]

This thesis covers the fourth demo, which originally was planned for Froan. Froan is a group of islands, 30 km from the mainland, in the municipality of Frøya in Norway with a population of 38 people. Necessary concessions for the installation of the demo proved to be hard to procure. This resulted in a temporary displacement of the demo to Rye, in the municipality of Trondheim. The demo is divided into two phases of operation. During the first, the system remains connected to the main grid, while during the second phase the goal is an off-grid system that requires less than 5 % connection to the main grid, annually. [13]

Rye microgrid consists of solar and wind power production that is planned to cover the load demand for two farm sites. The ESS is a hybrid system consisting of a lithium-ion battery and a hydrogen storage solution. The hydrogen ESS consists of an electrolyzer, provided by Hydrogenics, and fuel cell, provided by Ballard, while the battery is provided by LG Chem. The system in its entirety is designed by Powidian and TrønderEnergi. [13]
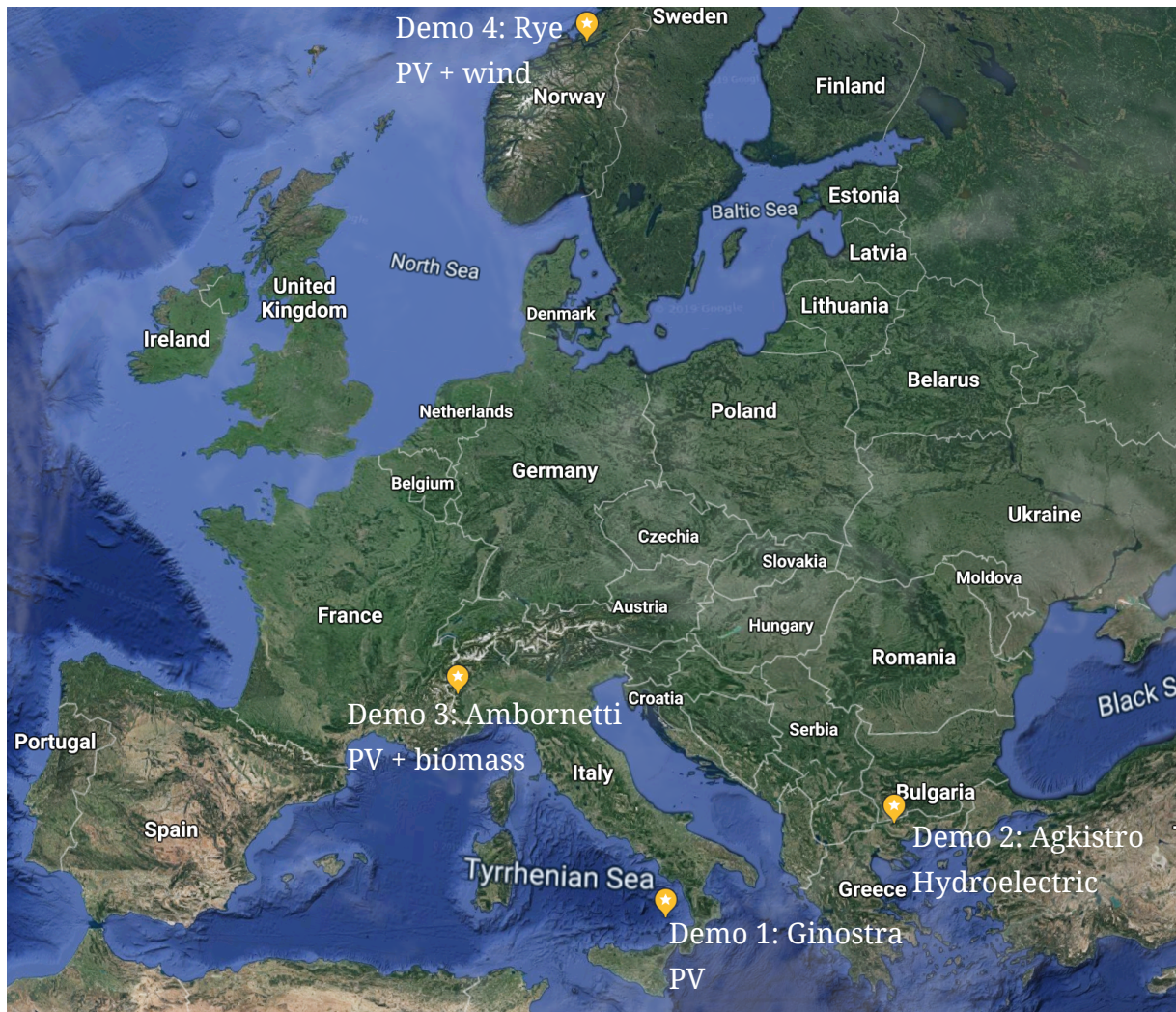
Figure 1.2.1: Map with the location of Project REMOTEs demos. Demo 1 is located at Ginostra, South Italy. Demo 2 is located in Agkistro, Greece. Demo 3 is located in Ambornetti, North Italy while Demo 4 is located at Rye, Norway. [10]

Problem statement

"Can active load management affect sizing of the energy storage system at Rye microgrid?".

The energy storage system planned for this project stands out as the part of the project with the highest investment costs.[13] This thesis aims to investigate the possibility of downsizing the lithium-ion battery by implementing active load management as a mean to shift peak loads to ideal time periods and reduce load demand with energy conservation strategies.

1.3 Objectives

In order to solve the main problem for this project, four key objectives were formulated to achieve this goal:

1. Make a model of the microgrid at Rye

2. Investigate the demand flexibility

3. Developing an ALM algorithm

4. Analyze the microgrid performance

1.4 Key assumptions and limitations

This thesis is limited by several factors and assumptions. Limited power production- and load demand data restricts the possibility to analyze annual variations, as this data is only available from the start of 2018. Smart meters on the farm sites were installed in February 2019, restricting the possibility of investigating seasonal variations in load demand for apartments and cowsheds.

Another limitation is the lack of component level metering. The smart meters installed at Rye only measure the total demand for the respective circuit it is connected to. Further assumptions regarding the load demand of appliances is consequently necessary. Loads with power rating under 1 kW is not considered in this thesis. Due to limited knowledge of household appliances, only the most certain appliances were studied.

The model and results are based on the assumption that all microgrid components were installed at the start of 2018, as the microgrid would be in phase two of project REMOTE. The PV system was installed in April 2019, while the ESS was not installed in the time frame of this thesis. As a consequence, uncertainty regarding solar power production has to be considered.

1.5   Approach

The thesis is based on four cases where investigating the possibility of downsizing the planned battery capacity is the goal for each of the cases. Case 1 acts as an reference case while active load management is performed in the other three cases.

Objective 1 was solved by utilizing a graphical programming software tool. Making a complete model also required simulations of the solar power production. Objective number 2 was achieved by performing a site survey in collaboration with TrønderEnergi and the farm owner Lars Hoem. Developing the ALM algorithm was the most time consuming part of this thesis, with the code amounting to over 4000 lines. Due to the scale of the script, its entirety is not attached as an appendix. Objective 4 is reached by combining all the other objectives in order to generate results, which are then analyzed to investigate the possibility of achieving the main goal.

1.6   Structure of the report

The outline of this thesis has been made with the mindset that it should be easy to read and peak the interest of readers with some knowledge towards microgrids and/or active load management. The theory chapters are written to reflect the methods utilized to achieve the different objectives.

The theory is divided into three separate chapters. Firstly, the microgrid at Rye is elaborated on in Chapter 2. This chapter consists of information on the different distributed generators (DGs) and demand sources the microgrid consists of. Chapter 3 elaborates on theory regarding how to harness solar energy. This is an area of focus due to the need for performing PV simulations. Chapter 4 presents theory on ALM and consumption of common household appliances.

The methods are introduced in two separate chapters. Chapter 5 presents the approach and results from the site survey, while Chapter 6 covers modeling and simulation.

Chapter 7 introduces the four cases. This chapter contains the methods and the corresponding results from each case. These results include an energy outlook, the effect of ALM and simulation results regarding ESS performance.

In Chapter 8, the methods and results are discussed and a case comparison is performed for further evaluation. In addition, what influences the actual flexibility of the regarded loads is considered.

Chapter 9 is the final chapter of this thesis. The thesis is ended with a conclusion and a section for further work. The problem formulation is answered and a course of action for future work is proposed.

1.7   Software

Different software tools have been utilized in order to achieve the goals for this thesis. MATLAB and Excel are used for different calculations and computing tasks. The load shifting algorithm was developed in MATLAB while the modeling and simulation of the microgrid was performed in Simulink. The solar power production was simulated using PVsyst as the preferred software tool.

1.8 Introduction to microgrids

This section aims to give a brief introduction to what defines and constitutes a microgrid. The following paragraphs cover the main elements microgrids consist of, and the possible benefits and challenges regarding microgrids.

Microgrids can be seen as means to manage reliability of supply and local optimization of energy supply by controlling distributed energy resources (DER). Microgrids also present the possibility of supplying remote areas with clean energy from renewable energy sources. [14]

Definition

An official definition for microgrids was formulated as late as 2017 by the Internationally Electrical Commission (IEC). Cited from their Electrotechnical Vocabulary database:

"Microgrid is a group of interconnected loads and energy resources at distribution voltage level with defined electrical boundaries that is either isolated from the grid or able to operate in both island mode and grid connected mode."[15]

Main elements in microgrid systems

In order to receive an overview of how microgrids operate, the five main elements in microgrids are listed below.

- Loads
- Energy production
- Energy storage
- Connection point
- Control and communication

Microgrids operating only in island-mode have to be able to deliver stable system voltage and frequency. This can be a challenge because of the intermittent renewable energy sources. In order to cope with this, there is a need for energy storage solutions and a control unit. The control unit includes voltage and frequency regulation, real and reactive power control, load forecasting and scheduling, microgrid monitoring, protection and black start.[4]

A connection point facilitates a connection between consumers, DGs and ESS. It can also serve as a connection to a main grid, but such a connection is consequently not included in an isolated microgrid.[16]

Chapter 2

Rye microgrid

Rye microgrid is estimated to be completed during 2019.[13] The configuration of the microgrid system including technical specifications of all components, in addition to theory regarding losses in the microgrid are covered in this chapter.

The microgrid is based on renewable energy sources. A hybrid solution with both solar and wind power generators supply the load demand of two farm sites, which consists of both residential and farming loads. The energy storage system consists of a lithium-ion battery and a hydrogen storage solution. [13]

The microgrid can operate both in island mode and in grid-connected mode in order to be able to sell excess power back to the main grid. It also acts as a backup in case of failure, and if both the DGs and ESS is unable to cover the load demand. During the first phase of the operation, the system will be connected to the grid. During the second phase, the goal is to achieve less than 5 % energy from the main grid each year in the time frame 2020 - 2021. [13]

The farm sites are supplied by the microgrid through the NS70261 substation (22 kV/230 V transformer). The wind turbine is separately connected to the grid through the NS70261 substation (400 V/22 kV transformer) while the solar power plant and ESS is connected through its own transformer (400 V/22 kV). The transmission line between the two substations is approximately 1 km. [13] A line diagram illustrating all the components in the system can be seen in figure 2.0.1.
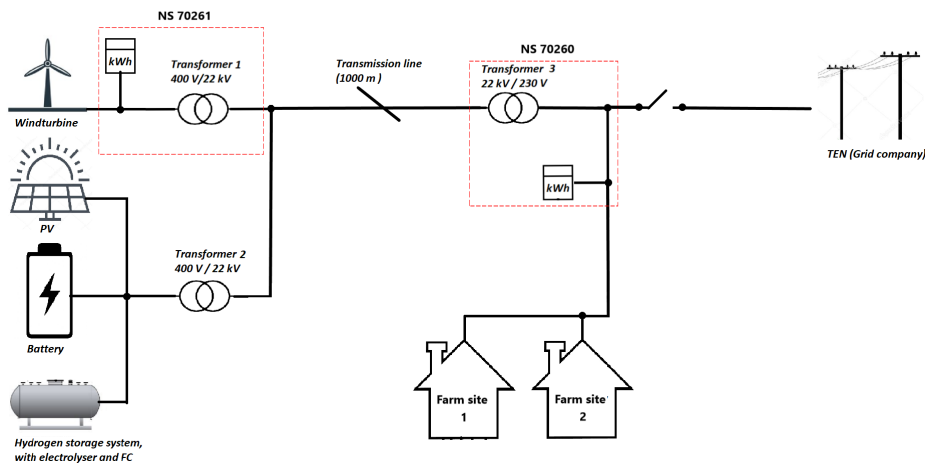
Figure 2.0.1: The microgrid configuration at Rye with all main components comprising of the powers generators, energy storage system and substations with measuring equipment. [13]

2.1 Distributed generators

This section covers information about the wind turbine and PV system at Rye. Technical specifications and configurations of the wind turbine and PV system is elaborated on.

Wind turbine

The wind turbine is a 225 kW Vestas V27, which has been in operation since 2015. The total production in 2016 was 179.5 MWh, while it was 175.1 MWh in 2017. The Vestas V27 turbine has the same technical specifications as the Vestas V29. This adds the possibility to increase the diameter from 27 m to 29 m with an extension set. As a result, an extra 50 000 kWh/year could be achieved. [13] Technical specifications are listed in table 2.1.1 while an image of the turbine is illustrated in figure 2.1.1.

Table 2.1.1: Specifications of the wind turbine at Rye.

Rotor		Generator		Operational data	
Diameter	27.0 m	Rated power	225 kW	Cut-in wind speed	3 m/s
Swept area	573.0 m^2	Voltage	400 V	Cut-off wind speed	25 m/s
Power density	392.7 m^2	-	-	Rated wind speed	14 m/s

Figure 2.1.1: The Vestas V27 wind turbine at Rye microgrid.

PV system

The PV system was installed and connected to the grid, 8th of April 2019. It consists of 288 modules, which adds up to a module area of 481 m^2. Two types of PV modules with different nominal power and cell types are used. All are provided by the Norwegian solar panel manufacturer REC. The module models are REC Twinpeak 2 and REC Twinpeak mono series. As of May 2019, the PV system at Rye is Norway's largest ground installed solar plant, and have a total installed nominal power capacity of 86.4 kWp. [13]

Three SolarEdge SE27, 6 kW inverters are installed to convert from DC to AC power. These inverters have an efficiency of 98 %. Each pair of modules are connected to a power optimizer, also from SolarEdge. Because of the different module nominal power, two types of power optimizers are used. The technical specifications of the components are listed in table 2.1.2. [13]

Table 2.1.2: The technical specification for the PV system at Rye.[17]

Cell type	Power [Wp]	Efficiency [%]	No. panels	Power optimizer
REC TP2 Monocrystalline	310	18.6	104	SolarEdge P750
REC TP2 Multicrystalline	295	17.7	184	SolarEdge P600

The PV system is oriented to the south (azimuth = 0°) with a fixed tilt angle of 35°. The distance between each row is 10 m. The modules are divided into three rows consisting of 96 modules each. There is one inverter for each row. Each inverter has three strings in parallel with 16 optimizers, where each optimizer is connected to a pair of modules. In result, this amounts to 288 modules. An overview of the PV installation is illustrated in figure 2.1.2. [13]
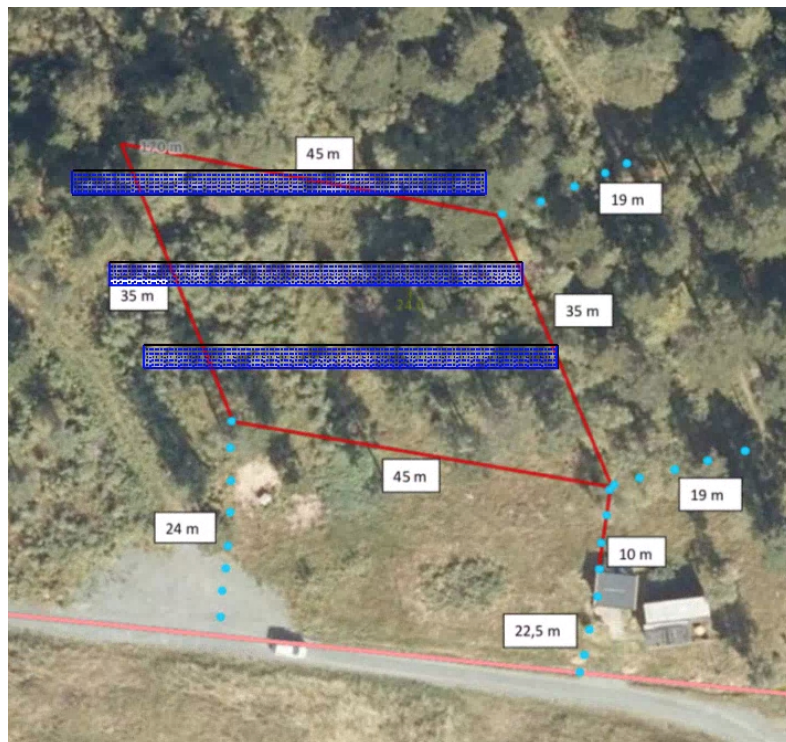
Figure 2.1.2: Illustration of the PV configuration at Rye. There are three rows consisting of 96 modules each. The red lines constitute the area where it is permitted to install the PV-system. [17]

2.2   The energy storage system

This section covers the technical specifications of the energy storage system that will be part of the microgrid. The planned ESS is a hybrid solution consisting of a lithium-ion battery and hydrogen based storage system which includes an proton exchange membrane (PEM) electrolyzer and PEM fuel cell. Both the battery and hydrogen ESS are expected to be installed during 2019.

Excess electrical production from PV and wind first serve to charge the battery bank. If the battery bank state of charge (SOC) reaches 80 %, then the electrolyzer starts to produce hydrogen. If the production is not sufficient to supply the load, then the load will be supplied by discharging the battery bank. If the load demand keeps being higher than the production, and the battery bank SOC reaches 20 %, the fuel cell starts. In this case, the fuel cell serves the primary load, and at the same time could be used to charge the battery. [13]

Battery storage

The lithium-ion battery has an installed capacity of 550 kWh, while the usable energy is 330 kWh due to the SOC restrictions elaborated on in the beginning of this section. The battery has a C-rate of 2C, which describes the rate of discharge relative to its maximum capacity. This means that the battery can perform two complete cycles in one hour.[18] The storage unit is designed for both island mode and grid connected mode. It is composed of one container that includes power conversion system (PCS), batteries and control unit. The control unit consists of programmable logical controller (PLC) to control the battery rack, measurement devices to measure frequency and power, communication interfaces, cooling, fire detection and extinguishing. The battery system is produced and supplied by LG Chem and the battery storage system is designed for 10 years useful life considering 400 complete cycles per year. [13] A display of the technical properties of the battery is shown in table 2.2.1.

Table 2.2.1: Technical specifications of Li-ion battery. [13]

Installed capacity	550 kWh
Usable energy	330 kWh
Voltage range	714 - 1000 V
C-rate	2C

The PCS includes a DC/AC converter. It has an efficiency of 98 %, while the total efficiency of the battery storage system is assumed to be 93 % based on information from TrønderEnergi.[13] Further technical specifications for the DC/AC converter are listed in table 2.2.2.

Table 2.2.2: Technical specification of DC/AC converter. [13]

Maximum DC voltage	1000 VDC
AC rated current	540 A
Efficiency	98 %
Network frequency	50/60 Hz
Cooling	Air, 40 °C max air inlet

Hydrogen storage

The hydrogen ESS acts as a backup solution if RES and battery ESS can not meet the load demand. Hydrogen is produced by a 55 kW PEM electrolyzer and is stored in a tank with a capacity of 100 kg at 30 bar. This is the same pressure as it is produced at. As a result, no compression is needed. The hydrogen is then used to produce electricity and deliver power to the microgrid through a 100 kW PEM fuel cell. [13]

Figure 2.2.1 illustrates the the different conversion processes. The conversion from power to gas is shortened to P2G, while the conversion from gas to power is shortened to G2P. The system in total can be described as a power to power system (P2P).
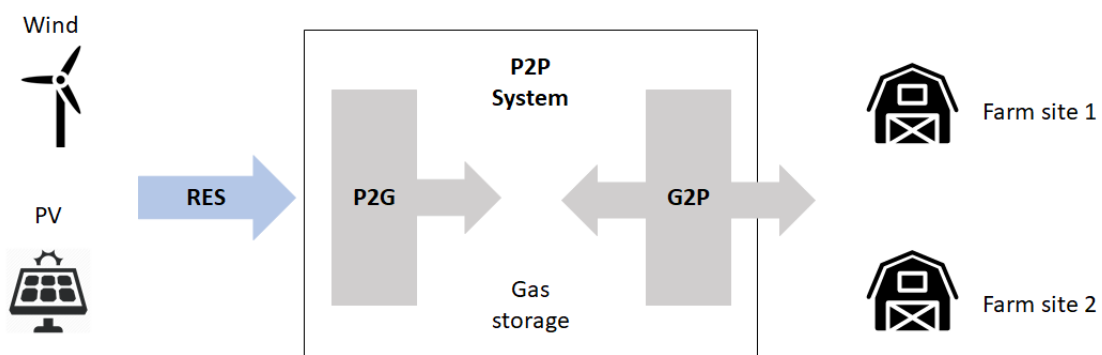
Figure 2.2.1: The different conversion processes in the hydrogen storage solution. Power from renewable energy sources can be applied to produce hydrogen gas. The hydrogen can then be converted to electricity and utilized to meet the load demand. Modified from source: [19]

Since hydrogen has an energy density by weight of 33.3 kWh/kg, 100 kg amounts to an energy capacity of 3.33 MWh.[20] The electrolyzer is manufactured and provided by Hydrogenics, while the fuel cell is supplied by Ballard power. Details on the specifications of the electrolysis- and fuel cell are illustrated in table 2.2.3. [13]

The efficiencies are excluded due to producer confidentiality.

Table 2.2.3: Technical specifications of the hydrogen system. [13]

Capacity of hydrogen tank	100 kg
Pressure in hydrogen tank	30 bar
Rated power of electrolyzer	55 kW
Outlet pressure of electrolyzer	30 bar
Rated power of fuel cell	100 kW

2.3   Site overview

This section presents an overview of the sites and how the load demand is measured. The microgrid consists of two farm sites and a power production site. Both farm sites have smart meters connected to the main circuits. These were installed in the beginning of February 2019. In addition, one smart meter for measuring the total load of both farm sites was installed in May 2018. The data gathered from these smart meters are used to map the individual loads on the two farm sites. [13] The sites are illustrated in figure 2.3.1.

Figure 2.3.1: Overview of the sites that constitutes the microgrid. There is a 1 km long transmission line between the power producing units and the farm sites.

There are production and total load demand data available from May 2018, provided by Safebase. One Safebase meter is placed in the substation NS70260 next to the farm sites, while one meter is in the substation NS70261 next to the wind turbine. These meters read and store the data at a 15 minute interval. [13] Figure 2.0.1 illustrates the placement of the substations.

Farm site 1

Farm site 1 consists of a house, Mastu (apartment) and one cowshed. The house is divided into three apartments (Main-, west- and east apartment). An eGauge smart meter is installed at this location and is measuring the loads from 5 different circuits yielding real time data. [13] Small current transformers (CT) are connected to each circuit measuring the current flowing through them. The smart meter read the CTs several thousand times per second, calculates the power, stores the data and creates a user interface to display the information. [21]

The different circuits connected to the eGauge smart meter on farm site 1 are listed below:

- Main apartment & west apartment

- East apartment

- Air-water heat pump & mastu

- Cowshed

- Silo

Farm site 2

Farm site 2 consists of one cowshed and a workshop. At this location there is a smart meter, called Smappee, connected to the breaker panel in the cowshed. This meter monitors the load down to a 5-minute resolution. The workshop has a minimal energy consumption and is therefore not metered.[13]

2.4   Transmission

The transmission consists of a transmission line with a length of 1 000 m, in addition to three transformers. This section elaborates on the transmission line and the transformers located in the microgrid.

There are two transformers at the production site and one at the farm site. Transformer 1 is placed in substation NS 70261. This transformer converts the voltage from 400 V to 22 kV. Transformer 2 transforms the 400 V from the ESS and PV to 22 kV. Transformer 3 is placed in substation NS 70260 at the farm sites. This transformer transforms the voltage from 22 kV to 230 V. An overview of the microgrid, with transmission, is displayed in figure 2.0.1. The transformers with corresponding rated power, primary and secondary voltages, no-load losses, and load losses at full load are listed in table 2.4.1. Transformer 1 and transformer 2 are the same models.[13]

Table 2.4.1: Technical specification of transformers in Rye microgrid.[13]

Transformer	Rated power [kVA]	U_p / U_s [V]	No load losses [kW]	Load losses at full load [kW]
1	315	22 000 / 400	0.360	2.900
2	315	22 000 / 400	0.360	2.900
3	100	22 000 / 230	0.202	1.264

There is a transmission line between the production site and the farm sites. As seen in figure 2.0.1, this line operates at a voltage of 22 kV and have a length of 1 000 m. This 22 kV line consists of the line type TSLF 3x1x50 Al. [13] This corresponds to a resistance of 0.6410 Ω/km per phase according to Nexans cable book.[22]

2.5 Transmission losses

This section elaborates on theory regarding calculation of losses in transformers and transmission lines. In addition, ratio of transformation and calculation of efficiency are covered.

Transformers

In general, transformers have a high efficiency. For larger transformers it can even reach 99.5 %, although there are several sources of loss. Copper losses, eddy currents, hysteresis, stray losses due to leakage flux and dielectric losses are all losses found in a transformer. Energy losses in transformers are dependent on the load and, because of this, it is useful to calculate the no-load losses and the load losses separately. The hysteresis and eddy current losses are dominating the no-load losses, since these do not vary with constant voltage. They can therefore be seen as constant over a specific time period. The load losses are dominated mainly by copper losses, which are very dependent on the load. [23–25]

The total losses in a transformer can be calculated using equation 2.5.1 where P_0 is the no-load losses, P_k is the load losses, S is the apparent power and S_n is the nominal apparent power of the transformer. From the equation it can be seen that the total losses of a transformer is dependent on the load of the transformer. [23, 24]

$$P_{loss} = P_0 + P_k \cdot \left(\frac{S}{S_n}\right)^2 \tag{2.5.1}$$

Ratio of transformation

The ratio of transformation for a transformer can be calculated using the primary and secondary voltage or current. Equation 2.5.2 shows the correlation between voltage, turnover ratio and currents of a transformer. U_p is primary voltage, U_s is secondary voltage, a is the ratio of transformation and I_p/I_s is primary and secondary current, respectively. [23]

$$\frac{U_p}{U_s} = a = \frac{I_s}{I_p} \tag{2.5.2}$$

Transmission line

Energy losses occur in every transmission line due to current flowing through a resistance. The losses take form as heat as the energy dissipates. These losses are often called I^2R-losses or copper-losses. In electrical transmission lines there will also be a capacitive effect between the phases and ground that will increase proportionally with the length of the line. However if the transmission line is under 2 km and the voltage is under 132 kV, these effects can be neglected when calculating losses. [26]

To calculate the power losses for a transmission line, the total resistance of the line per phase and the current flowing through it is essential information. When these values are known, equation 2.5.3 can be used to calculate the losses. P_{loss} is the total losses, I is the current running trough the cable and R_{phase} is the total resistance per phase. [23, 26]

$$P_{loss} = I^2 \cdot R_{phase} \cdot 3 \tag{2.5.3}$$

The resistance per phase and meter of a specific cable or line can be found in cable books from different manufactures. If the resistance per phase is known, the total resistance per phase can be calculated from equation 2.5.4. In the equation r is resistance per phase given in Ω/m or Ω/km and l is the length of the cable or line in meters or kilometers. [26]

$$R_{phase} = r \cdot l \tag{2.5.4}$$

Efficiency

The efficiency of a transformer, transmission line or in general can be calculated by using equation 2.5.5. The equation reveal that the efficiency is dependent on the power going out of a component divided by the power going in. [23, 26]

$$\eta = \frac{P_{out}}{P_{in}} \cdot 100\% = \frac{P_{out}}{P_{out} + P_{loss}} \cdot 100\% = \frac{P_{in} - P_{loss}}{P_{in}} \cdot 100\% \tag{2.5.5}$$

2.6 Battery cycles and lifetime

This section elaborates on the theory on how the number of battery cycles are calculated. In addition, factors that impacts the lifetime expectancy of lithium-ion batteries are elaborated on.

To define how the number of battery cycles are calculated, it is first important to understand how a cycle is defined. A full cycle is when the accumulated SOC of a battery reaches 100 %. Another key aspect is that the maximum capacity of a battery is not fixed as time goes by. When a battery is used, electrochemical reactions occur, which puts strain on the battery. Over time, this results in a lower maximum capacity. When this capacity reaches 80 % of its original value, the battery is considered to be at the end of its lifetime. The number of cycles before this occurs is called the cycle life. [27]

To calculate the number of cycles a battery has performed, it is necessary to know the total amount of energy passed through the battery and the maximum capacity of the battery at all times. In this thesis, a simplification where it is assumed that the maximum capacity does not change over time is applied. The resulting equation for calculating the number of performed cycles is illustrated in equation 2.6.1. E_{Acc} and E_{Cap} is the accumulated energy and battery capacity, respectively. [27]

$$NOC = \frac{E_{Acc}}{E_{Cap}} \tag{2.6.1}$$

The lifetime expectancy of lithium-ion batteries depends on several factors. These batteries degenerates with usage and storage. This includes chemical and mechanical degradation caused by factors like temperature, state-of-charge histories, electricity current levels, cycle depth and frequency. All these factors have to be considered to accurately predict the lifetime expectancy. [28]

Chapter 3

Harnessing solar energy

This section covers the basics regarding harnessing energy from the sun and focuses on the parameters that have been important for completing the simulations in this thesis. This includes the different types of solar irradiance and how to measure it, the different components the PV system consists of and the losses that occurs in these systems.

The sun supplies energy in the form of radiation. Because of the long distance between the sun and the earth, a fraction of about two millions reach the surface. The amount of energy that reaches the earth amounts to approximately $1 \cdot 10^{18}$ kWh annually. This is equivalent to $10\,000$ times the worlds energy requirement which means that only 0.01 % would need to be harnessed to cover the total energy demand. [29]

3.1 Solar radiance

When finding the potential for solar energy, solar irradiance is one of the most important factors to consider, but it is also a factor with high uncertainty in northern latitudes. Plant specific factors like module inclination, azimuth and shading will also be reviewed as this has an influence on the energy output of a PV system. The next paragraphs cover the radiance potential, especially in northern latitudes.

The radiation that reaches the outer part of the atmosphere fluctuates between $1\,325$ W/m^2 and $1\,412$ W/m^2. The fluctuation is caused by the distance between the sun and the earth which varies between 147 and 152 million km. [29] A portion of the solar radiance is reduced due to reflection of light, scattering in the earths atmosphere, and absorption because of certain molecules, such as O_2, O_3, H_2O, and CO_2. On a very good day, irradiance may reach about $1\,000$ W/m^2 on the surface. When looking at the annual energy content of the solar irradiation, the result is the global annual irradiation in kWh/m^2. [29, 30]

There are several factors that decide the intensity of the solar irradiance. The latitude is one of the main factors. In northern latitudes the seasonal variation is substantial because of the difference between summer and winter insolation. There are also other factors, like variations through the day and local weather conditions, such as temperature, wind, snow and clouds.[31] According to the Norwegian solar association, the irradance on a horizontal plane in Norway is between 700 - $1\,000$ kWh/m^2 annually. The highest irradiance occurs between the months of May and July, whilst the lowest is found between December and January. [32] The worldwide distribution of annual solar irradiance is shown in figure 3.1.1.
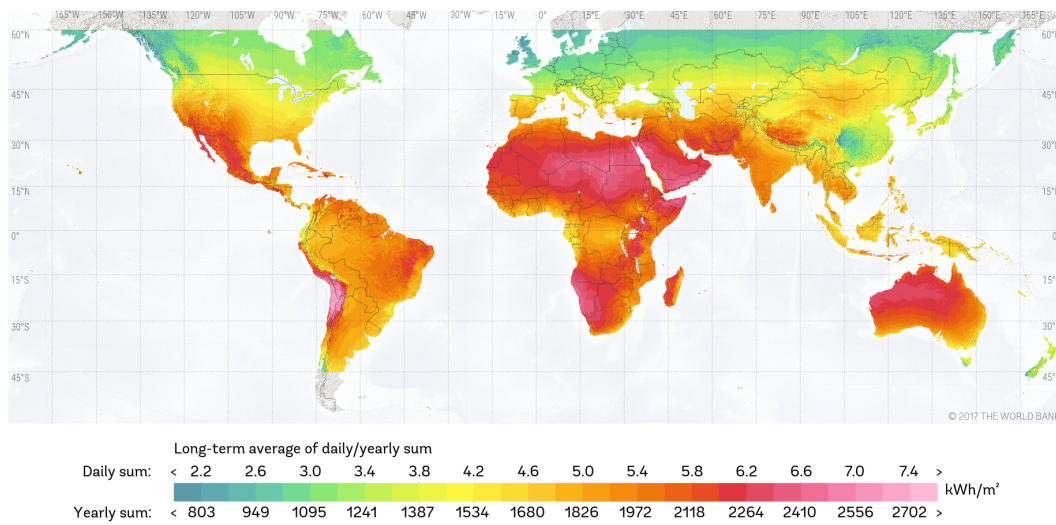
Figure 3.1.1: Worldwide distribution of annual solar irradiance in kWh/m^2. This illustration reveal the lack of data for northern latitudes.[33]

Types of solar irradiance and ground reflection

Different sub-factors have direct impact on the power output of PV systems. The following paragraphs explain the difference between direct and diffuse radiation, and also the albedo effect, as these are factors that have to be considered in order to perform valid simulations when planning a PV system.

The irradiation reaching the surface is the sum of three different components. This is direct, diffuse and reflected irradiation. A portion of the sunlight is reflected by clouds, and as a result, the difference between direct and diffuse radiation has to be distinguished. The direct sunlight comes directly from the sun and is the portion that casts shadows of objects. The diffuse radiation has no direction as it is scattered into all directions. Because of variations in weather and solar altitude through the day, the direct and diffuse radiation vary greatly. [29]

The reflective component from the ground is called the albedo effect. Inclined planes receive reflective irradiance from the ground, which varies depending on the ground surface. The higher the irradiance, the more light is reflected by the surface. Fresh snow typically has an albedo effect of 0.8 - 0.9, whilst grass has a value of about 0.25 depending of the month of the year. [29] Figure 3.1.2 illustrates the different types of irradiance and the reflective component due to the albedo effect.
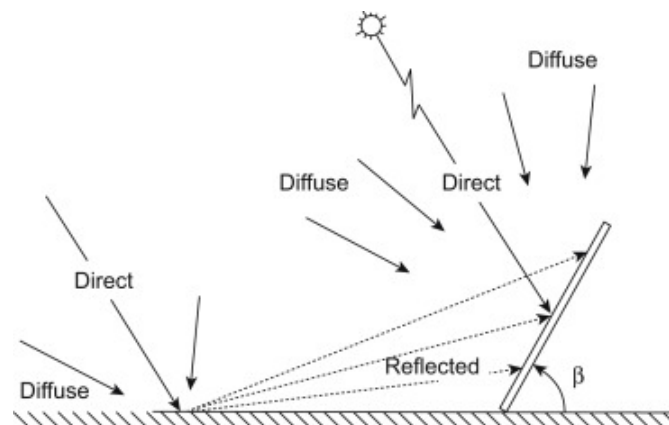
Figure 3.1.2: Illustration of the different components of solar irradiation on a tilted plane. [34]

Orientation and positioning of PV modules

In order to calculate accurate values for irradiance values and the power production of solar energy systems it is vital to have knowledge about the sun's path. The altitude of the sun can be described at any location by the solar altitude and the solar azimuth. When describing solar energy systems, south is generally given as $\alpha = 0°$. [29] Figure 3.1.3 illustrates the different angles to consider when planning a PV system.

PV modules are usually installed with an angle of attack (β) relative to the horizontal plane in order to achieve a higher annual yield. The angle size depends on the latitude of the site location, but also on the time of the year. The optimal angle is larger in the winter compared to the summer time. For fixed planes, the optimal angle in Norway is found to be 30° in Oslo, but is higher in the northern parts of the country. [31]
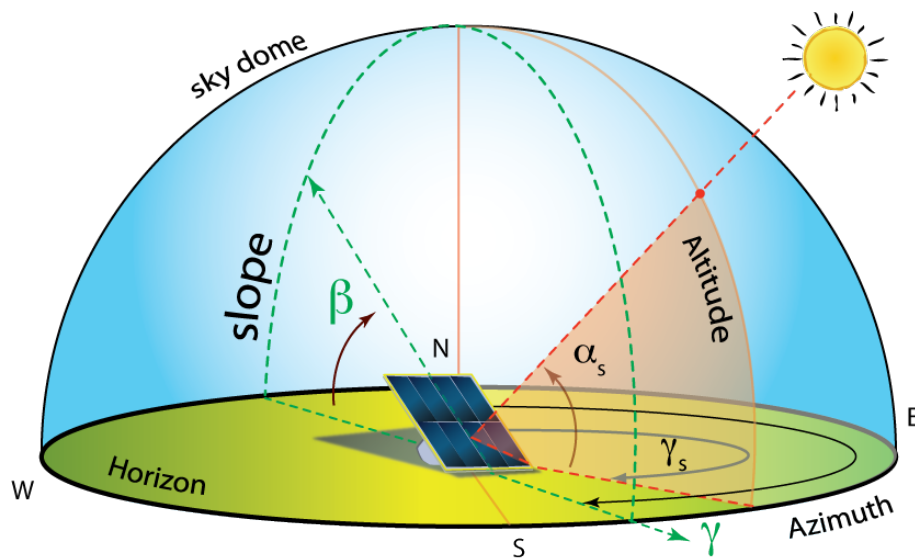
Figure 3.1.3: An illustration of different angles that is of importance when planning a PV system. [35]

Measuring solar irradiance

As previously stated, measuring solar irradiance is a source of substantial uncertainty when planning a PV system, especially in northern latitudes. The following paragraphs cover the two most common methods used for gathering solar data and why this data can have a high uncertainty.

Ground stations represent the ground truth and can be a reliable source of irradiation data if the equipment is well maintained and calibrated.[36] There are two large worldwide surface radiation networks operating today, which are the World Radiation Data Centre (WRDC) and Baseline Surface Radiation Network (BSRN).[37] WRDC only have one station in Norway which is located in Bergen, while they have 16 located in Sweden.[38] BSRN does not have any stations located in Scandinavia. [39] There are several other stations in Norway, but it can be difficult to assess their validity.

Satellite data is the other main method for measuring solar irradiation. There are two types of weather stations, which includes polar-orbiting and geostationary platforms. The geostationary platforms are preferred for solar-resource monitoring because they view the same part of the earth continuously and thus produce the hourly site specific data time series used for solar engineering applications. [36] Uncertainty is determined by astronomic and geographical factors. The most important factor is sun elevation, but other factors like terrain, coastal zones and areas with increased occurrence and variability of snow and ice can increase the uncertainty. Areas in northern latitudes also have a disadvantage because of the curvature of the earth as this limits the usability of satellite images. It is argued that the usability ends between 60 - 66°N. [36] Trondheim is located at a latitude of 63°, so satellite data alone might not give accurate results. The orbits of goestationary and polar-orbiting satellites are illustrated in figure 3.1.4.
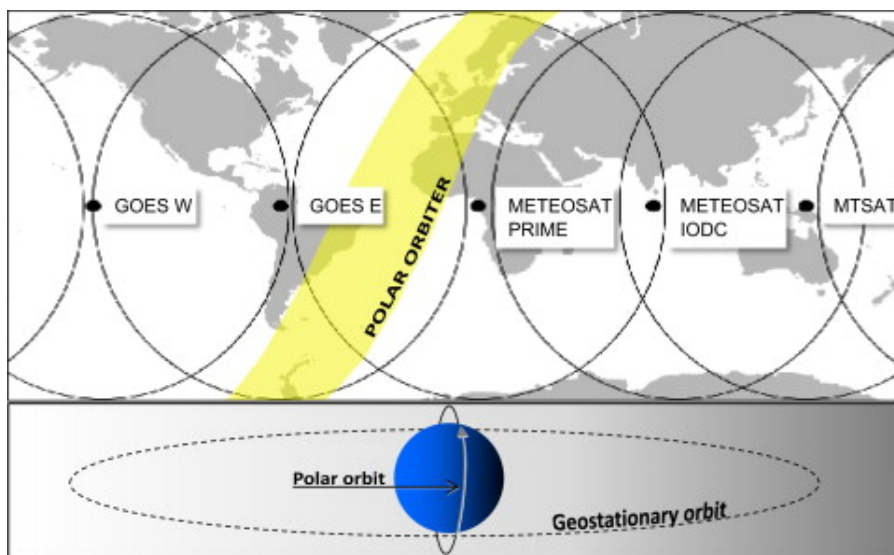
Figure 3.1.4: An illustration of geostationary and polar-orbiting satellite orbits, and their operational field of view. [36]

There are many meteorological data sources available. The source used for this thesis is Meteonorm version 7.2. Meteonorm is a software that provides monthly meteorological data for any location on earth and is the provider used for simulating power production in PVsyst. Meteonorm has a database containing a total of 8 325 ground stations. Regarding Europe, if there are no radiation measurements available closer than 50 km from the selected location, satellite data is used. If the nearest site is more than 10 km away, a combination of ground measurement and satellite data is used. [40]

3.2   Components in PV systems

PV systems can have different configurations based on its utilization. Different components are needed for it to function in an optimal manner. This section focuses on the main components installed at Rye.

The following components are reviewed:

- PV modules

- Power optimizers

- Inverters

PV modules are the power producing component and consists of several low-voltage cells connected in series in order to get a useful voltage. If n cells are connected in series, the module voltage is n times the cell voltage, and the module current will be the same as the cell current. To increase the current, modules have to be coupled in parallel. Modules are often coupled together in large numbers forming an array. Modules in an array may be coupled in series, parallel or a mixture of the two. [41] An illustration of this is shown in figure 3.2.1.
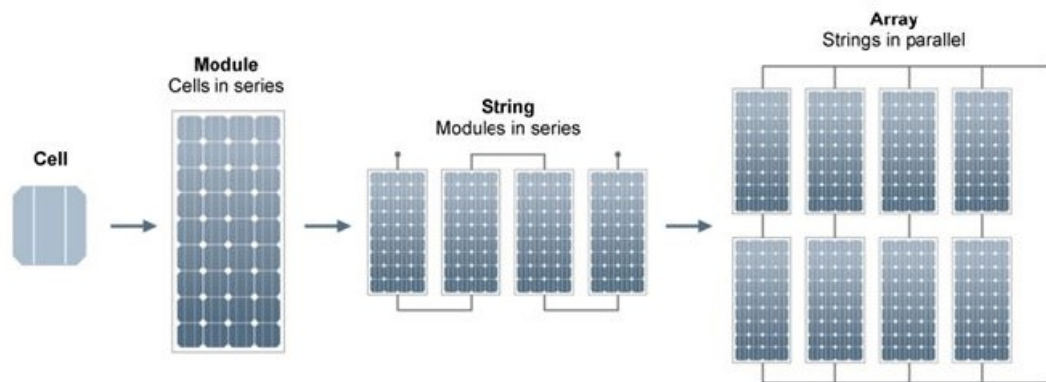
Figure 3.2.1: An illustration of the difference between cell, module, string and array.[42]

Power optimizers serve as DC/DC converters that turn modules into smart modules. These devices are constantly tracking the maximum power point (MPPT) of the modules individually, and maintain an optimal string voltage for DC/AC conversion at the inverter, and thus optimizing the power output. The fixed string voltage also provides safety benefits as they reduce the module voltage to a safe level whenever the inverter or grid is shut down. Having MPPT on each module also allows for more flexible PV array design as mismatched modules can be serially-connected in a string. [43]

The solar inverter is an essential part of a PV system and is also called a DC/AC converter. It is used to convert the solar DC electricity generated by the PV array into AC power and to adjust the frequency and voltage to the same level as the grid.[29] Figure 3.2.2 presentes an example of how solar modules, power optimizers and inverters are connected together.
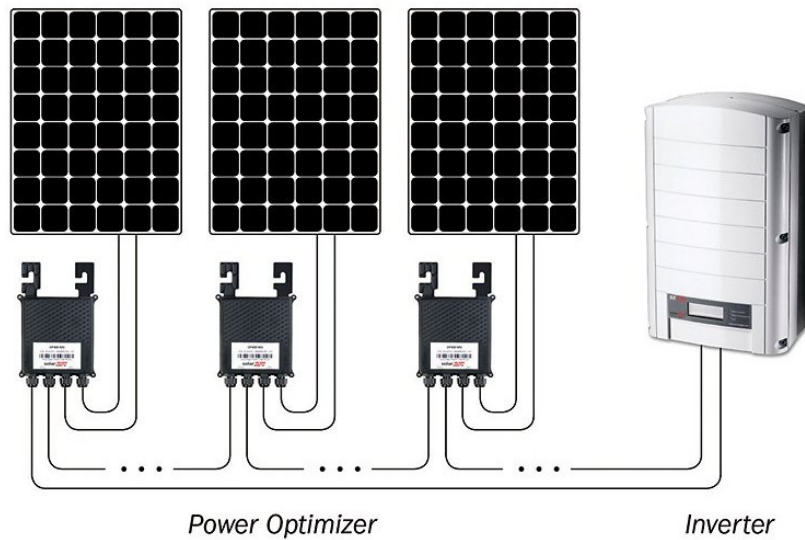
Figure 3.2.2: An illustration of power optimizers connected to PV modules in series forming a string, which is then connected to an DC/AC inverter. [42]

3.3 Losses in PV systems

There are different factors contributing in decreasing the total efficiency of PV systems. This section reviews the most important losses, but only goes into detail on the losses that were adjusted in the simulations. Other losses were predefined and are therefore not covered in this thesis.

Shading losses

Far and near shading are two types of shadings leading to power losses in a PV system. Far shading affects the system in a global way. These shadings are, as stated in section 3.1, created by the direct sunlight and casts shadows of objects and is described by a horizon line. The distance between the PV system and these objects are typically ten times the size of the PV field size. Near shading is caused by objects in the immediate surroundings of the PV module, such as vegetation. Simulating these shadings is particularly complex compared to far shadings and need detailed 3D description of the PV system and its environment. [40]

Soiling losses

Soiling losses is losses due to accumulation of dirt on the PV modules. The effect of snow covering the modules is also part of these losses, which can have a strong negative effect on the performance of the PV system. This factor is dependant on the local climate as regular periods of rain will prevent this accumulation. In these areas the effect can be negligible (less than 1 %) [40]. As Norway has long periods with snow the effect of soiling losses could be substantial in several months of the year and is therefore something that should be taken into account in the planning process.

Array and system losses

All the parameters that reduce the available array output energy with respect to the PV-module nominal power under standard test conditions (STC), can be defined as array losses. Under STC contidions, an ideal PV-array should yield one kW/kWp. This means that if the collector plane receives 1 kW of irradiance it should produce 1 kWh per installed kWp. In other words the array losses are the difference between the ideal array yield at STC and the effective yield as measured at the output array. [40]

The system losses include losses in the components outside the PV array (power optimizers, inverters etc.), losses due to system unavailability and auxiliary consumption. System unavailability is a loss factor due to maintenance or system failures, while auxiliary consumption is the energy used for managing the system (fans, electronic devices, lights etc.). [40]

Chapter 4

Theory on active load management

Active load management (ALM) is the control of electricity consumption. It is also known as demand side management (DSM) and is a broad concept which includes many different strategies to adjust or control the load demand. The goal is often to cut energy costs, achieve more efficient power systems, avoid expensive infrastructure investments etc. [44] Since this thesis focuses on a microgrid that is planned to operate in island mode, energy prices are consequently not an issue.

Concepts from ALM are used to shift loads to more suitable hours, reduce energy consumption and try to increase the load factor. The end goal is to investigate the possibility to downsize the battery storage capacity by implementing ALM. This chapter reviews the concepts taken from ALM, how the different load classifications are defined and the power consumption of relevant appliances.

The concept of ALM was introduced in the 1970s as a response to the middle east oil crisis.[45] Today, utilities around the world are using ALM in their strategic planning, as a mean to maximize profits. ALM aims to actively shape the daily and seasonable electric load profiles in order to achieve a better overall system utilization. ALM offers several programs for controlling the load profiles in order to achieve the objectives. [46] The objectives for this project are:

- Shift loads to times within a day where the power production is sufficient
- Reduce energy consumption
- Achieve a load factor as close to 1.0 as possible

4.1   Load factor

The load factor is the ratio between the peak load and the average load over a time period. It is defined by the power demand of appliances and/or systems, and the consumption habits of the end users. The load factor is preferred to be as close to 1 as possible. [47]

$$LF = \frac{\text{Average load}}{\text{Peak load over a given time period}} \tag{4.1.1}$$

4.2   Active load management strategies

The most common ALM techniques are energy conservation to save energy and demand response programs to shift and reschedule the energy consumption. [48] The methods of load shifting and energy conservation are reviewed in this section. Figure 4.2.1 illustrates the two ALM methods used in this thesis.
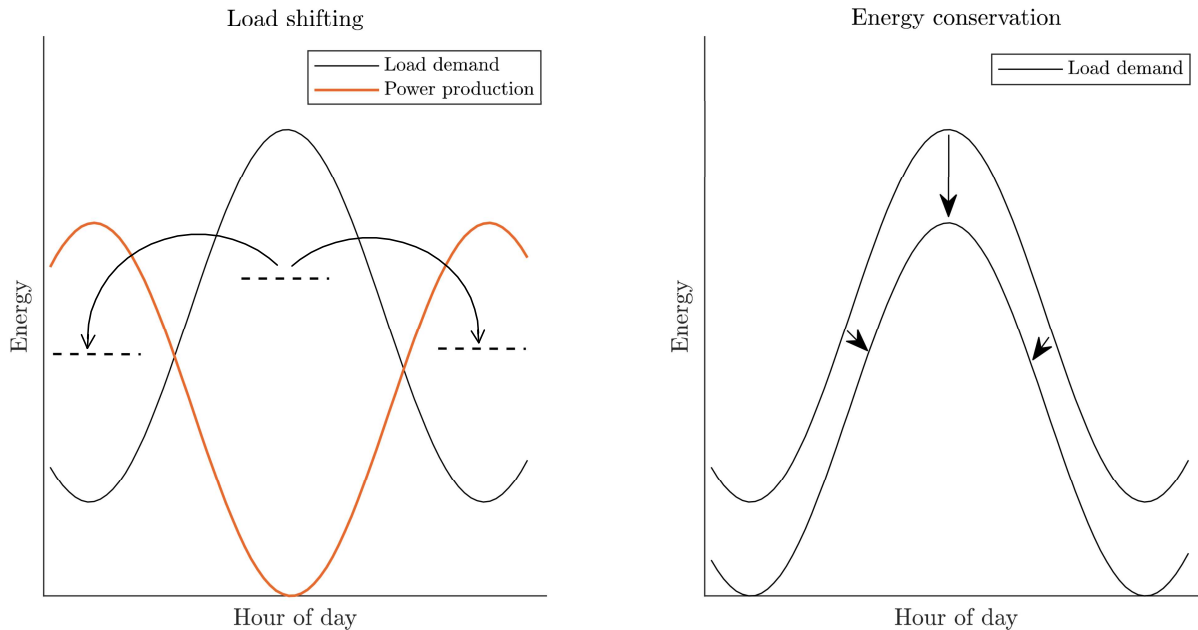
Figure 4.2.1: Example of load shifting where the peak load is shifted to a time with a higher power production (left) and energy conservation which is an ALM method to reduce the overall load demand (right). Modified from source: [48]

Load shifting

Load shifting is widely considered as the most effective load management technique. It takes advantage of time independence of loads and shifts the energy consumption to periods where the power production is sufficient to cover the demand. This does not decrease the total energy consumption, but may decrease the peak demand. [44, 49] On the other hand, if the power production is great, it may result in a higher peak demand at that hour than what was prior to the shift.

Energy conservation

Energy conservation is based on decreasing the power consumption by using more energy efficient devices or changing the usage pattern to reduce overall demand. On a small scale, this can include replacing filament lamps with LEDs, or using other energy efficient appliances. In other words this method reduces the total power consumption, unlike load shifting that only shifts the load in time. [48, 50]

4.3 Load classification

Electrical appliances are loads that can be classified by their flexibility. When searching for literature on this topic it was found that there are many different ways to classify loads. In the case of this project the loads have been classified as either flexible, non-flexible or power shiftable. Further definition of the three is listed below.

- **Flexible loads:**
  Flexible loads are defined as time-shiftable. E.g. loads that can be shifted to periods where the power production is high or the demand is at its lowest.

- **Non-flexible:**
  Non-flexible loads have fixed power requirements and operation period. E.g. heating.

- **Power shiftable**
  Power shiftable loads can be operated using less power. E.g. lights.

4.4 Consumption of common household appliances

This section covers theory on common household appliances that are of importance to this thesis. Average energy consumption and probability of start time for washing machines and dishwashers are presented first, before water heaters and lighting are elaborated on.

Washing machines and dishwashers

Some household appliances such as dishwashers and washing machines are called shiftable atomic loads. This means that their starting time can be shifted to more ideal times, but once they have started they can not be interrupted. [51] Figure 4.4.1 display load profiles for these appliances per cycle with a minute resolution.

The power consumption of these appliances can vary significantly depending on the size of the load and the selected program of the machine. The load profiles presented are based on average energy consumption for common dishwashers and washing machines. [52]
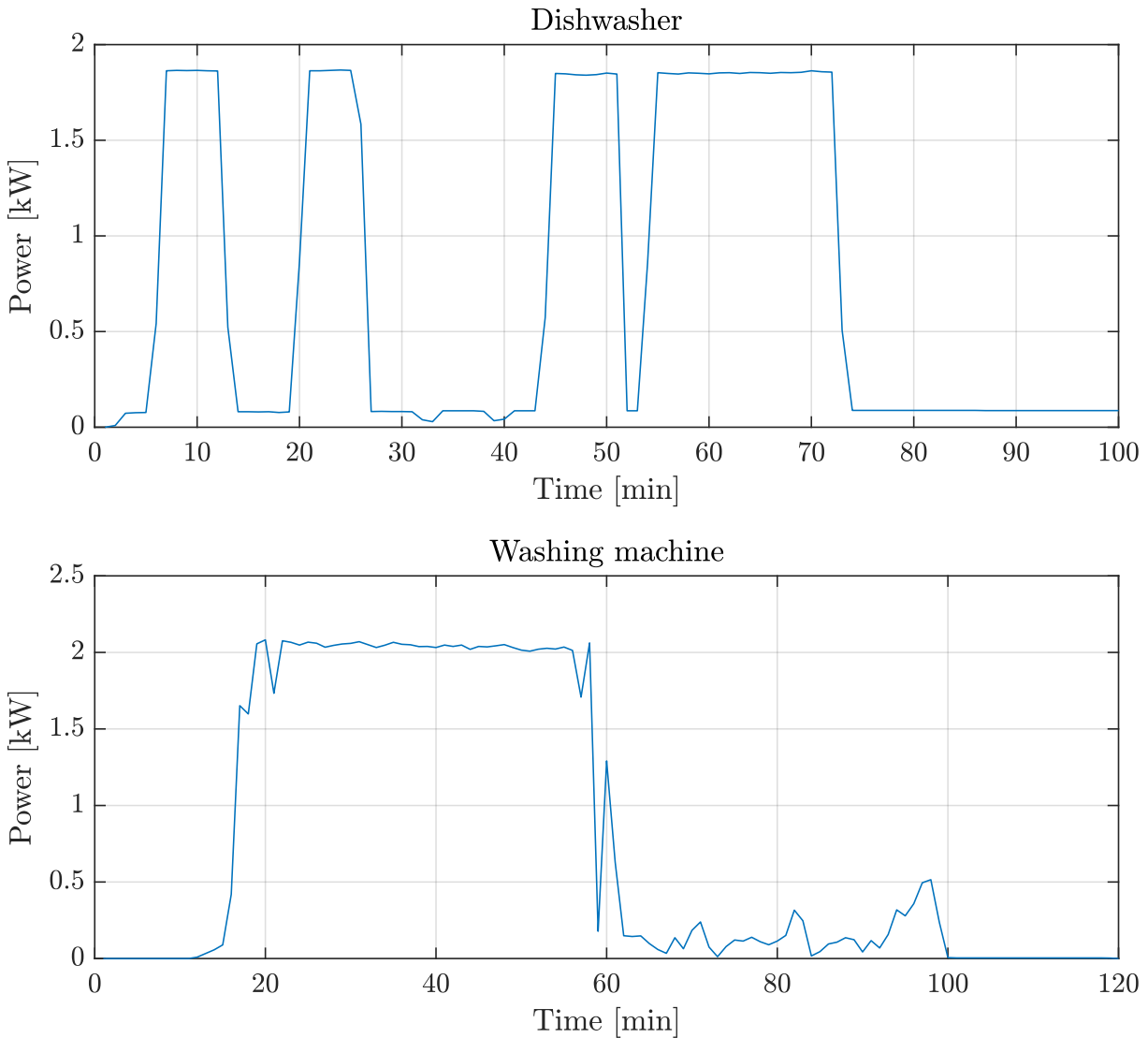
Figure 4.4.1: An illustration of the average power consumption per cycle for dishwashers and washing machines. Data provided by SINTEF Energy. [53]

When applying ALM on household appliances that varies in time-of-use, it is not as easy as taking a portion from one hour and move it to the next. It is important to have access to consumption profiles of individual loads in order to estimate the flexibility potential. If component meters are not available, time-based probability-of-use profiles are necessary. [51] Figure 4.4.2 illustrates the probability of start time for dishwashers and washing machines for average Norwegian households.
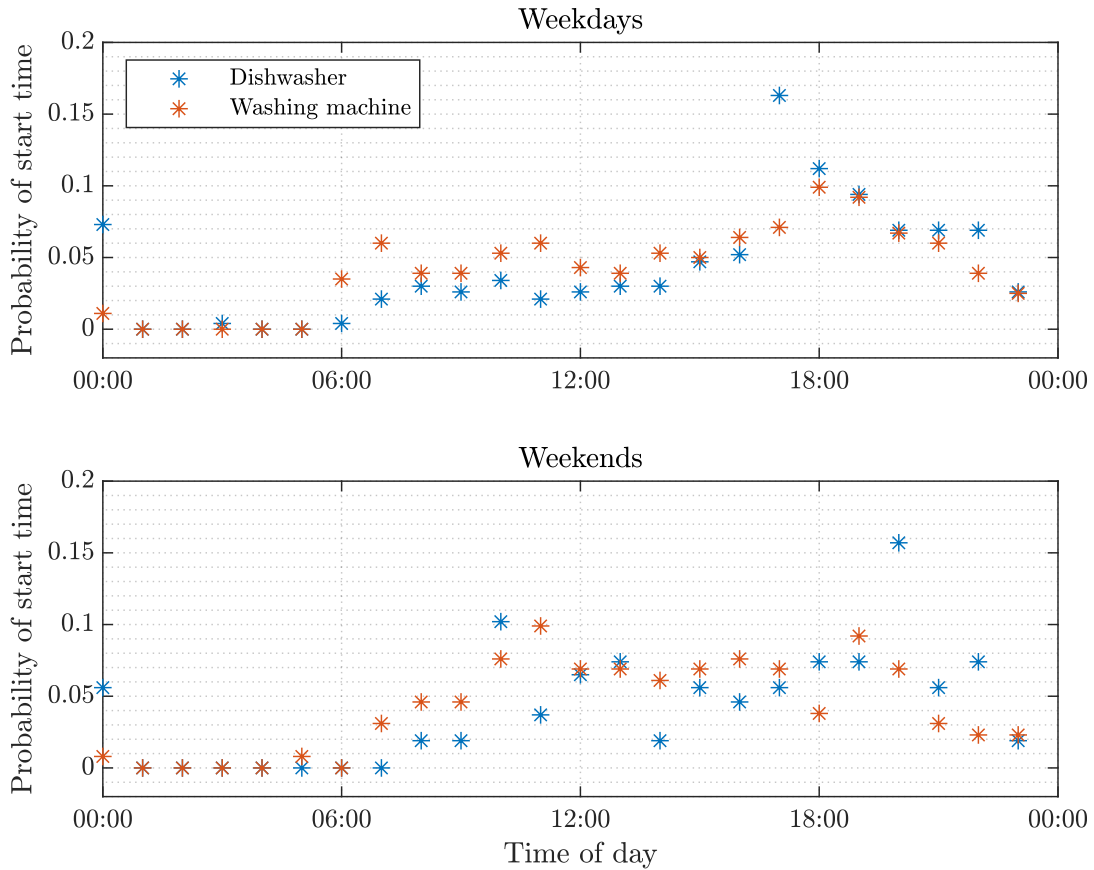
Figure 4.4.2: An illustration of the probability of start time for typical household appliances for average Norwegian households. Data provided by SINTEF Energy. [53]

From figure 4.4.2 it can be seen that the probability of start time on weekdays for dishwashers and washing machine has a peak value at 17:00 and 18:00, respectively. On weekends the probability intensifies earlier in the morning hours but has earlier peak values, with dishwasher probability of start time at its highest at 10:00 and washing machine at 20:00.

The average number of washing machine uses per week in an average European household is found to be 3.8 based on numbers from 2011. SINTEF Energy have calculated the probability that the washing activity takes place in a weekday to be 48.7 %, while there is a minimal difference between the weekdays. Although, it is found that it is most likely that the use of washing machines happens at Sundays and Thursdays, while it is least likely on Tuesdays. [52]

Water heaters

Water heaters are the loads that can be considered most flexible, and is well suited for load management due to its thermal inertia. Water heaters can be idle for a long time without power supply and at the same time keep a relative constant temperature, due to its minimal heat loss. [53]

In this thesis the standard SN/TS 3031:2016 from "Energy performance of buildings - Calculation of energy needs and energy supply" is used to make a load profile for the water heaters. The standard is based on an annual energy consumption of 25 kWh/m^2 for small houses and 10 kWh/m^2 for light industry buildings. A general load profile for water heaters, based on the consumption data from the standard is illustrated in figure 4.4.3. [54] The consumption is given in Wh/h, which can be seen as an anomaly, but it is commonly used to describe energy per hour.
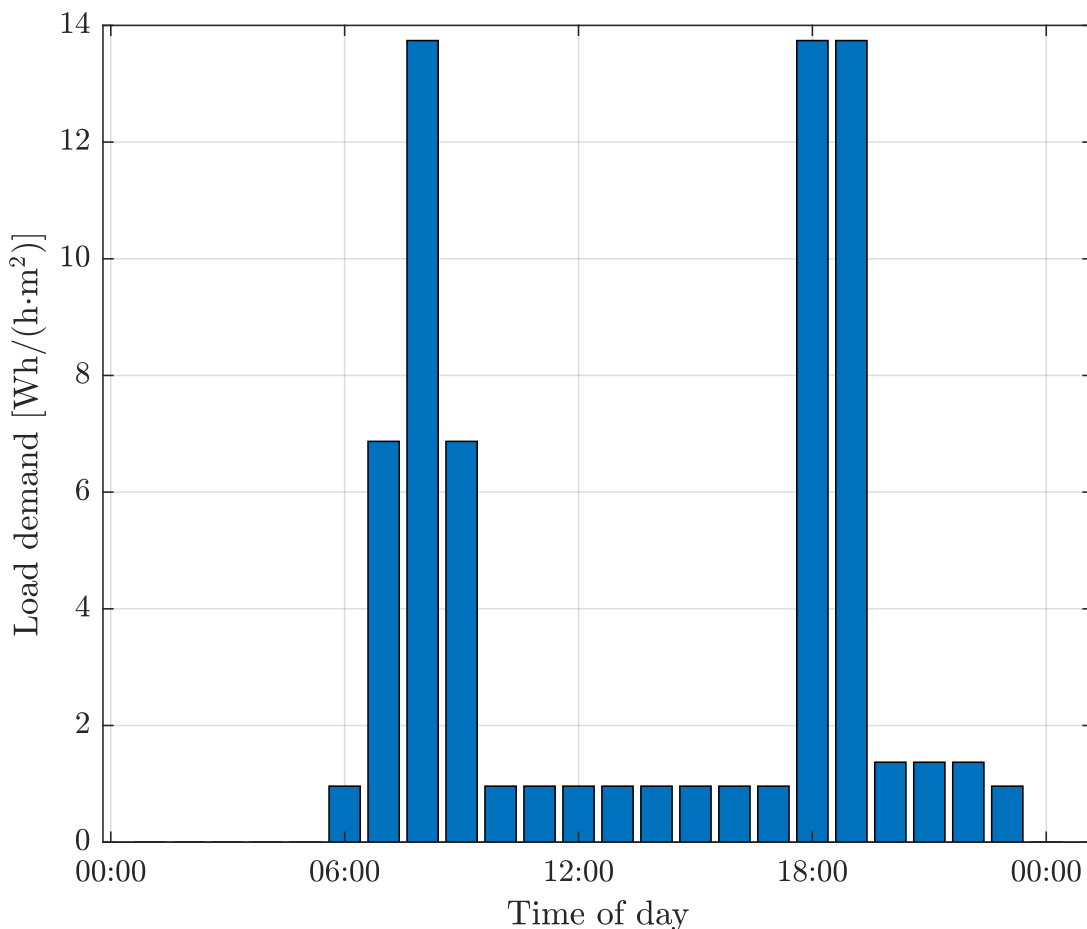
Figure 4.4.3: An illustration of a daily load profile for water heaters based on data from Norsk standard.

Lighting

The standard SN/TS 3031:2016 is also used to make a load profile for the lightning in the apartments. The standard is based on an annual energy consumption of 11.4 Wh/m^2. According to this standard the energy consumption for lighting appliances can be reduced by 20 % if a control system based on utilization of daylight or sensors is applied. [54]

Chapter 5

Defining demand flexibility at Rye

Mapping of loads and defining the demand flexibility of the two farm sites are core parts of this thesis. A site survey was performed, in addition to personal communication with the farmer Lars Hoem to get an overview of the different loads and their respective usage pattern. This chapter covers this process and the findings from the site survey.

Data from the smart meters (eGauge & Smappee) are used to plot load profiles for the time period February 19th - April 1th 2019. A comparison with temperature was implemented with data from the Norwegian Meteorological Institute to see the correlation between temperature and heating in the apartments. [55] The temperature data is measured at Voll weather station in Trondheim. This was found to be the nearest location that was also reliable.

As elaborated on in section 2.3, the main- and west apartment are on the same circuit, while the east apartment, cowshed and silo are on individual circuits. The mastu is not included in any of the circuits connected to the eGauge smart meter. Load profiles for all the flexible loads are attached in appendix A.

5.1   Site survey

The site survey at the two sites was performed on March 20th 2019 in order to map the different loads and classify them according to their flexibility properties. This was accomplished in cooperation with the farmer Lars Hoem and TrønderEnergi. This section presents the findings from the site survey.

On beforehand, it was planned to map as many appliances over 2 kW as possible from the two sites. But as some loads (motors, compressors etc.) runs at the same time, also loads down to 1 kW were considered. The power rating of each appliance was noted along with their respective usage pattern, in order to define their flexibility.

All loads are classified as flexible, non-flexible or power-shiftable. Each appliance is given a limit which defines the number of hours their respective load can be shifted between, during a day, or its potential energy reduction. These values are either based on information from the farmer, SINTEF Energy or Standard Norge. Data from SINTEF Energy and Standard Norge are used, since there are no measurements on a component level.

Farm site 1

The loads on farm site 1 can be divided into household appliances and appliances related to the cowshed. There are, in addition to the cowshed, a total of 4 apartments. Only the main- and east apartments were in use in 2018, while the mastu was inhabited only in 2019. The west apartment was not in use for the scope of this thesis. The apartments vary in size and their respective areas are listed in table 5.1.1. These values are used to calculate the energy consumption of water heaters and lighting based on data from Standard Norge.

Table 5.1.1: Area of the apartments and cowshed at farm site 1.

Apartments	Area
Main apartment	312 m^2
West apartment	64 m^2
East apartment	200 m^2
Mastu	50 m^2
Cowshed	700 m^2

Household appliances

All apartments have dishwashers and washing machines. These loads are classified as flexible and are assumed to have the same energy consumption per cycle. Their starting time are based on probability data presented in section 4.4. These appliances are set to be flexible within a limit of 24 hours since their starting time could be predefined.

Cookers are found in all apartments. These loads are classified as non-flexible based on that consumers prepare food when they are hungry, and their usage pattern are hard to predict.

Heating in the main apartment is provided by an air-to-water heat-pump, while the east apartment has an air-to-air heat-pump. The heating demand in the mastu is only covered by heating cables. Heating is defined as non-flexible as it is automatically regulated by defined temperatures.

There are water heaters in all the apartments. The water heaters are classified as flexible, with exception to the water heater in the main apartment. This water heater is supplied with heat from the air-to-water heat-pump, which - again - is classified as non-flexible. The water heaters have a power rating between 2 - 3 kW. They are set to be flexible within a time limit of 12 hours due to their thermal inertia and minimal heat loss. All loads mapped in the apartments are listed in table 5.1.2.

The energy consumption of lighting is based on standards elaborated on in section 4.4. A limit of 20 % energy reduction is given, based on the same standard.

Table 5.1.2: Overview of loads mapped in the apartments at farm site 1. Empty cells are due to lack of information regarding the respective appliance, or due to non-flexible loads.

Electrical appliance	Power rating [kW]	Consumption	Classification	Time of use	Limit
Dishwasher x 3	-	1.28 kWh/cycle	Flexible	100 min	24 hr
Washing machine x 3	-	1.55 kWh/cycle	Flexible	2 hr	24 hr
Water heater x 3	2.0 - 3.0	-	Flexible	-	12 hr
Lights	-	1.84 Wh/m^2	Power shiftable	16 hr	20 %
Cooker x 3	-	-	Non-flexible	-	-
Air - water heat pump	8.0	-	Non-flexible	-	-
Air - air heat pump x 2	1.8 x 2	-	Non-flexible	-	-

Cowshed

Nine individual loads were registered in the cowshed at farm site 1. Most of them are related to husbandry of cows. There are three silos with a 1.5 kW motor each, which are responsible for providing concentrates. These motors run independently of each other, at no predefined times, and is therefore classified as non-flexible.

The process of milking the cows is done automatically by a milking robot where the cows enter the machine at their own will. Since this process does not follow a predefined pattern, the load is defined as non-flexible. The milk is stored in a tank and emptied approximately every second day. The heat element is part of the machine that cleans the milk storage tank, which is done right after the tank is emptied. This load is defined as non-flexible as the usage pattern depends on an external company that collects the milk when it is needed.

The largest individual load on farm site 1 is a grass silo. There are two motors that operate simultaneously, amounting to a maximum power rating of 44 kW. This load is connected to the same circuit as the air-to-air heat-pumps and its load profile can be seen in figure 5.1.1. The load operates in the evening every day, except between the period June - November, with a few exceptions. The silo is classified as flexible because this operation can be performed at any time of day, although a person must be present. Its limit is set to 16 hours since the component is placed in the immediate vicinity of the farmers home, but is unlikely to be operated in the night time.

There is a water heater in the cowshed which have an assumed power rating of 2 - 3 kW, based on information from the farm owner. The energy consumption is defined by data from the standard for small industry buildings, and the area of the cowshed. Its limit is - like the water heaters in the apartments - set to 12 hours.

The telecommunication company Telenor is renting an area in the cowshed which contains equipment connected to the microgrid. Telenor pay 15 000 NOK/year, but the power consumption is unknown. Assuming an average price of electricity (numbers from 2018) of 1.10 NOK/kWh including taxes and grid rent, this amounts to a total annual consumption of 16 500 kWh. Assuming a flat load and dividing on the total number of hours in a year, this amounts to approximately 1.9 kW [56, 57].

The grain dryer operates approximately 14 days in September. This load operate continuously in this period as long as there is grain to dry. As a result, this load is classified as non-flexible. The increased demand due to this load can be observed from the load profile of the total demand in figure 6.5.1. All loads mapped from the cowshed can be seen in table 5.1.3.

Table 5.1.3: Overview of loads in cowshed at farm site 1. Empty cells are due to lack of information regarding the respective appliance, or intentionally left blank due to non-flexible loads.

Electrical appliance	Power rating [kW]	Consumption [kWh/day]	Classification	Time of use	Limit
Water heater	2.0 - 3.0	-	Flexible	-	12 hr
Silo	44.0	22.0	Flexible	30 min	16 hr
Telenor	1.9	45.6	Power-shiftable	Constant	100 %
Lights	-	-	Power-shiftable	24 hr	20 %
Motor x 3	4.5	-	Non-flexible	-	-
Heat element	12.0	6.0	Non-flexible	30 min	-
Milking system	5.9	-	Non-flexible	-	-
Grain dryer	32.0	-	Non-flexible	14 days	-

The silo is the individual load that has the highest power rating of the flexible loads. When comparing the total load profile to the profile of the silo alone, it is easy to identify because of its high and regular peaks. This is illustrated in a subplot in figure 5.1.1. As the silo is classified as a flexible load, it is important to know its usage pattern in order to make sure that non-flexible loads are not mistaken for being flexible when it is shifted.
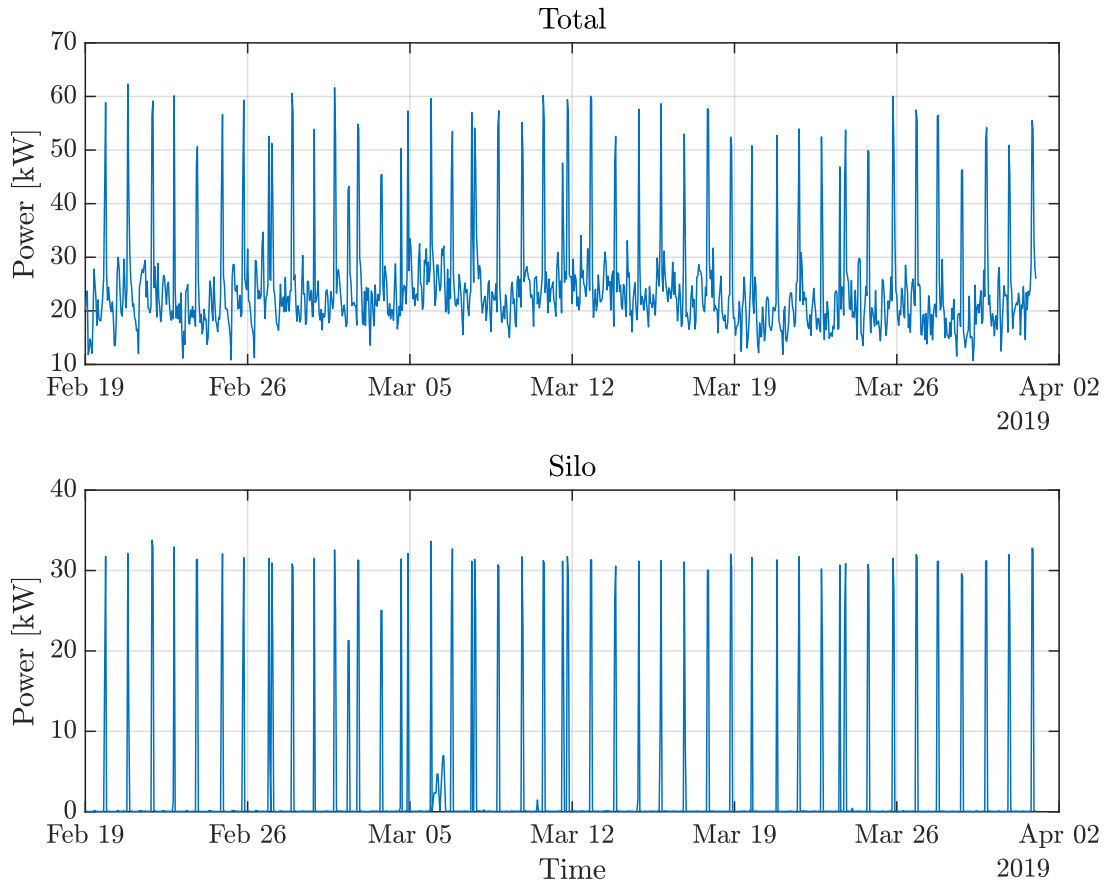
Figure 5.1.1: Comparison of the total load and the silo at farm site 1. It is illustrated that the peak loads in the total demand comprise of the silo.

Farm site 2

At farm site 2 there are few loads in the cowshed, amounting to a small load demand. The only load considered flexible is the water heater. According to the farm owner, the water heater at this site is mostly idle. An overview displaying the different appliances and their respective classification is presented in table 5.1.4.

Table 5.1.4: Overview of loads at farm site 2. Empty cells are due to lack of information regarding the respective appliance, or intentionally left blank due to non-flexible loads.

Electrical appliance	Power rating [kW]	Consumption	Classification	Time of use	Limit
Water heater	2.0 - 3.0	-	Flexible	-	12 hr
Heat lamps x 4	1.0	-	Non-flexible	24 hr	-
Lights	-	-	Power-shiftable	24 hr	20 %

5.2   Component flexibility

This section presents a comparison of apartment load profiles and the probability of start time, which is elaborated on in section 4.4.

When comparing the probability data with the load profiles of the apartments, it can be observed from figure 5.2.1 that the probability of start time for both dishwasher and washing machine corresponds fairly well with the load demand. The load profile in the comparison plot is for a random weekday. The load will never be consistent and the results will thus vary depending on the day and time of year. The demand is plotted in hourly values, and is illustrated with markers. The lines between them are applied to illustrate the trend.
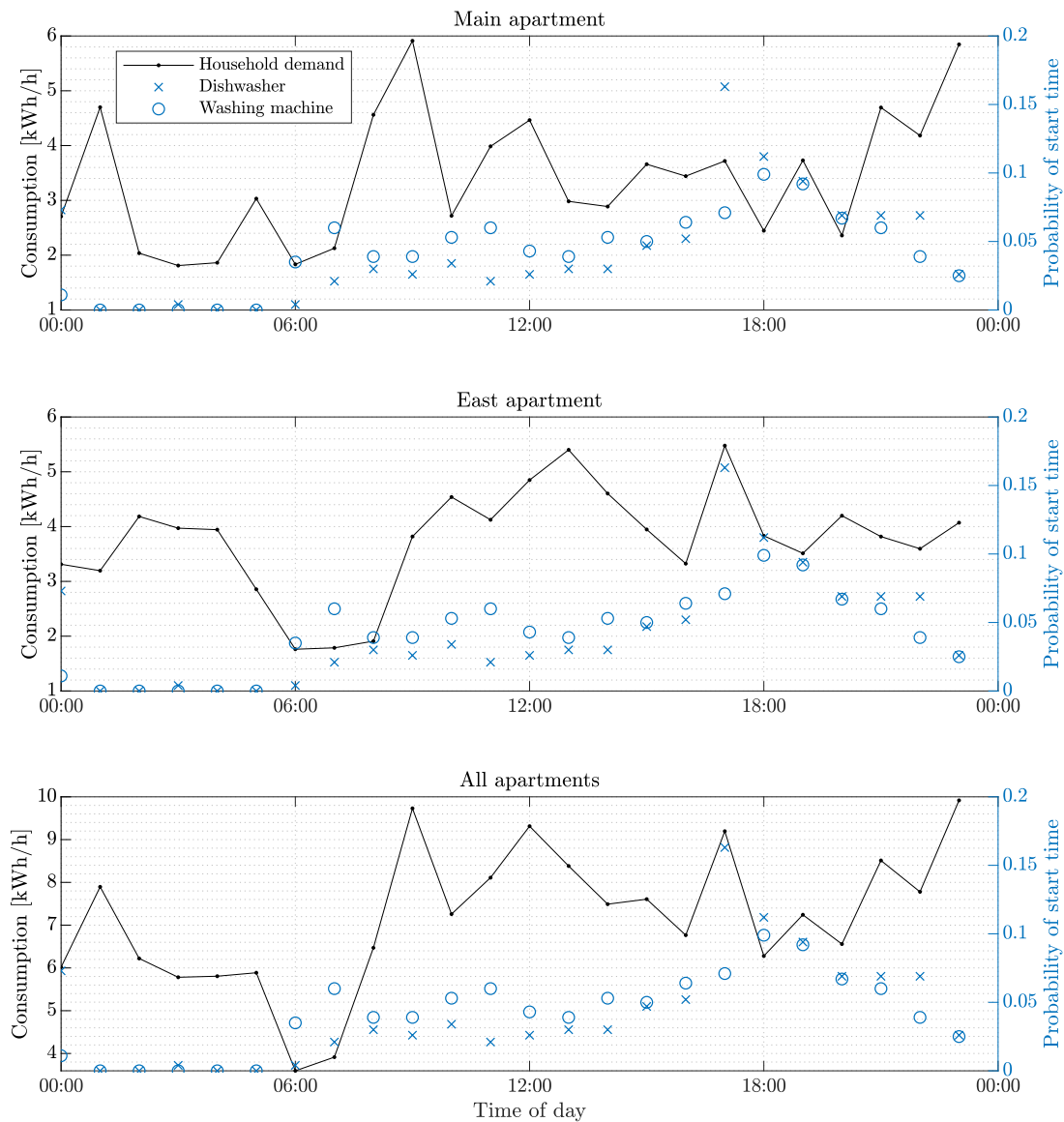
Figure 5.2.1: Probability of start time for dishwasher and washing machine compared to load demand for the apartments at farm site 1. Note that the right y-axis belongs to the dishwashers and washing machines.

5.3   Demand fluctuations

This section presents a comparison of load demand and ambient temperature at the two farm sites. In order to investigate the amount of heating demand, and to avoid shifting the heat demand, a comparison between the load demand and ambient temperature is performed.

Farm site 1

When comparing the combined load profile for all apartments with temperature, an apparent correlation between load demand and outside temperature is observed. This is as expected as the specific time period is in the winter season where substantial temperature fluctuations occur. The correlation is especially apparent around March 5th when the temperature is below -10 °C, while the demand reaches one of the highest peaks of the time period.

For the cowshed on the other hand, this correlation can not be observed as there is no significant heating demand. The load demand in the cowshed is stable and highly predictable. Comparing the two plots, it becomes clear that the base load changes with temperature in the apartments, while it stays relatively constant in the cowshed. Figure 5.3.1 illustrates this comparison for the time period where the eGauge smart meter has been installed.
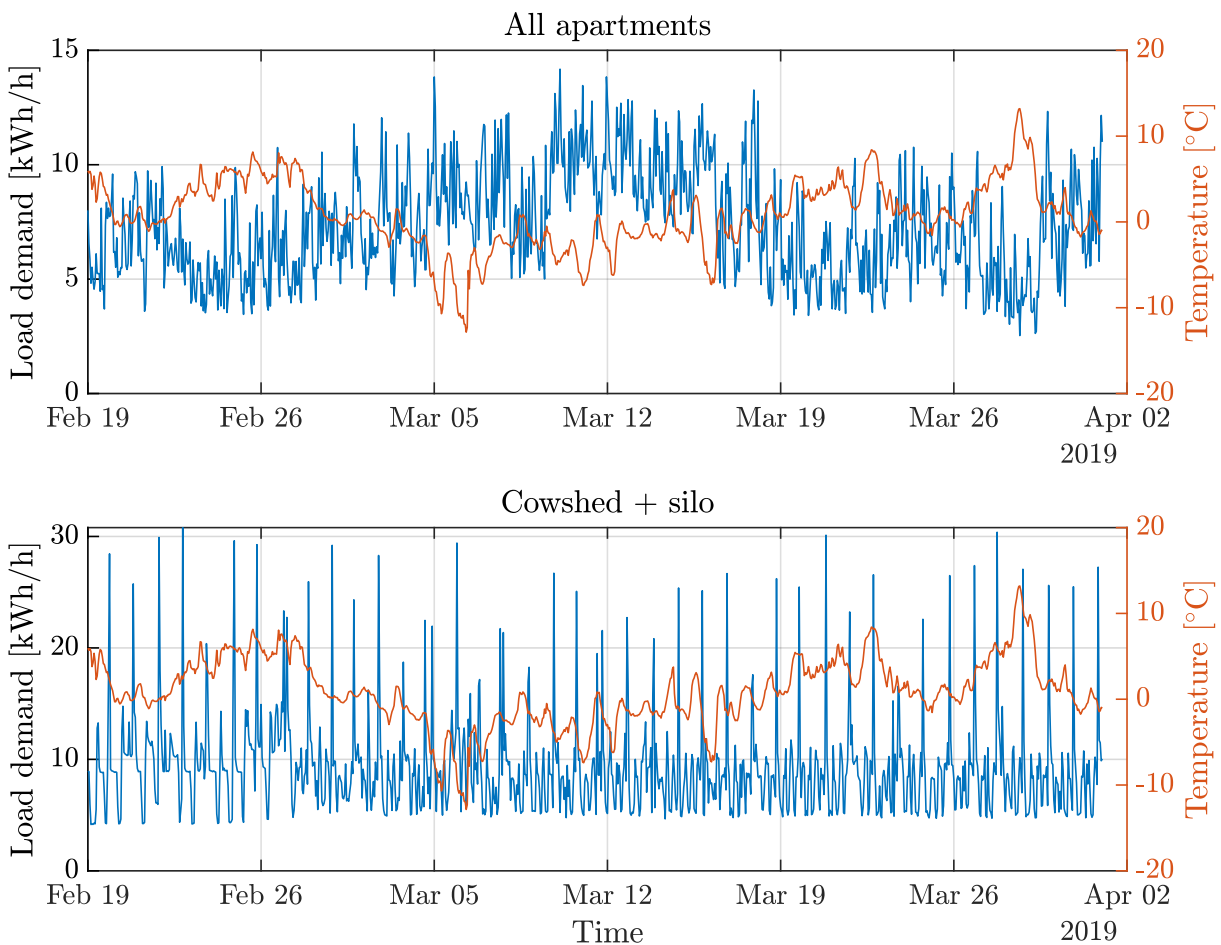
Figure 5.3.1: Load profile for all apartments and cowshed + silo, compared to ambient temperature. A correlation is found for the apartments, but not for the cowshed and silo.

Farm site 2

When comparing the load demand on farm site 2 to the ambient temperature, it can be observed that there is a correlation between the two. The correlation is especially apparent on March 4th and March 11th. Another observation is that the load demand is higher than what would be expected according to the mapped loads from this site. Discussions with the farmer Lars Hoem did not result in an explanation for the deviation.
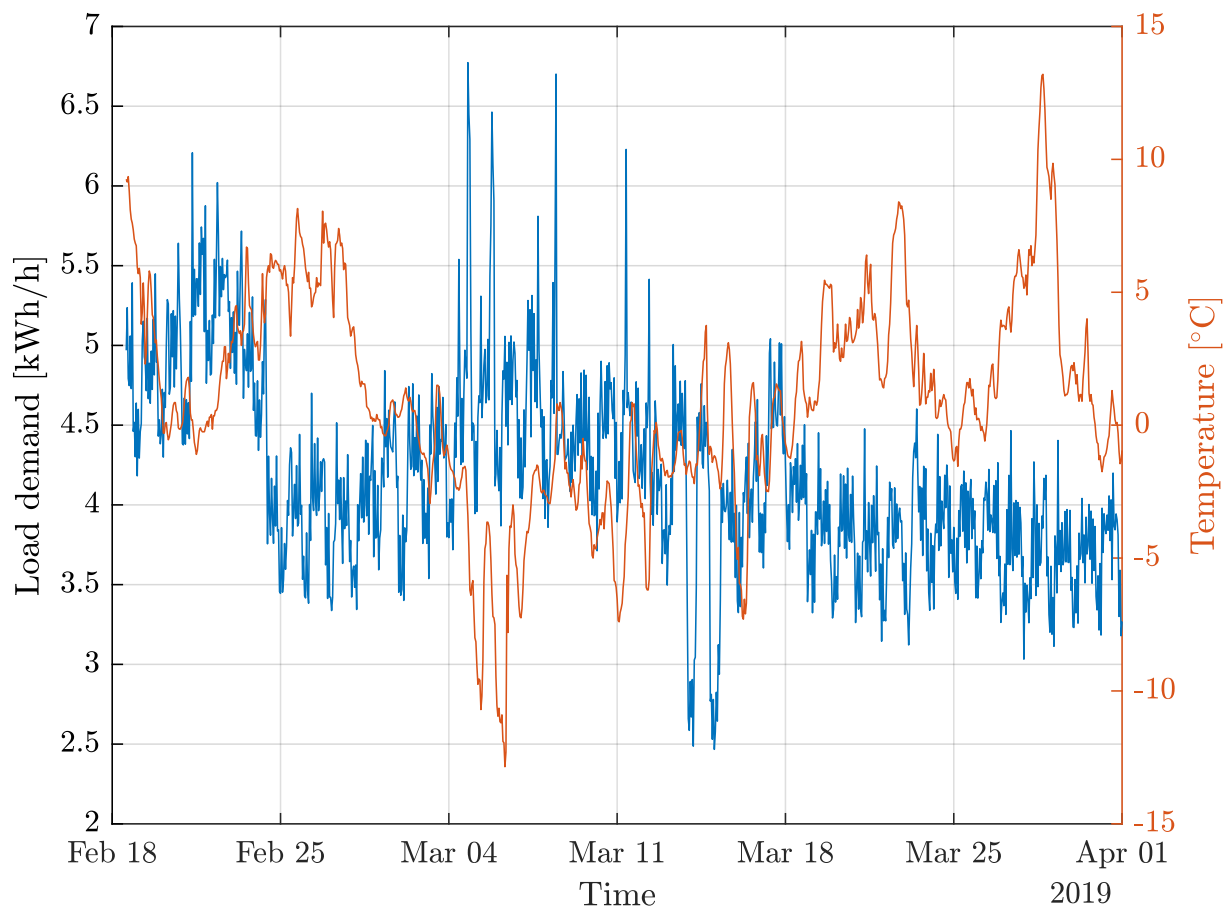
Figure 5.3.2: Load profile at farm site 2 for the time period where the smart meters were installed compared to ambient temperature. A correlation between the two can be observed.

Total

Figure 5.3.3, displays the load profile from January 2018 to April 2019 together with the temperature from the same time period. It can be observed that during the colder periods, the base load rises, while it decreases in the warmer periods.

If the figure is studied further, it can be seen that the demand varies greatly during the winter, early summer and fall while it remains relatively constant in the mid- to late summer months. This is due to the use of the silo. Also there is a three-week period in September 2018 where the demand remained high. The reason is the grain dryer, which operates for about two weeks every year, which is elaborated on in 5.1. These observations are also confimerd by the farm owner.
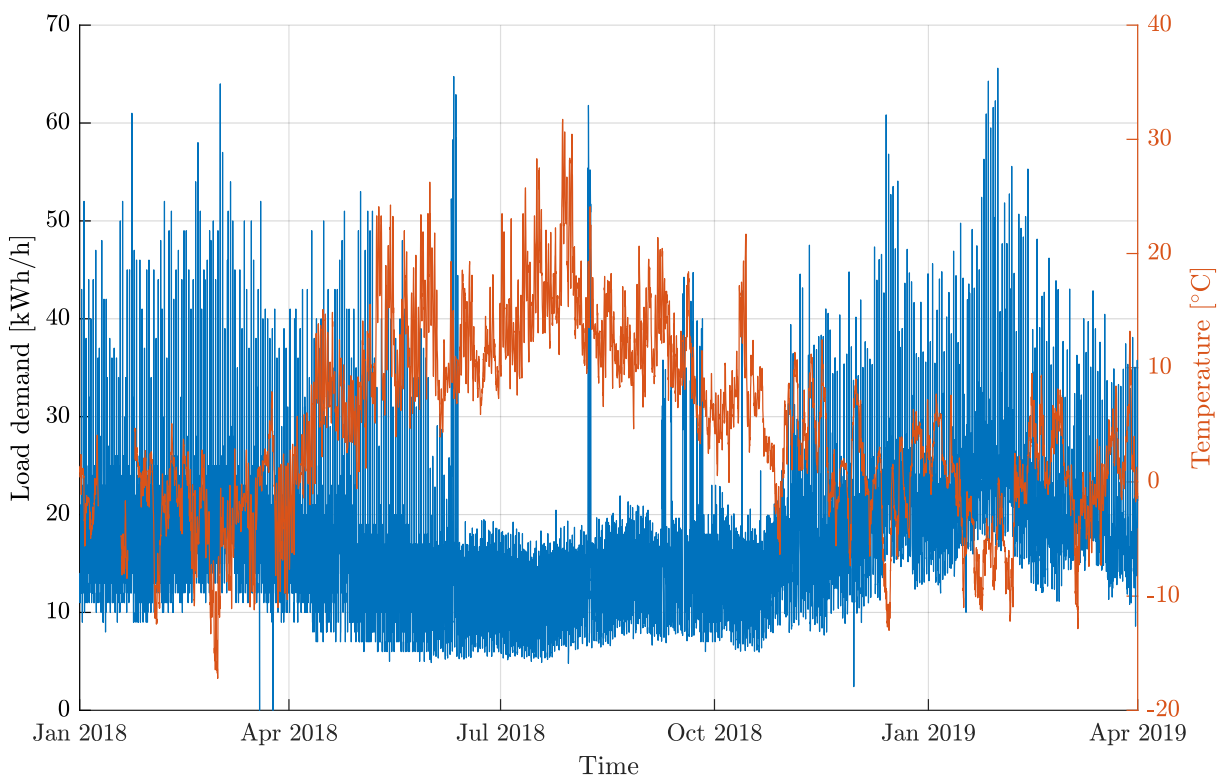
Figure 5.3.3: Comparison of the total load demand and ambient temperature for the time period January 2018 to April 2019.

Chapter 6

Modeling & simulation

This chapter is based on the systematic approach to the different software tools and procedures that is used to solve the problem of this thesis. This includes all procedures needed to simulate for the different cases which are further elaborated on in Chapter 7. The following five steps are described in this chapter:

- Simulating power production from PV
- Calculation of transmission losses
- Developing a load shifting algorithm
- Modeling the microgrid in Simulink
- Processing of data sources

6.1   Performing simulations in PVsyst

As the PV system at Rye was installed in March 2019, simulations had to be performed in order to gather production data over a one year time horizon. PVsyst was the chosen software tool used for the simulations, based on recommendations from the managing director at Solbes, Eirik Lockertsen. This section reviews the different parameters implemented in PVsyst. The full simulation report is attached in appendix B.

PVsyst is one of the leading PC software package for the study, sizing, simulation and data analysis of complete PV systems. It deals with both grid-connected and stand-alone PV systems, and includes extensive meteo data and databases for PV system components, as well as general solar energy tools. [40]

The configuration of the PV system at Rye was set beforehand and PVsyst was used to simulate the energy production over a one year time period, based on the configurations listed in section 2.1. PVsyst provides the option of variant analysis, which has been used in some cases to test the effect of some parameter changes.

Selecting meteorological data

Finding a source of meteorological data was the starting point of the evaluation of this PV project. It is important to note that meteorological data is the main source of uncertainty. The reasons for this are covered in section 3.1.

The solar data provider Meteonorm (version 7.2) was used to gather the data needed to simulate the PV production in PVsyst. Meteonorm is a part of the PVsyst database of meteo providers. The coordinates for the site location were found from google maps and used to define the site location in PVsyst.

Orientation

One of the main parameters required is the orientation of the PV system. As the PV system at Rye has a fixed tilted plane of 35° and is placed facing south, the field type and parameters are selected accordingly, as shown in figure 6.1.1.
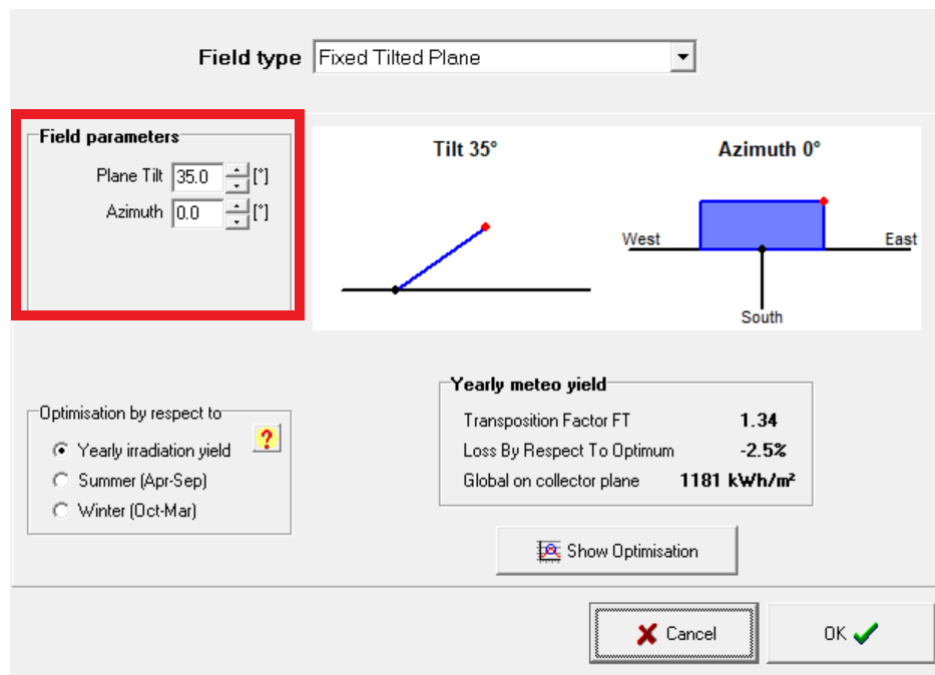
Figure 6.1.1: The field parameters are implemented in PVsyst according to the system configurations at Rye. The red box illustrates how the plane tilt and azimuth are defined.

System parameters

A step-by-step method of defining the system parameters in PVsyst is described in the following paragraphs. Each step is illustrated in figure 2.1. With the following parameters set, all the components and component configurations corresponds with the system at Rye.

(1) When defining the system parameters, the first step was to assign three sub-arrays, one for each row of modules. A compromise had to be made as it is not possible to select multiple module types in a single sub-array. As a result, the "top row" uses 96 REC310NP modules and the two other rows uses REC295TP2. This amounts to 96 of the 310 Wp modules and 192 of the 295 Wp modules.

(2) The second step was to select power optimizers. The correct model for the 310 Wp modules is not available in PVsyst. Therefore, a slightly larger P700 optimizer was selected. Variant analysis with a smaller optimizer was performed, but the results concluded that it had no effect on energy yield. The correct P600 was chosen for the 295 Wp modules.

(3) The third step was to select inverters. Here, the correct string configuration had to be applied. There is one inverter for each sub-array. Then the strings were defined for the system. The number of optimizers in series was set to 16 as there is one optimizer per pair of modules. The number of strings in parallel was set to three. In sum, there are three strings per inverter with 16 optimizers per string. With two modules per optimizer, the total of modules per row is 96. It can be seen in figure 6.1.2, that the inverter power is slightly oversized. This was not taken into consideration as the inverters used in the simulations are the same as in the real system.
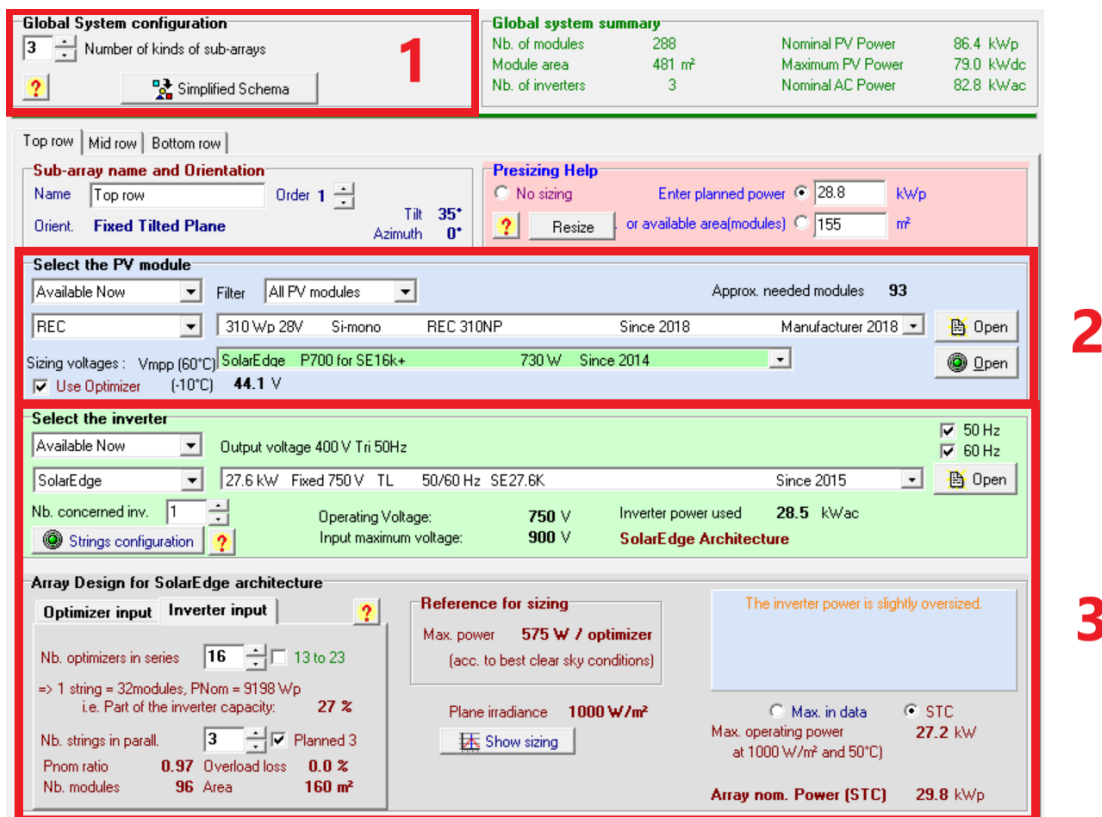
Figure 6.1.2: Step-by-step method of defining the system parameters in PVsyst. The red box marked as 1 illustrates how sub-arrays are defined. The red box marked as 2 illustrates where the PV modules and Power Optimizers are chosen, while the third box show where the inverter and array design are defined.

Detailed losses

Array loss parameters are initially set to reasonable default values. The soiling loss was defined for the whole system and was the only loss factor that was modified. Monthly soiling loss values were set for the whole year. These values were provided by the solar company Solbes. The selected values can be seen in figure 6.1.3.

Figure 6.1.3: The red box illustrates where the soiling loss values are implemented for each month of the year in PVsyst.

Shading loss

In order to implement the effect of near shading in PVsyst, a 3D model of the whole system with its environment has to be made. As this was already done by SOLbes, they provided the file containing the complete 3D model. This file was implemented to create a new shading scene in PVsyst.

Simulation and results

After running a simulation, PVsyst generates a comprehensive report with system details and results including system performance and detailed losses. PVsyst generates CSV-files containing the hourly data that is needed for implementing it in the Simulink model. The data for the simulated power production was exported as an xls-file and imported into MATLAB in order to plot the estimated production over a year. It is also used for comparing the PV production against the wind power production. These results can be found in section 7.1.1.

6.2 Calculation of losses

This section presents the methods used for calculating losses in the transmission line and transformers considered in the microgrid. The equations introduced in section 2.5 are applied here.

Transmission line losses

To calculate the losses in the transmission line the current flowing through the line is needed. The smart meter installed measures the current flowing at the secondary side of transformer 3 as shown in figure 6.2.1. Using equation 2.5.2, and rearranging for I_p, yields the current flowing trough the transmission line:

$$\frac{U_p}{U_s} = a = \frac{I_s}{I_p} \rightarrow I_p = \frac{I_s}{a}$$
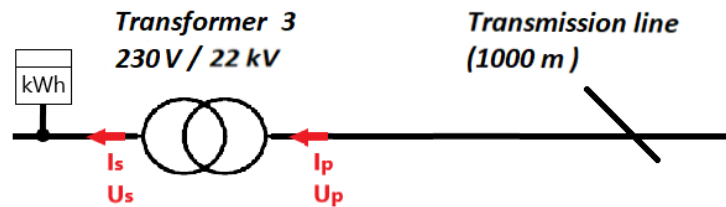
Figure 6.2.1: Line schematic illustrating that the current is measured at the secondary side of transformer 3, while it is the primary current flowing through the transmission line.

Calculating the total resistance per phase of the line is done using equation 2.5.4. values for r and l are as elaborated on in section 2.4.

$$R = r \cdot l \ = \ 0.641 \ \Omega/km \cdot 1.00 \ km = \underline{0.641 \ \Omega}$$

Equation 2.5.3 is applied in MATLAB to calculate the total power loss in the transmission line. Figure 6.2.2 illustrates the losses in the transmission line over the period, 31th May 2018 15:00 - 1th April 2019 00:00. The reason for lack of data during the start of 2018 and the middle of September 2018 is because there were no measurements of current during this time period. It can be seen in the figure that the maximum losses are 8.4 W. This results in an efficiency very close to 100 % and because of this, losses in the transmission line is neglected in further simulations and analysis.
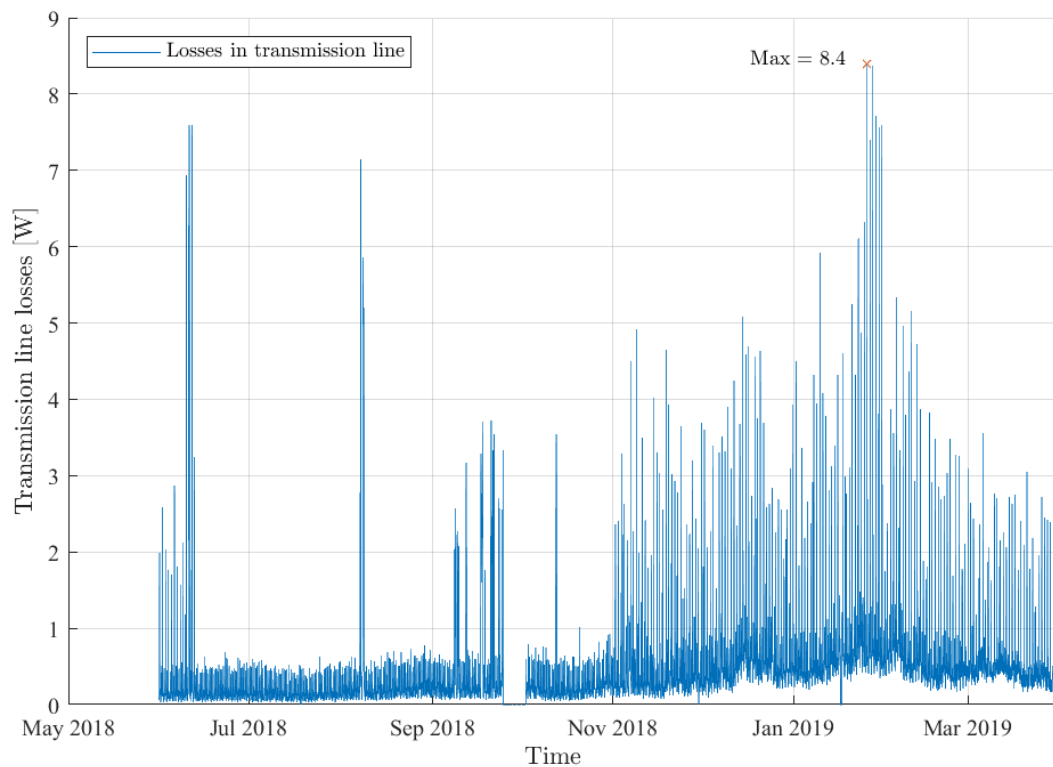
Figure 6.2.2: An illustration of the losses in the transmission line. It is plotted for times with available current data.

Transformer losses

The losses in transformers vary depending on the transformer load. Applying data found in table 2.4.1 and equation 2.5.1, figure 6.2.3 is made. The figure illustrates the total losses in each transformer based on the load, given in percent of full load. The terms T1, T2, T3 are used for transformer 1, 2 and 3. Since T1 and T2 are of the same type, they are graphed together. In addition, it can be noted that the maximum loss for T1 and T2 are 3 260 W and 1 466 W for T3.
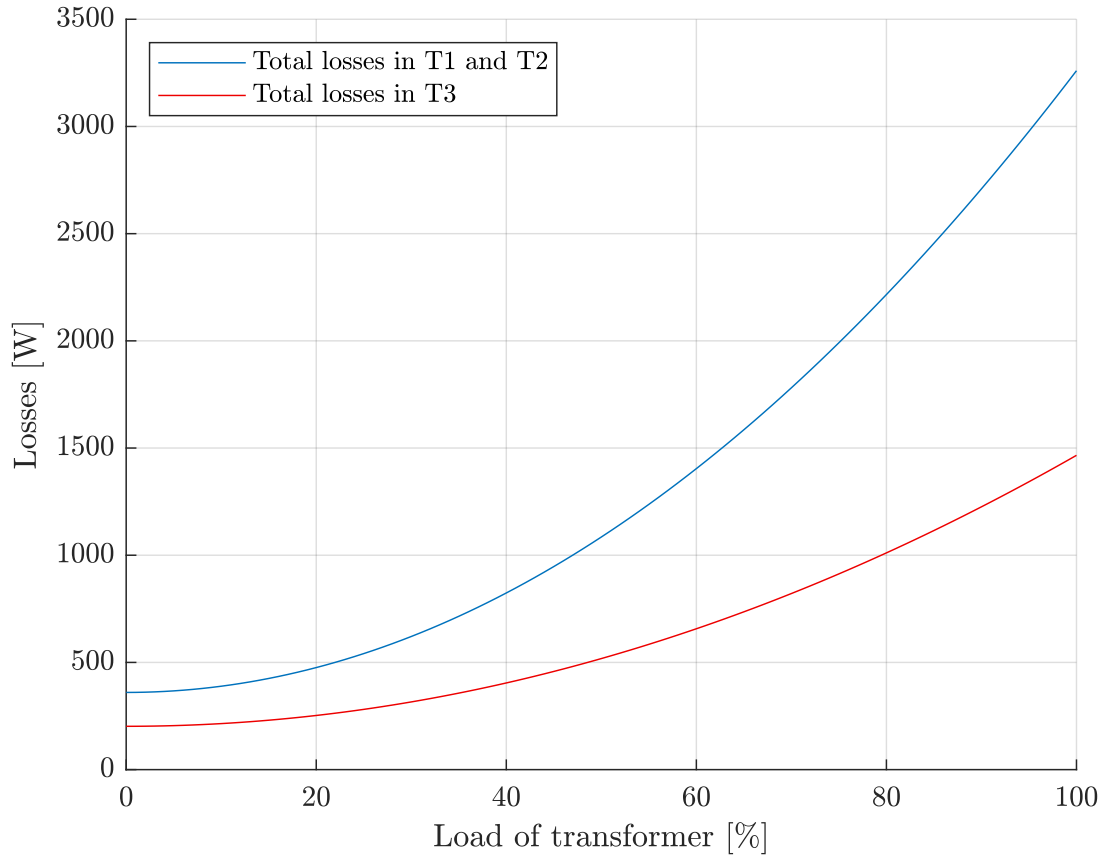
Figure 6.2.3: An illlustration of total losses in the transformers. The losses are based on percentage of full load. T1 and T2 are of the same type and are consequently plotted together.

The equipment measuring the apparent power has been operating since 31th of May 2018. As a result, there is a lack of data in the beginning of 2018. In addition there are missing data where the equipment was out of order. Consequently, the transformer losses were implemented as mean efficiencies in the model, instead of time series data. T2 was not installed at the time of writing this thesis, but is the same model as T1. The efficiency of T2 is therefore set to the same value as T1.

In order to calculate the mean efficiencies, the mean losses of each transformer had to be calculated. Equation 2.5.1 was applied, substituting the apparent power, S for mean apparent power S_{mean}. The mean efficiencies, displayed in table 6.2.1, were then calculated by implementing equation 2.5.5. It can be observed that T1 and T2 have a mean efficiency of 96.1 %, while 98.3 % is for T3.

Table 6.2.1: Resulting transformer efficiencies.

Transformer	Efficiency [%]
Transformer 1	96.1
Transformer 2	96.1
Transformer 3	98.3

6.3   Development of the ALM algorithm

This section covers the methods applied when active load management is implemented. As mentioned in chapter 4, the chosen ALM strategies are load shifting and energy conservation. To implement these strategies, an algorithm is developed and programmed in MATLAB. The inspiration for the algorithm, illustrated in figure 6.3.1 comes from the Masters Thesis written by P. Hategekimana at the University of Agder.[49] A flow chart of the algorithm is illustrated in figure 6.3.1.
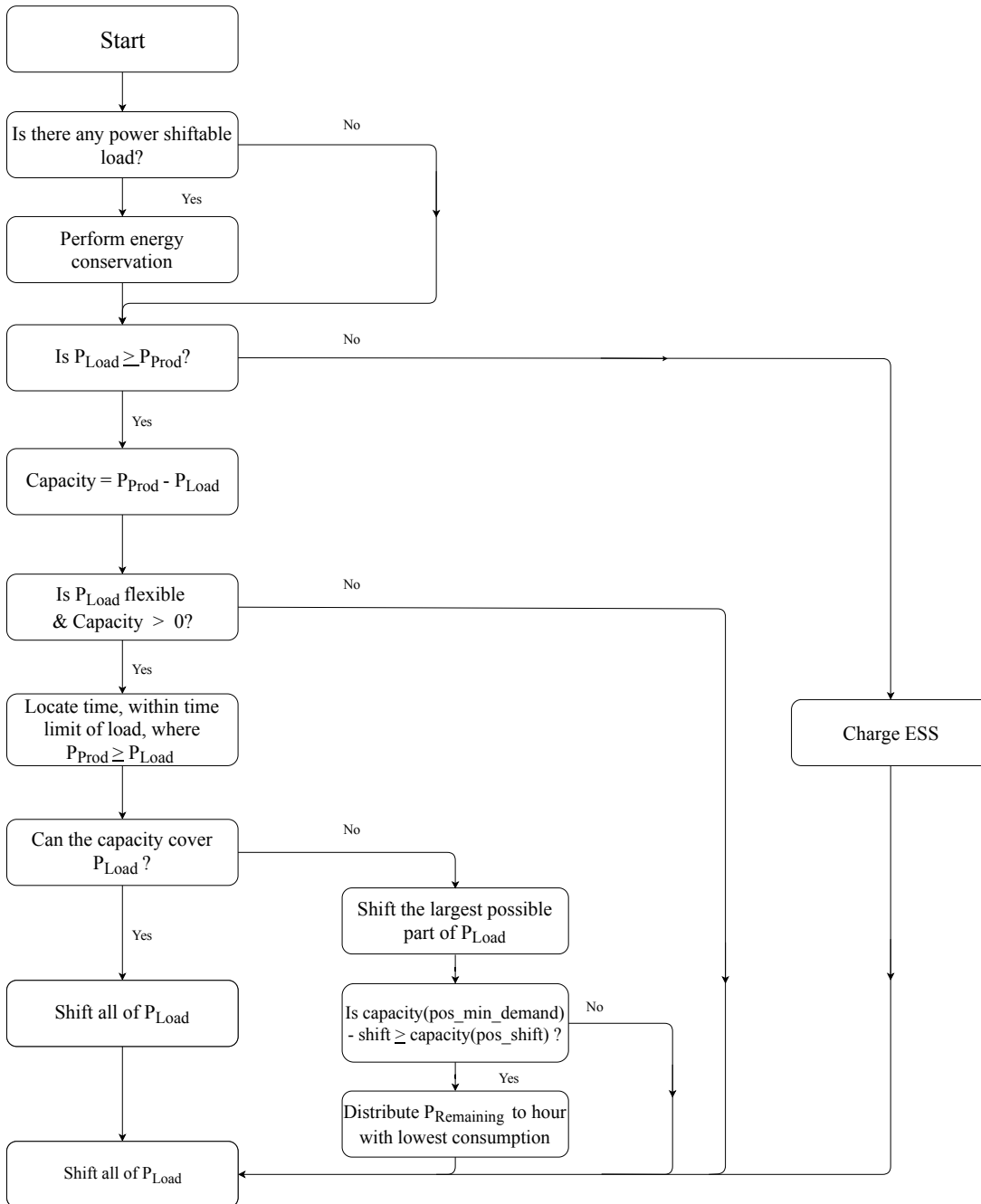
Figure 6.3.1: A flowchart presenting the ALM algorithm. Energy conservation is performed, before flexible loads are shifted to hours with high capacity. The remaining flexible loads are then distributed to hours with lowest consumption.

Energy conservation has the highest priority in order to decrease the load demand. As a result, the necessity of load shifting may also decrease. Shifting flexible loads to hours with the highest capacity is the second priority, as a mean to utilize the energy production more efficiently. The third priority is to shift flexible loads to hours with the lowest consumption to increase the system load factor. It is important to note that capacity and battery capacity is differentiated in this thesis. When explaining the criteria for shifting loads, capacity is defined as the difference between production and demand.

The algorithm starts by checking if there are any power-shiftable loads. If this is true, energy conservation is applied. Then it is checked if the load is greater than the production for a given hour of the day. If yes, it is checked if the load is flexible. If no, the ESS is charged. Then, the algorithm locates a time within the set time limit of the load, where the production is greater than the load. It then evaluates if the production is great enough to cover the whole load. If it is, the whole load is shifted. If not, the largest possible portion, if any, is shifted. If there is any remaining flexible load, it is distributed to the hour with the lowest consumption. This hour is defined by "pos_min_demand" in the flowchart. The criteria for this to be executed is that the capacity at the hour with the lowest consumption, after shift, has to be greater than the capacity at the hour where energy is shifted from. This is due to maintaining the State Of Health (SOH) of the battery. The hour where the load is shifted from is defined by "pos_shift" in the flowchart.

Figure 6.3.2 is used to illustrate the parts of the algorithm performing load shifting. The topmost plot presents the original load profile, while the middle plot illustrates the part when the flexible load is only shifted to hours with sufficient production. The lowermost plot presents the load profile after the remaining flexible load has been distributed to hours with the lowest consumption. The demand and production are plotted in hourly values, and are illustrated with markers. The lines between them are applied to illustrate the trend.

It can be observed that the peak demand between 18:00 to 22:00 is partitioned throughout the day to fully utilize the power production. By only applying the second part of the algorithm, there is still some flexible load left at 13:00 and between 18:00 to 22:00, but no capacity at any hours of the day to shift it to. By executing the third part of the algorithm, the remaining flexible load between 18:00 to 22:00 is distributed to the time period between 02:00 to 06:00. The exception to this is at 03:00. This is not done since the capacity at 03:00 would be lower than at 13:00 if the remaining flexible load is shifted to this hour. A more detailed example with corresponding MATLAB script is illustrated in appendix D.
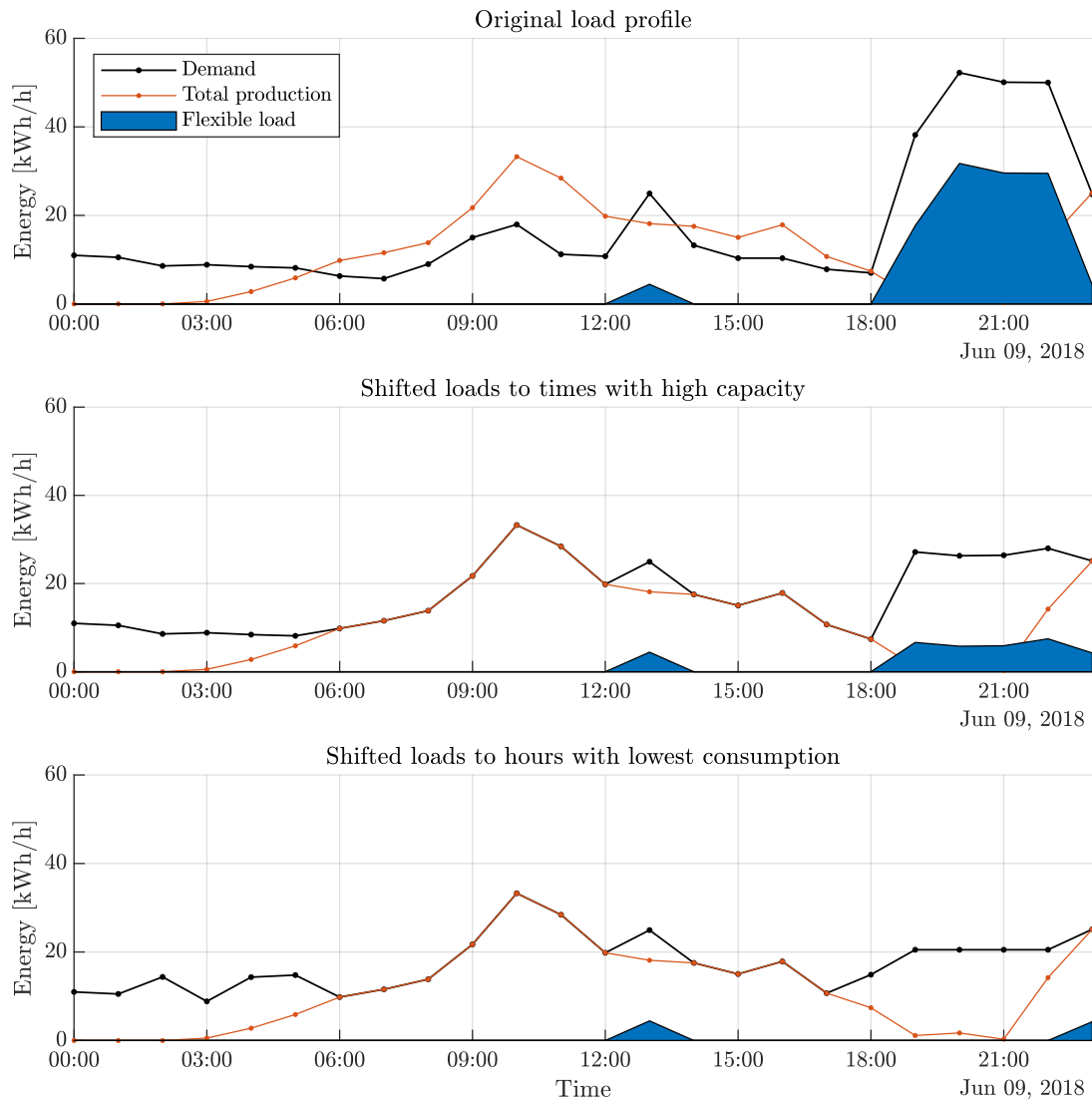
Figure 6.3.2: Example of how load shifting is performed. The original load profile is displayed in the topmost plot. The load profile after loads are shifted to hours with sufficient capacity is illustrated in the middle plot. The lowermost plot presents the load profile after remaining flexible loads are shifted to hours with the lowest consumption.

6.4 Modeling of the microgrid

This section covers the process and methods used to make a model of the microgrid for the following simulation performed in Simulink. Simulink was chosen over other simulating programs because of the wide range of online documentation.

The goal for the model is to have the whole microgrid in one simulation model, where the status of the energy storage system is calculated. Energy needed from the main grid and throttled energy is also calculated.

The model applies load- and production measurements to create an energy storage system based on logical and mathematical blocks. It is based on the planned microgrid, with its corresponding parameters, as presented and explained in Chapter 2. Figure 6.4.1 illustrates the different blocks applied to complete the model of the microgrid. A more detailed description of how the blocks are applied is attached in appendix C.
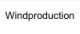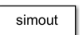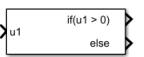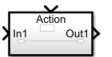
Block symbols	Block name	Block function
	Sum	Sum or subtract values for two or more inputs
	Integrator	Integrates input signal. Can be used as accumulator
Windproduction	From workspace	Imports data from MATLAB workspace
simout	To workspace	Exports input signal to MATLAB workspace
if(u1 > 0) else	IF	The IF block gives a "true" or "false" signal. 1 is true and 0 is false. Elseif conditions can be applied.
Action In1 Out1	IF action	The IF action block recieves a true or false signal from the IF block. If signal is "true", the action is executed
-K-	Gain	Multiplies the input with a function or constant value
	Rate limiter	Limits the rising and falling slew rate of input
1 / 1	In / out port	Creates in / out port for subsystems

Figure 6.4.1: List of the blocks used in Simulink for making the model of the microgrid.

Main system model

To make the model systematic, several subsystems are made. The subsystem created for the production units in the microgrid is displayed as figure 6.4.2. A subsystem is created for production, farm site 1, farm site 2 and the energy storage system. These systems make up the main system of the model. Figure 6.4.3 illustrates the main system where all subsystems are displayed.
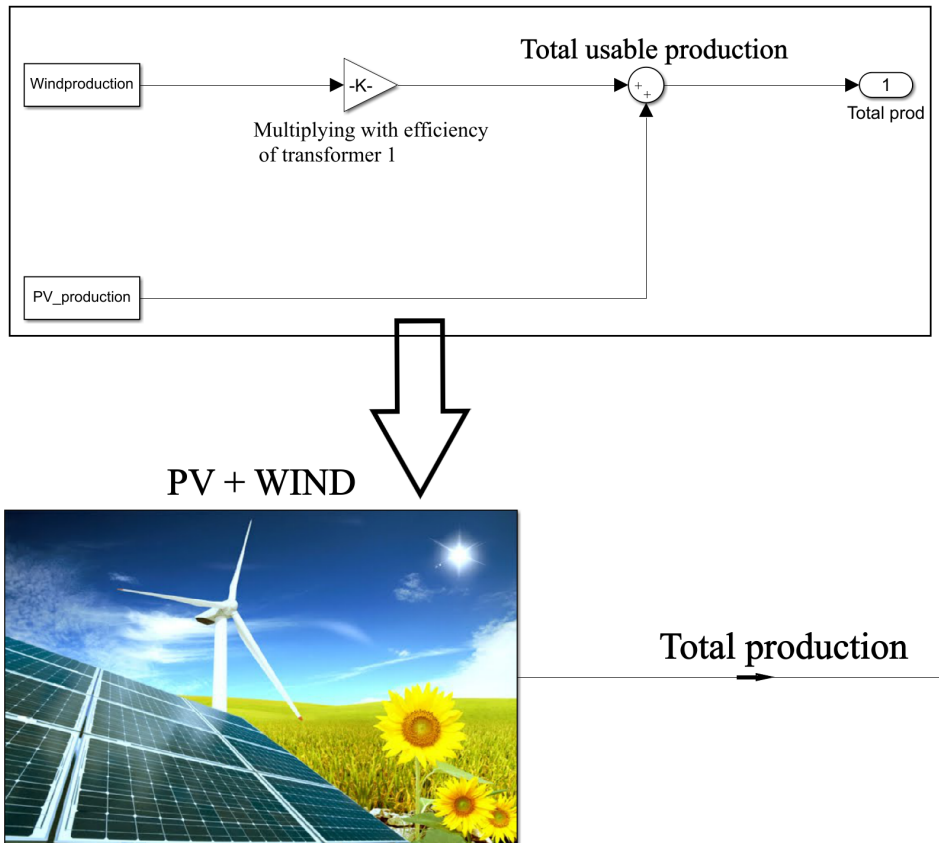
Figure 6.4.2: Illustration of the subsystem for production in Simulink, describing how the total usable production is calculated, and how the efficiency of transformer 1 is implemented.
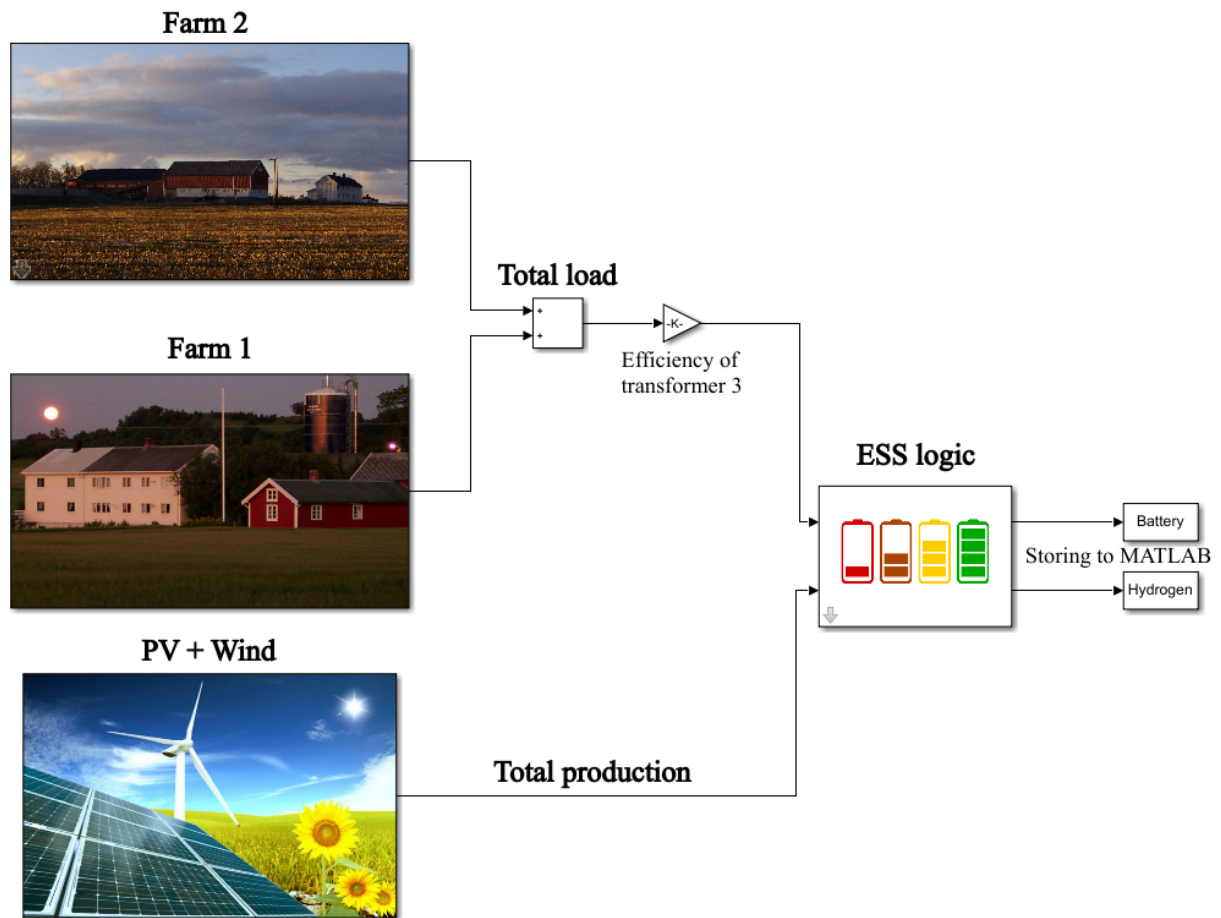
Figure 6.4.3: Presentation of the main system model of the microgrid, consisting of four subsystems. The total load is calculated by summarizing the load demand from the farm sites. It is then multiplied by the efficiency of transformer 3. Total production and demand are inputs to the ESS subsystem.

As shown in figure 6.4.3, two calculations are performed outside of the four subsystems. The total load is calculated by summarizing the load demand from the two farm sites. The total load is then multiplied by the efficiency of transformer 3, because the total load goes through this transformer and the losses can be seen as an increase in demand.

The production system is, as mentioned earlier, presented in figure 6.4.2. The total production is found by multiplying the wind production with the efficiency of transformer 1 and then summarizing it with the PV production. Load data from each of the circuits are summarized in the subsystem of farm site 1 and 2, to get the total load from each site. The last operation performed in the main system is to export the battery status and hydrogen status from the ESS subsystem, from Simulink to MATLAB. The model does not consider the no-load losses of the transformers during a no-load situation.

The ESS model

The ESS model is based on a logical algorithm, presented as a flowchart in figure 6.4.4. The algorithm illustrates that at the start of each iteration, the model imports the total load and total production based on time input. These are then summarized to find if the net energy is positive or negative. If net energy is positive and the battery SOC is under 80 %, then the battery is charged. When the battery SOC reaches 80 % and there is still a positive net energy, then the energy is used to charge the hydrogen storage. If the net energy is negative and the battery SOC is above 20 %, then the battery is discharged. Upon reaching a SOC of 20 %, the hydrogen storage is discharged. This logical algorithm is the baseline for the ESS model.
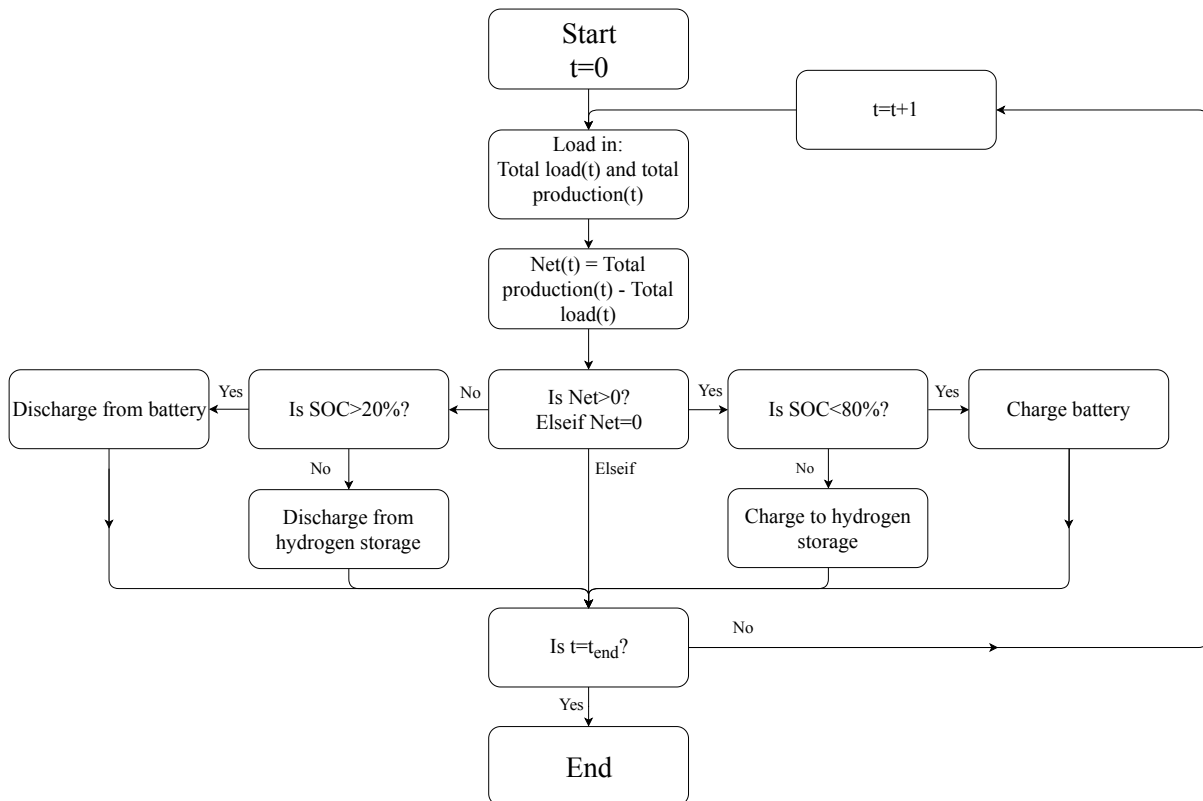
Figure 6.4.4: Flowchart illustrating the algorithm for discharging and charging the ESS.

Figure 6.4.5 presents the resulting ESS model. The model consists of three colored areas. The red area contains calculations for the battery, the green area calculates the hydrogen storage and the blue area calculates throttled energy and energy needed from the main grid.

The area calculating battery status is built up using the algorithm described in figure 6.4.4. In addition, efficiencies are implemented and cycles are calculated using equation 2.6.1. The efficiencies for the battery and transformer 2 is implemented for charging and discharging. This is a simplification, since the energy from PV does not flow through transformer 2. This can be seen in figure 2.0.1. The energy is then accumulated in an integrator block to make the battery status over the simulation time. This integrator block is set to upper and lower limits for the battery capacity and is therefore needed to be changed when testing for other battery capacities. The accumulated energy goes through a rate limiter which defined by the C-rate of the battery. After going through the rate limiter, the battery status is stored in MATLAB before entering the green area.

The hydrogen storage status is calculated in the green area. It is also a subject to the algorithm in figure 6.4.4. In addition, the efficiency of the electrolyzer is added for charging, and the efficiencies of the fuel cell and transformer 2 are added for discharging. The efficiency of transformer 2 is added because the energy discharged from hydrogen storage goes through transformer 2. The accumulated energy needed from hydrogen storage is also calculated and stored in MATLAB. The hydrogen status is then accumulated and summarized with the difference due to the battery rate limiter, to calculate a new hydrogen status. This is done to account for the excess or deficit of energy when charging or discharging the battery. The accumulated values of the hydrogen status goes through the hydrogen rate limiter, which is set to a rising slew rate of 55 and a falling slew rate of - 100. This represents the power rating of the electrolyzer and the fuel cell, respectively.

The hydrogen status, battery status and net energy then enters the blue area. This area checks the throttled energy and the energy needed from the main grid, and is not a part of the main ESS algorithm. Instead, the algorithm applied is as follows: If the ESS is full and the net energy is positive, then the positive net energy is throttled along with the positive difference from the hydrogen storage rate limiter. The Elseif condition checks if the ESS is empty and net energy is negative. If so, the negative net energy and the negative values from the hydrogen rate limiter are supplied by the main grid. A flowchart of this algorithm is displayed in figure C.1.2.

As a summary, table 6.4.1 presents the inputs and outputs from the model.

Table 6.4.1: Inputs and outputs from the model of microgrid made in Simulink.

Inputs
Load demand
Wind production
PV production
Outputs
Battery status
Hydrogen status
Number of cycles in battery
Accumulated energy from hydrogen
Throttled energy
Energy from main grid
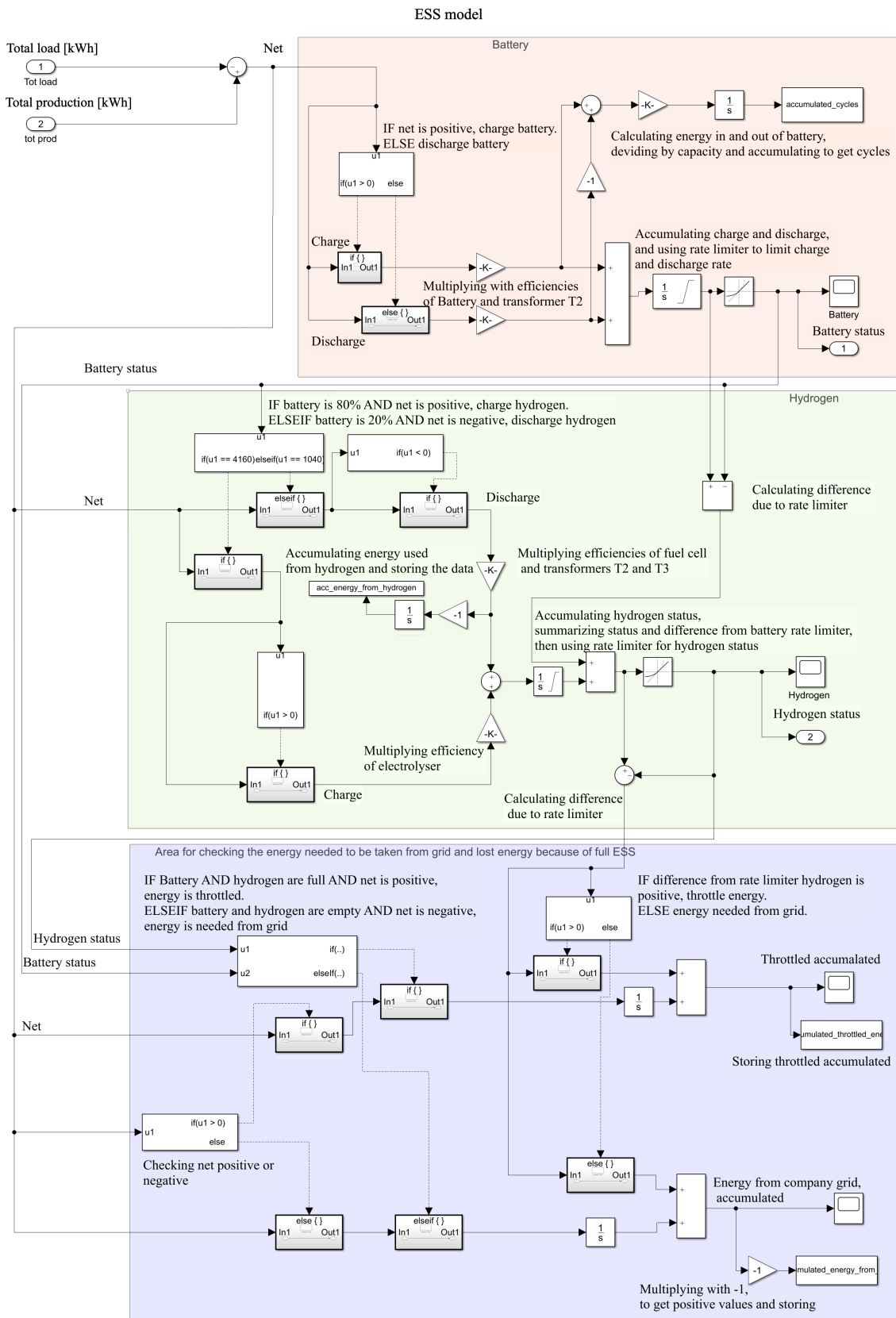
Figure 6.4.5: Illustration of the ESS subsystem. The red area contains calculations for the battery, the green area calculates the hydrogen storage and the blue area calculates throttled energy and energy needed from the main grid.

6.5 Data sources

This section presents the use of different data sources to make up the load demand and total power production for the time period January 2018 to April 2019.

Figure 6.5.1 displays the consumption and total production throughout the time period. Due to lack of complete data and downtime of sensors, two sources of data was used to complete the data set. Data source 1 was provided by TrønderEnergi, while data source 2 was obtained from the Safebase meters in substations NS 70260 and NS 70261.
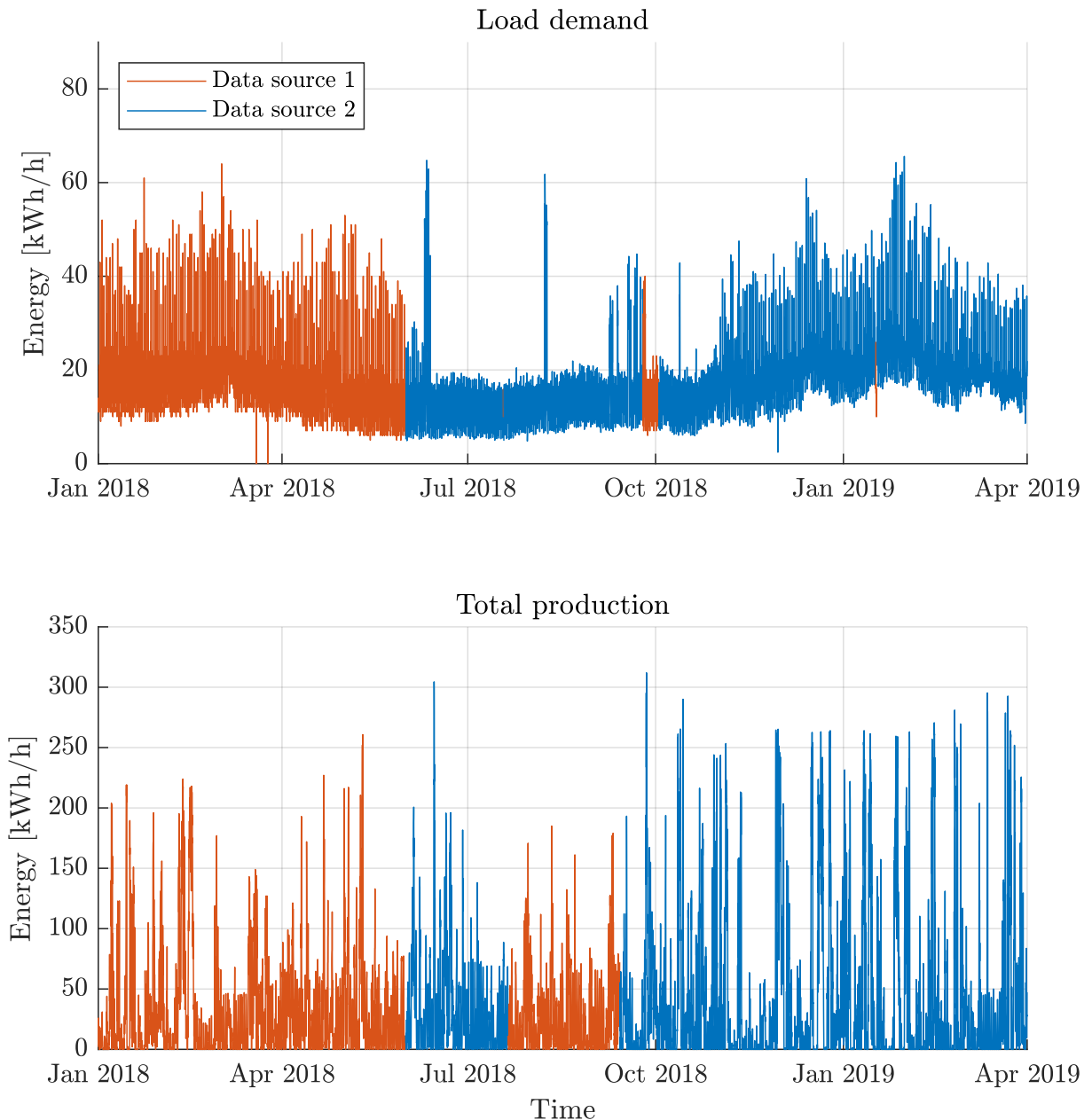
Figure 6.5.1: Plot illustrating how two different data sources are combined to get a continuous load profile for the time period 1th January 2019 to 1th April 2019.

Chapter 7

Performance results

This chapter introduces the performance results of the microgrid with respect to power production, load demand and how it behaves in different cases. Four cases are presented with an aim to investigate the effect of active load management, ESS performance and load factor. The first case acts as a reference, while active load management is implemented in the other cases with different methods applied.

The cases are based on the load demand and production in the period from 1th January 2018 to 1th of April 2019. When quantifying the results, only 2018 is considered since annual values provide the best basis for comparison.

Each case is presented in their own section with the corresponding methods and results. The main areas of focus in this chapter are listed below.

- Power production and load demand
- Effect of active load management
- ESS performance
- Load factor

The goal for the project is to achieve less than 5 % connection to the main grid. Simulations are performed in each case to test this and other parameters with different battery capacities. The planned battery capacity of 550 kWh is used as a reference for all cases.

7.1 Energy outlook

This section presents the simulation results from PVsyst and compares the annual production and demand. To be able to evaluate the performance of the microgrid, it is necessary to have access to historical data containing production and demand. This was provided by TrønderEnergi, with exception to power production from PV. Solar production had to be simulated in PVsyst, which is elaborated on detail in section 6.1.

7.1.1 Power production from PV

Monthly energy output simulated in PVsyst is presented in figure 7.1.1. Energy production per installed kWp and losses in the PV system are presented. All array losses are accounted for in "Collection loss", which are illustrated by the green parts of the bar chart. It is clear from these results that most of the losses in the PV system are due to these collection losses, while the system losses, illustrated in red, only account for a small portion. See section 3.3 for details about system and array losses.
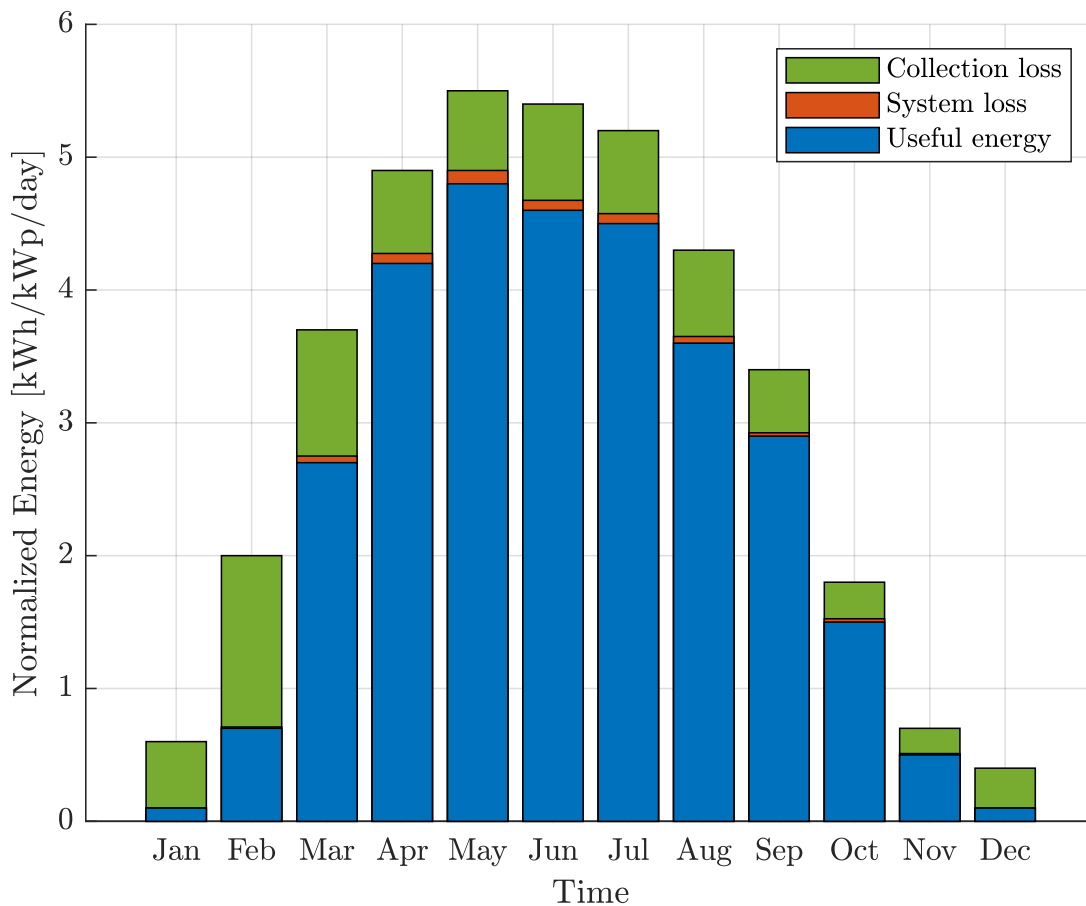
Figure 7.1.1: Solar power production per installed kWp/day. Normalized production (per installed kWp): Nominal power 86.4 kWp. Modified from original chart from simulation report found in appendix B.

Other observations from these results are that the collection loss is at its highest in February, while the system losses seems to be at its lowest in the same time period. The system losses are at its peak in the month of May. All losses taken into account, February is the month with the highest amount of losses. It should be noted that when comparing the losses to the useful energy in percent, the loss factor is greatest in January and February, due to the low power production in these months.

Table 7.1.1 presents the main results from the simulations in PVsyst. They are displayed in monthly values. The average temperature from the Meteorological Institute has also been included. The total energy from the PV system over a one year time horizon is estimated to be 80.2 MWh. It can be observed that there is a difference between the temperatures from Meteonorm, which has been used in the simulation, and the temperatures from the Meteorological Institute. The mean difference over the year is 0.51 °C.

Table 7.1.1: Main results from simulation performed in PVsyst, with comparison between temperature values from Meteonorm and Meteorological Institute.

Months	$\mathbf{T}_{Meteonorm}$ [°C]	$\mathbf{T}_{Meteorological}$ [°C]	Usable energy [MWh]
Jan	0.25	-1.23	0.15
Feb	-0.60	-3.47	1.93
Mar	1.03	-2.60	7.34
Apr	5.76	5.21	10.9
May	9.33	12.9	12.9
Jun	12.1	11.1	12.1
Jul	15.2	17.3	12.0
Aug	14.6	13.2	9.89
Sep	10.9	10.8	7.43
Oct	6.57	5.83	4.20
Nov	2.91	3.50	1.27
Dec	0.30	-0.16	0.07
Year	**6.57**	**6.02**	**80.2**

The PV system was installed and connected to the grid 8th of April. Production data for April 2019 is used for comparison. In the time period between 8th April and 29th April 2019 a total of 11.37 MWh was produced.[13] Comparing this to the simulated production it can be seen that PVsyst assumed 0.47 MWh less than the actual production in April, with a week of less production.

7.1.2   Combined wind & solar

Figure 7.1.2 displays the individual and total production from wind and solar from January 2018 to April 2019. The solar power production is simulated for one year. The resulting data is consequently used for both 2018 and 2019.

When comparing the production data it can be seen that the two DGs complement each other well. Production from wind is at its highest in the months where the PV production is low. This makes the total production fairly stable over the year. Variations can be observed between the early months of 2018 and 2019. The wind production in January 2018 is significantly lower than January 2019, while the opposite is true for February. This variation demonstrates the unpredictability of wind power production.
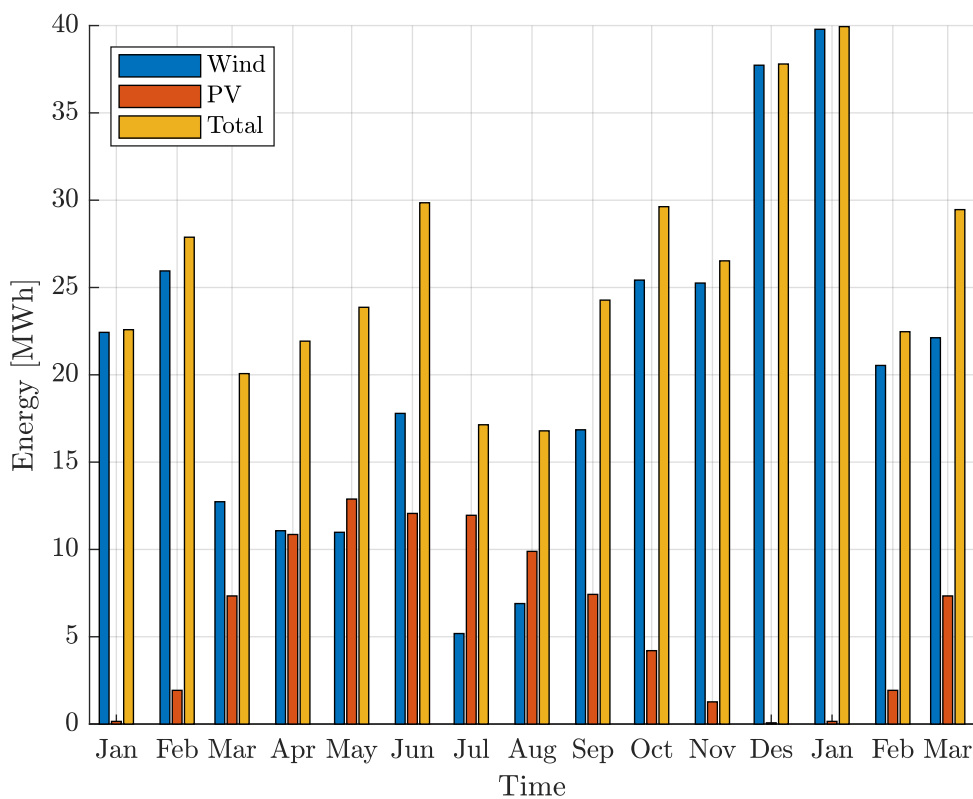
Figure 7.1.2: Power production from wind and solar compared to the total power production. The power production from wind is based on data from from January 2018 to April 2019, while PV production is based on simulated values.

7.1.3   Load demand

Table 7.1.2 presents the individual performances of the DGs, the annual total power demand and the total power production for 2018 and the first quarter of 2019. By comparing the production and demand, it can be observed that the amount of produced energy is substantially larger than the demand for both periods. This is further illustrated in figure 7.1.3.

Table 7.1.2: Overview of annual power production and energy demand. The data for 2019 is during the period from 1th January to 1th April.

Period	Solar [MWh]	Wind [MWh]	Total production [MWh]	Total demand [MWh]	Net Energy [MWh]
2018	80.2	218.3	298.3	131.0	167.4
Jan - Apr 2019	9.4	82.5	92.0	44.6	47.4
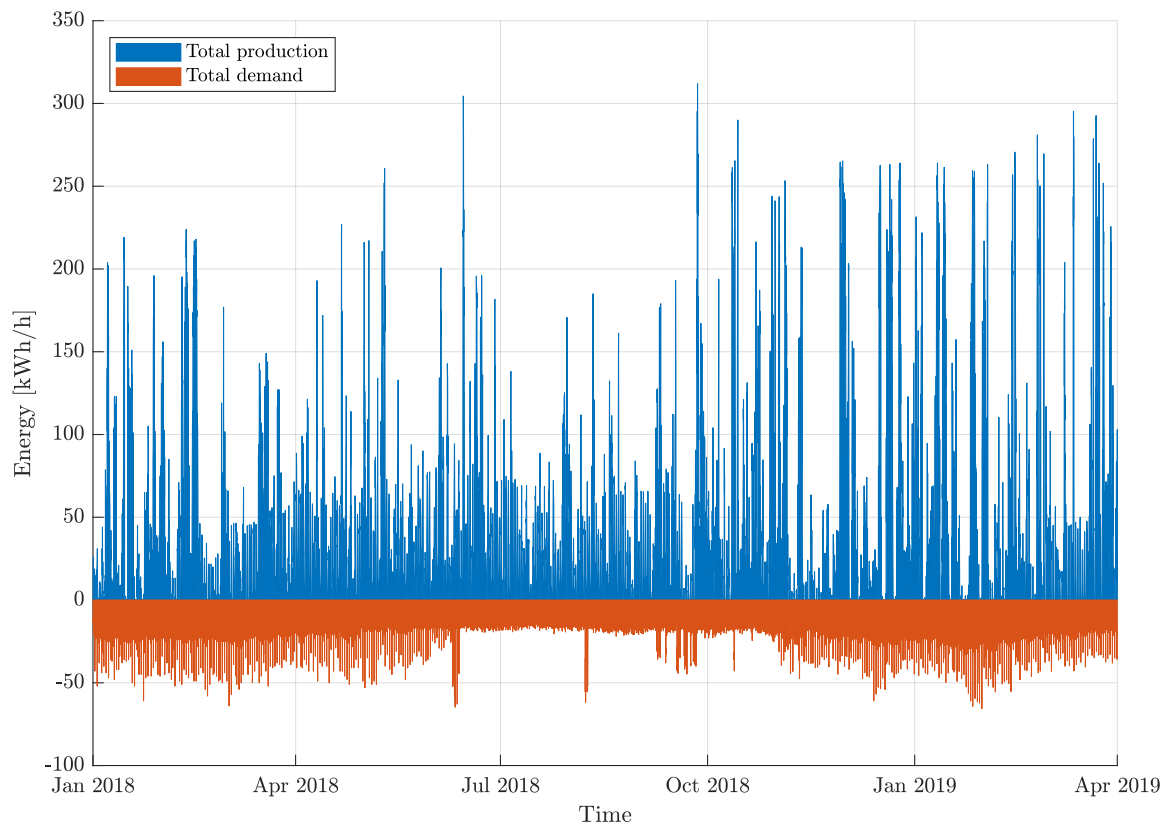
Figure 7.1.3: Plot illustrating total production and total demand for the time period 1th January 2018 - 1th April 2019. The demand is shown as negative values.

The most evident observation from figure 7.1.3 is that although the total energy production is greater than the total energy demand for many hours, there are periods where the demand is greater. It can be observed that these periods occur more often in the early and late months of the year.

7.2 Case 1

This case acts as a reference case for the other three cases, as no load management is applied. This section goes through the necessary methods regarding simulation and presents the correlating results. The goal is to apply the results from this case as a reference to the other cases. This makes ground for comparison.

7.2.1 Disconnect from grid with & without fully charged ESS

After running simulations starting with and without fully charged ESS, it is found that there is a substantial difference in how much energy that was needed from the main grid in 2018.

Table 7.2.1 display the resulting energy needed from the main grid in MWh and in percent of total demand. A difference of 1.40 MWh and 1.07 % of total energy for 2018 is found. As there is no way of knowing the ESS capacity in the beginning of future years, all simulations are performed starting with empty ESS, since this would be a worst case.

Table 7.2.1: Comparing energy needed from the main grid in 2018 with or without fully charged ESS from start of disconnection.

Fully charged ESS	Empty ESS
6.64 MWh	8.04 MWh
5.07 %	6.14 %

7.2.2 Load factor

Equation 4.1.1 is applied in each case to calculate the load factor. An illustration displaying the calculated load factor for each day is shown in figure 7.2.1. For this case, the average load factor lies at 0.485. It can be seen that the load factor differs from the summer to the rest of the time period. This is due to the absence of the silo in the summer, which reduces peak demand.

Figure 7.2.1: Illustration of the daily development of the load factor in Case 1 throughout the time period, 1th January 2018 - 1th April 2019. The average load factor is also included.

7.2.3 ESS performance

It can be observed from table 7.2.2 that with the planned battery size of 550 kWh, 6.14 % of the energy demand in 2018 has to be supplied from the main grid. This is more than the planned goal of less than 5.00 %. Further simulations are performed to investigate the battery size needed to achieve this goal, which is found to be 1.05 MWh for this case. Other simulations are also performed to investigate how independent the system could be, by increasing the battery size. The lowest percent of energy needed from the main grid in 2018 is found to be 1.10 %. In order to achieve this, a battery size of 5.30 MWh is needed.

Because of the ESS priority where the battery is discharged first, the energy from hydrogen storage decreases when increasing the battery size. The number of annual battery cycles drop substantially with an increase in battery capacity.

Table 7.2.2: Comparing ESS performance results for different battery capacities in Case 1. Results are shown for 2018. Values regarding the reference battery are marked with bold.

		2018		
Battery capacity [kWh]	Cycles [-]	Energy from grid [%]	Energy from hydrogen [MWh]	Energy throttled [%]
550	**453.1**	**6.14**	**47.2**	**35.0**
1050	237.3	4.96	36.1	38.1
5300	47.90	1.10	8.74	42.7

Battery lifetime expectancy

The lifetime expectancy for the different battery capacities are listed in table 7.2.3. It is found that the lifetime expectancy for a 550 kWh battery would be 8.80 years. This is 1.20 years less than the 10 years the reference battery is expected to have. With this method the lifetime expectancy for the largest battery is found to be 83.5 years, which is not a realistic result as it does not consider other factors.

Table 7.2.3: Life time expectancy for different battery capacities based on a expected lifetime of 10 years with 400 annual cycles in Case 1.

Battery capacity [kWh]	550	1050	5300
Lifetime expectancy [yr.]	8.80	16.9	83.5

7.3 Case 2

This case is based on a statistical method to define flexible loads. The objective is to investigate the validity of using statistics for defining flexible loads by comparing it to the other cases. This section elaborates on this method of load classification and the results of implementing ALM with this method.

7.3.1 Defining extreme values & time limit

A method applying quartiles is used to detect extreme values in the historic demand data. These extremals are defined as outliers, which are then characterized as flexible loads. This method defines an outlier as a value larger than 1.5 times the interquartile range (Q_{Inter}) above the third quartile (Q_3). This can be applied to find a lower bound as well, using the first quartile (Q_1), but since the energy consumption never reaches negative values, the lower bound has been manually set to zero. An illustration of the method is displayed in figure 7.3.1.

To increase the validity of this method, an upper bound is calculated iteratively for each week. This is done to adequately detect outliers within a timeframe where trends do not change too much. This means that if there is a value above the upper bound within a given week, it is classified as flexible and can be shifted. The time limit for when a load can be shifted is set to 24 hours in this case.
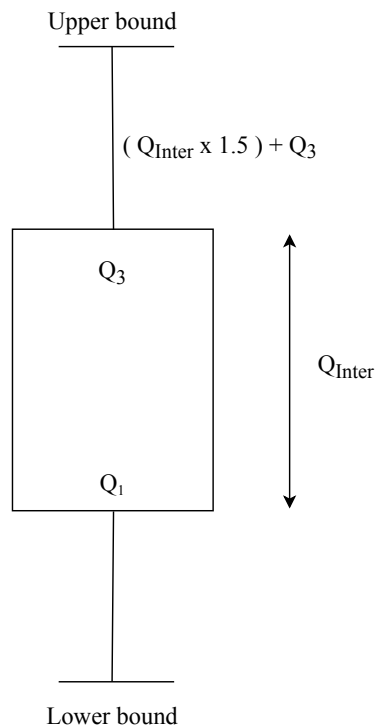
Figure 7.3.1: Illustration of method applied to calculate an upper bound, using the interquartile range (Q_{Inter}) and third quartile (Q_3).

7.3.2 The effect of active load management

Figure 7.3.2 illustrates a comparison of the load profile before and after implementing the ALM algorithm. It also displays the amount of shifted load in the lowermost plot. A great amount of the larger peaks above the upper bound is shifted to periods within the set time limit, without affecting the base load. It can be observed that new peaks are created. This is due to sufficient capacity at the hour of the new peak. An example of this occurrence can be seen in October 2018. Most of the shifting occurs in the early and late months of the year. This corresponds well with the usage pattern of the silo, as elaborated on in section 5.1.
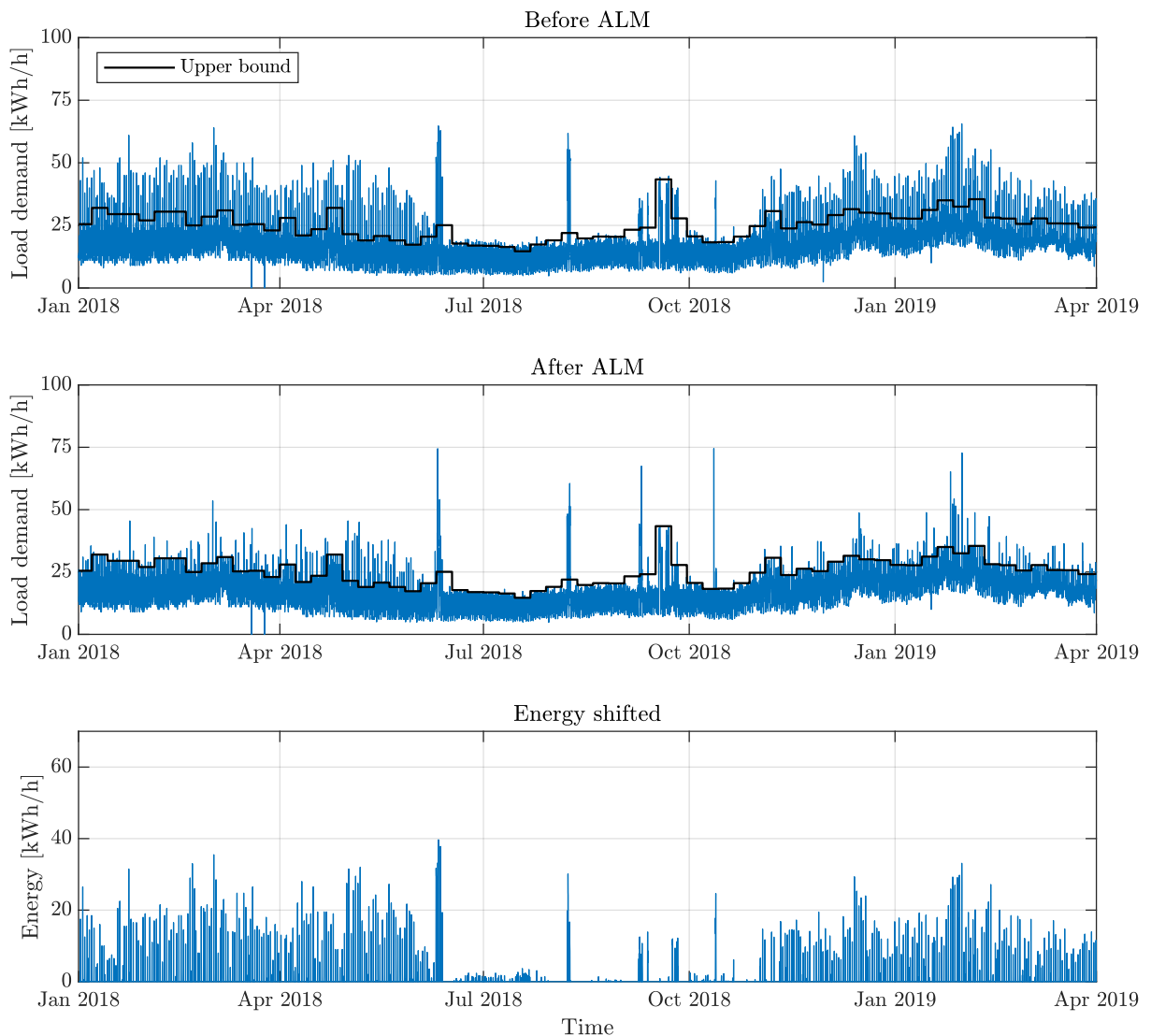
Figure 7.3.2: Plot illustrating the effect of active load management in Case 2, for the time period 1th January 2018 - 1th April 2019. The lowermost plot illustrates the amount of shifted energy.

Table 7.3.1 quantifies the effect of the ALM algorithm. It illustrates the amount of shifted load and the shifted load in percent of the total demand. With the applied method, 5.14 MWh is shifted for 2018. Compared to the total demand, this value makes up 3.92 %.

Table 7.3.1: Results from implementing active load management in Case 2.

Period	2018
Total flexible load [MWh]	5.54
Total shifted load [MWh]	5.14
Percentage shifted of total demand [%]	3.92

Load factor

Figure 7.3.3 illustrates the daily load factor for Case 2. The average load factor is 0.577. It can be observed that it does not vary much, with exception to the time period between April to June in 2018 where the load factor is low. This is due to the small amount of shifted load and a new peak load in the same time period. This can be seen in figure 7.3.2. The reason for the low variation is that every extreme value, which is classified as flexible, is shifted to periods with sufficient capacity. After this is accomplished, the remaining flexible load is distributed to times with the least demand, as elaborated on in section 6.3. Another observation is that there is two occurrences where the load factor reaches below 0.3. If figure 7.3.2 is studied it can be seen that larger peaks have been created after load shifting for the same periods, and thus decreasing the load factor.
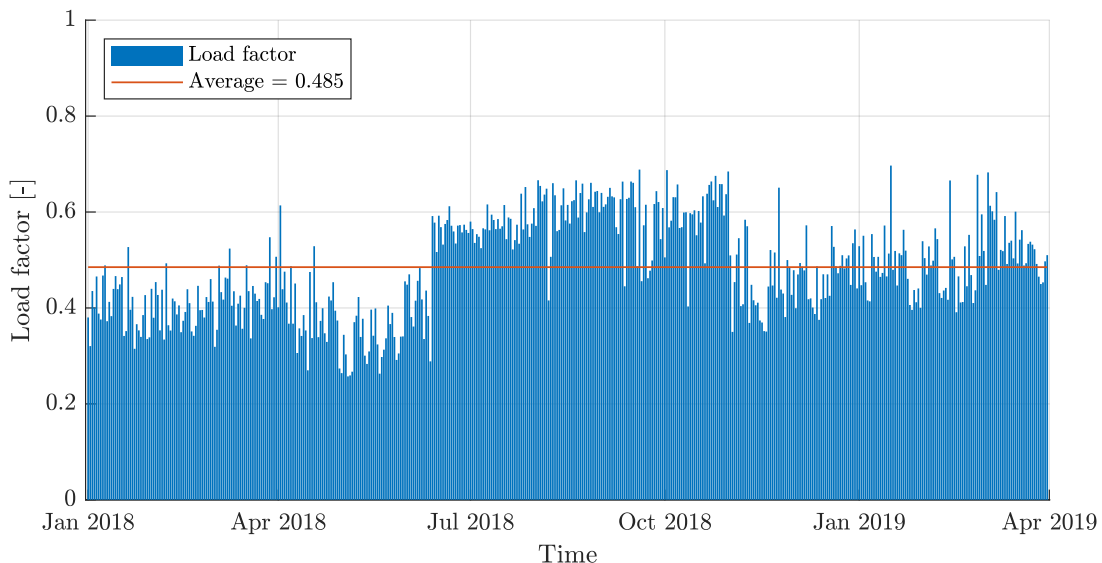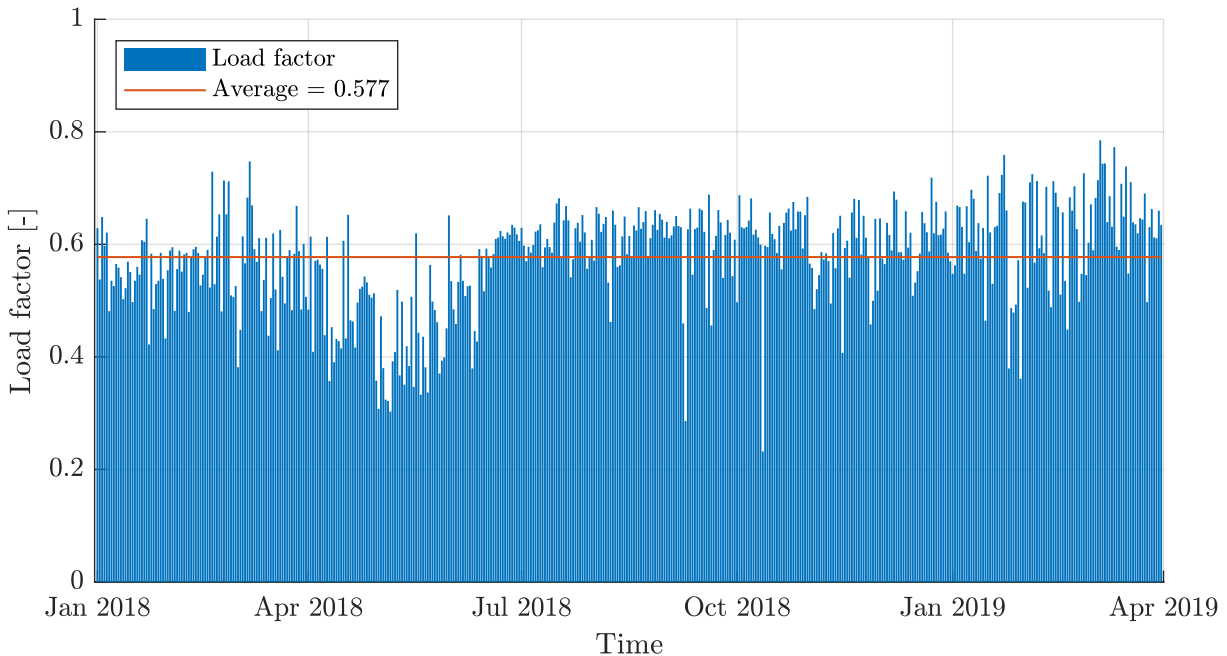

Figure 7.3.3: Illustration of the daily development of the load factor in Case 2 throughout the time period, 1th January 2018 - 1th April 2019. The average load factor is also included.

7.3.3 ESS performance

In this case it is found that by applying ALM this would decrease the amount of energy needed from the grid from 6.14 % to 5.97 %, with the planned battery capacity (550 kWh) for 2018. The battery capacity could be downsized to 500 kWh without exceeding the energy needed from the main grid, compared to the reference case.

Further simulations were performed to investigate the battery capacity needed to achieve less than 5.00 % connection to the main grid, and as low as possible. It is found that a capacity of 1.00 MWh is needed to reach 4.90 % energy needed form main grid while a capacity of 5.10 MWh is needed to reach the lowest possible percentage of 1.04 % energy needed from main grid.

The number of battery cycles decrease with an increase in battery capacity. But compared to Case 1, the number of cycles decrease by 11.4 cycles in 2018 with a capacity of 550 kWh. The new lifetime expectancies are calculated and compared in section 8.1. The results are found in table 7.3.2.

Table 7.3.2: Comparing ESS performance results for different battery capacities in Case 2. Results are shown for 2018. Values regarding the reference battery are marked with bold.

2018				
Battery capacity [kWh]	Cycles [-]	Energy from grid [%]	Energy from hydrogen [MWh]	Energy throttled [%]
500	485.8	6.11	47.6	35.2
550	**441.7**	**5.97**	**46.2**	**35.5**
1000	242.9	4.90	36.2	38.3
5100	47.60	1.04	8.62	43.0

Figure 7.3.4 illustrates the status of the hydrogen storage for different battery capacities for the whole time period. The difference of energy between the respective battery capacities is also included. With a decrease in battery capacity the energy from hydrogen storage increases. It can be observed in the figure that more of the hydrogen storage capacity is used, especially in the early and late months of the year. The first subplot reveals that in February 2018, the effect of downsizing the battery capacity leads to a total discharge of the hydrogen storage capacity. As a consequence, more energy is needed from the main grid. This can be seen, as all bottom points are decreased and more energy is needed from the main grid when the hydrogen storage status is at 0 %. Another observation is that there is a large amount of unused hydrogen capacity, especially in the time period between June and August where no energy from hydrogen storage is used.

Figure 7.3.4: Comparison of the hydrogen storage capacity status for a battery storage capacity of 500 kWh and 550 kWh, and the difference of utilized energy from hydrogen storage between the two in Case 2. Negative values in the lowermost plot illustrate the extra energy utilized from hydrogen storage with the smaller battery.

Battery lifetime expectancy

The lifetime expectancy for the different battery capacities is listed in table 7.3.3. It is found that the lifetime expectancy for a 550 kWh battery would be 9.06 years. This is 0.26 years more than the 8.80 years found in the reference case, for the same battery capacity. The lifetime expectancy for the largest battery is found to be 84.03 years, which is not a realistic result as it does not consider other factors.

Table 7.3.3: Lifetime expectancy for different battery capacities based on a expected lifetime of 10 years with 400 annual cycles in Case 2.

Battery capacity [kWh]	500	550	1000	5100
Lifetime expectancy [yr.]	8.23	9.06	16.47	84.03

7.4 Case 3

The objective of this case is to implement ALM on all the loads classified as flexible and power shiftable in section 5.1. Load shifting of water heaters, dishwashers, washing machines and the silo is performed. Energy reduction of lighting and Telenor is also implemented. ALM is performed with a priority order where energy conservation is the first priority. The second priority is shifting of the biggest loads. Because the silo is the largest flexible load and can not be partitioned, it has the highest priority. The following order is applied:

1. Telenor and lighting

2. Silo

3. Water heater east

4. Water heater mastu

5. Dishwashers

6. Washing machines

Because of limitations on detailed historical data, a load profile is generated for the silo. This is achieved by using statistics in similar fashion as described in section 7.3.1. By applying this method on the already existing load profile for the total demand, the hours of operation was found. These time periods and the average consumption of the silo is used to make up the new load profile. The average consumption was used for the period without historical data because the exact load demand is unknown. The exception is the peak in August 2018. Because it is easy to read the load demand at that hour, a value of 20 kWh/h was set. The completed load profile consists of the average values, the 20 kWh/h peak and measurements from eGauge. This is illustrated in appendix A.

The energy consumption of the water heaters is based on standardized values, elaborated on in section 4.4, and the area of the respective apartment, introduced in section 5.1. Since the east apartment has the largest area compared to the mastu, its water heater has the largest energy consumption and, consequently, has a higher priority. When applying the standard on the cowsheds, the energy consumption exceeds the power rating of the water heaters and give unrealistic values for lightning at the respective locations, and is consequently neglected. When applying ALM, the power ratings in table 5.1.2, 5.1.3 and table 5.1.4 were set as maximum limits. This was done in order to ensure that the energy consumption after shifting never exceeded the respective appliance's power rating.

The starting times of the dishwashers and washing machines are based on the probability data elaborated on in section 4.4. The dishwashers are assumed to operate once every day, with starting time at 17:00 on weekdays and 20:00 at weekends. The washing machines are assumed to operate 4 times a week with the configuration shown in table 7.4.1. The appliances in the mastu only takes effect from the beginning of 2019 as it was uninhabited in 2018. All load profiles made and used are illustrated in appendix A.

Table 7.4.1: Usage pattern for the washing machines. The days the respective washing machine is considered to be used are marked.

	Monday	Tuesday	Wednesday	Thursday	Friday	Saturday	Sunday
Main apartment	x			x	x		x
East apartment				x	x	x	x
Mastu			x	x	x		x

7.4.1   The effect of active load management

Figure 7.4.1 displays the load profile before and after active load management is implemented. To further illustrate the effect of ALM, a plot presenting how much energy that is conserved and shifted is included. It can be observed that the amount shifted is greatest during the start and end of the year. This is due to the operation of the silo and the larger amount of production during these periods. In August 2018 there is a peak at approximately 60 kWh. It is found that roughly 20 kWh is shifted from the evening to an earlier part of that day. Another observation is the reduction in base load. This is due to the energy conservation-strategy, where lights have been reduced by 20 % and Telenor by 100 %. This is apparent in the plot illustrating the energy conserved and shifted, because of the 2.1 kWh minimum, which is the sum of Telenor and lighting. It can also be observed that there are several occurrences in the summer where the demand is zero. This is due to the inaccuracy of the standards applied in this case.

Figure 7.4.1: Plot presenting the effect of active load management in Case 3, for the time period 1th January 2018 - 1th April 2019. The lowermost plot illustrates the amount of conserved and shifted energy.

Table 7.4.2 quantifies the effect of the ALM algorithm. It illustrates the amount of shifted and reduced load, and the shifted load in percent of the total demand. With the applied method, 15.3 MWh is shifted for 2018. Compared to the total demand, this makes up 11.7 %. The amount of reduced energy is 17.8 MWh for 2018. It can be detected that the amount reduced is greater than the amount shifted.

Table 7.4.2: Results from implementing the load shift algorithm in Case 3.

Period	2018
Total flexible load [MWh]	22.3
Total shifted load [MWh]	15.3
Percentage shifted of total demand [%]	11.7
Energy reduction [MWh]	17.8
Percentage reduced of total demand [%]	13.6

Load factor

Figure 7.4.2 displays the daily development of load factor in this case. It can be seen that the average load factor is calculated to be 0.489. The overall trend is a higher load factor during the summer compared to the rest of the timer period.

Figure 7.4.2: Illustration of the daily development of the load factor in Case 3 throughout the time period, 1th January 2018 - 1th April 2019. The average load factor is also included.

7.4.2   ESS performance

With the previously mentioned load shifting criteria, this case results in a decrease of 1.96 % in energy needed from the main grid with the planned battery size, compared to the reference case. Here, the goal of under 5.00 % energy needed from the main grid is achieved with a battery capacity down to 320 kWh. It is also found that the capacity can be decreased to 110 kWh without exceeding the energy needed from the main grid compared to the reference battery in the reference case. The lowest percentage of grid connection was found to be 1.00 % with a battery capacity of 3.00 MWh.

A decrease of 14.57 battery cycles, compared to the reference case, is achieved with a battery capacity of 550 kWh. With the decrease in battery capacity to 110 kWh, the annual cycles increase dramatically.

As the energy needed from the main grid decreases with larger battery capacities, the throttled energy increases. Comparing the amount of throttled energy in this case to the reference case, it is found that 7.84 % more energy is being throttled with the 550 kWh battery in this case. All the mentioned results are found in table 7.4.3.

Table 7.4.3: Comparing ESS performance results for different battery capacities in Case 3. Results are shown for 2018. Values regarding the reference battery are marked with bold.

2018				
Battery capacity [kWh]	Cycles [-]	Energy from grid [%]	Energy from hydrogen [MWh]	Energy throttled [%]
110	2193	6.11	59.9	36.2
320	753.7	4.96	42.0	41.3
550	**438.5**	**4.18**	**35.4**	**42.9**
3000	80.40	1.00	10.5	48.8

The hydrogen storage capacity is utilized in a much larger extent when decreasing the battery capacity. This results in more energy needed from the main grid. Figure 7.4.3 illustrates this as it can be observed that more of the previously unused capacity is utilized. Despite this, there is still a lot of unused capacity, especially in the period April to September 2018. This is due to the low load demand during the summer months. See figure 7.1.3 for a comparison of total production and load demand.
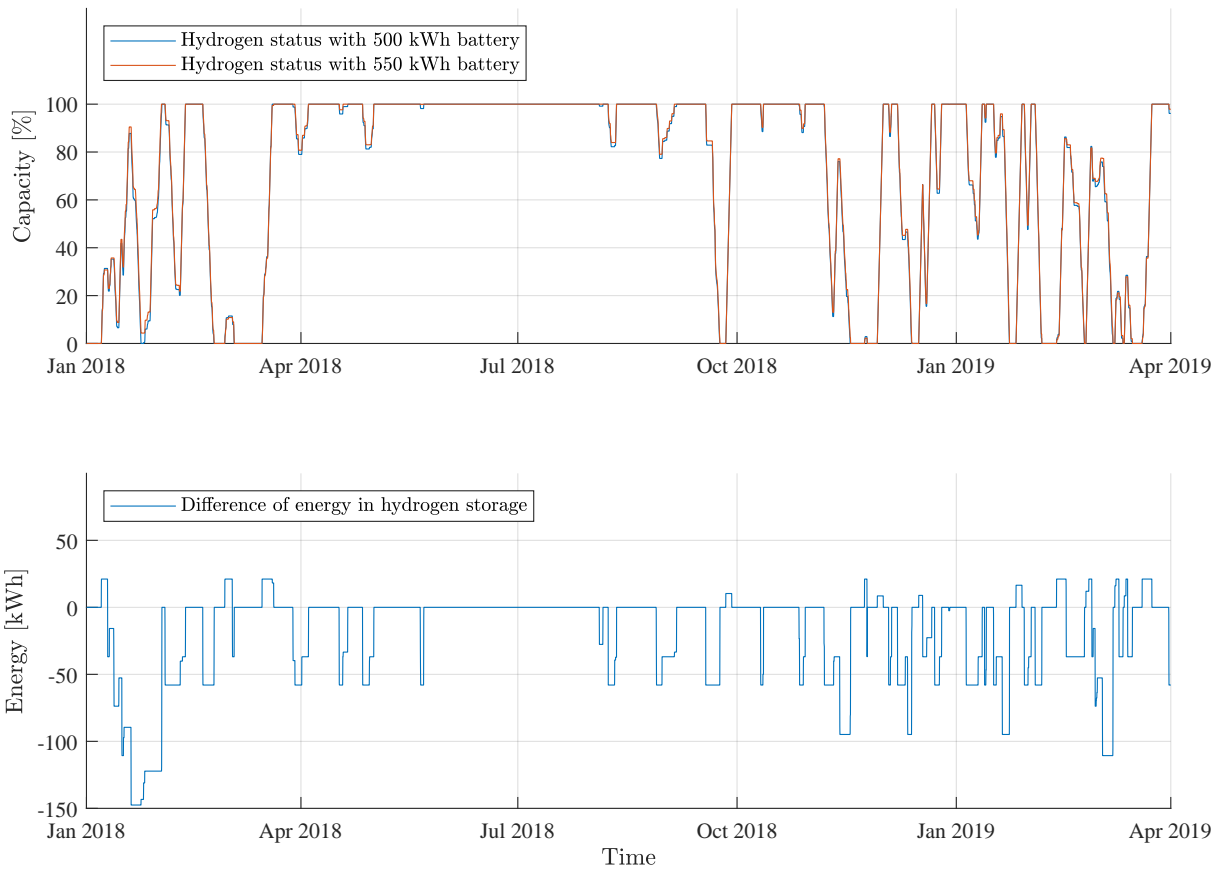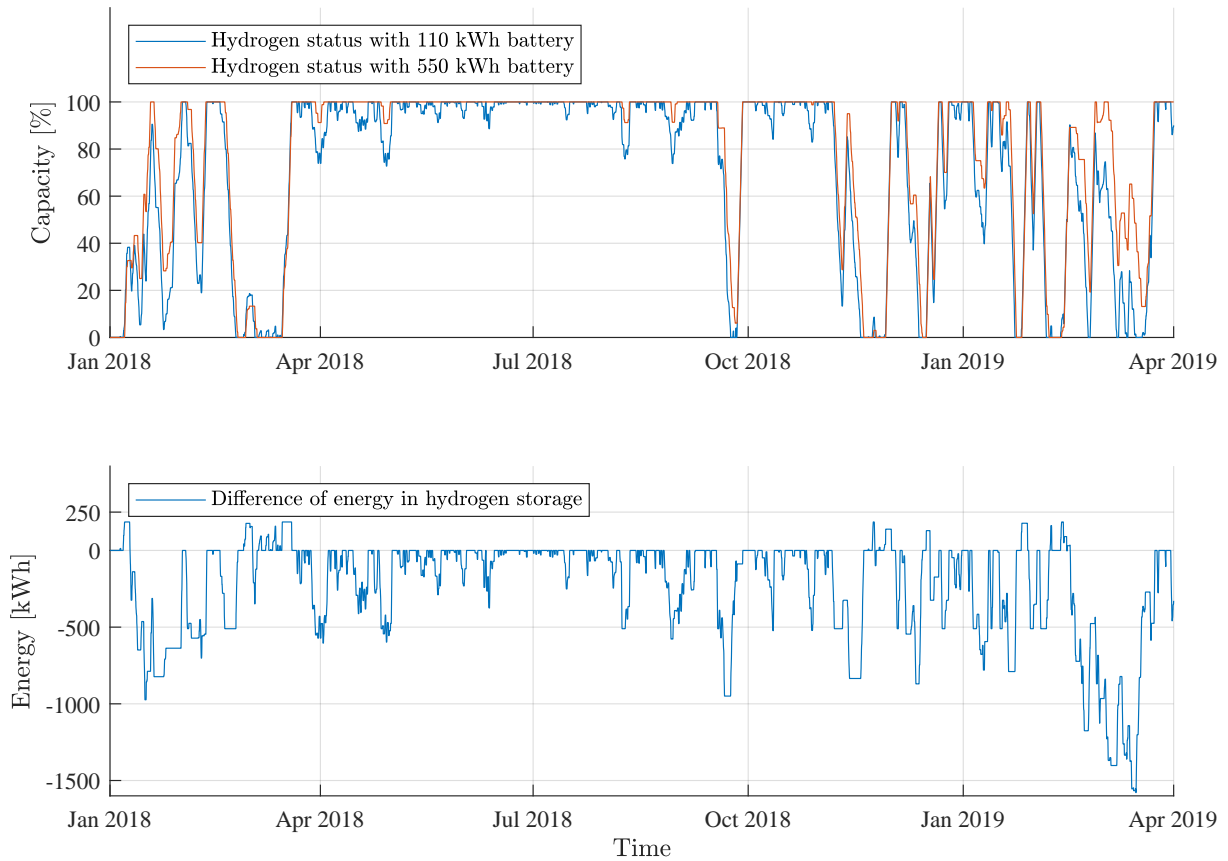
Figure 7.4.3: Comparison of the hydrogen storage capacity status for a battery storage capacity of 110 kWh and 550 kWh, and the difference of utilized energy from hydrogen storage between the two in Case 3. Negative values in the lowermost plot illustrates the extra energy utilized from hydrogen storage with the smaller battery.

Battery lifetime expectancy

The lifetime expectancy for the different battery capacities based on load demand and production data for 2018 is listed in table 7.4.4. It is found that the lifetime expectancy for a 550 kWh battery would be 9.12 years. This is 0.32 years more than the 8.80 years found in the reference case, for the same battery capacity. The lifetime expectancy for the largest battery is found to be 49.75 years, which is not a realistic result as it does not consider other factors.

Table 7.4.4: Lifetime expectancy for different battery capacities based on a expected lifetime of 10 years with 400 annual cycles in Case 3.

Battery capacity [kWh]	110	320	550	3000
Lifetime expectancy [yr.]	1.82	5.31	9.12	49.75

7.5   Case 4

This case is made to be the most conservative of the four cases. The goal is to investigate the effect of implementing ALM when only the most certain of the flexible loads are subject to ALM. The loads considered in this case are the silo, apartment lights and Telenor. The priority order in this case is that the energy consumption of apartment lights are reduced by 20 % from standardized values, while Telenor is removed entirely. Then, the silo is shifted according to the ALM algorithm elaborated on in section 6.3. As the load of the silo can not be partitioned throughout the day, a criterion for the shift to take place is that the maximum capacity is great enough to cover the whole load.

7.5.1   The effect of active load management

Figure 7.5.1 presents a comparison of the load profile before and after the implementation of ALM. An illustration of the shifted and conserved energy is also included. By studying the figure, it can be observed that the base load is lessened because of the energy reduction of lights and Telenor, which is apparent in the lowermost plot. It can also be observed that some of the peaks have been shifted. An example of this is the peak at roughly 60 kWh in the middle of August 2018 being shifted and reduced to about 50 kWh.
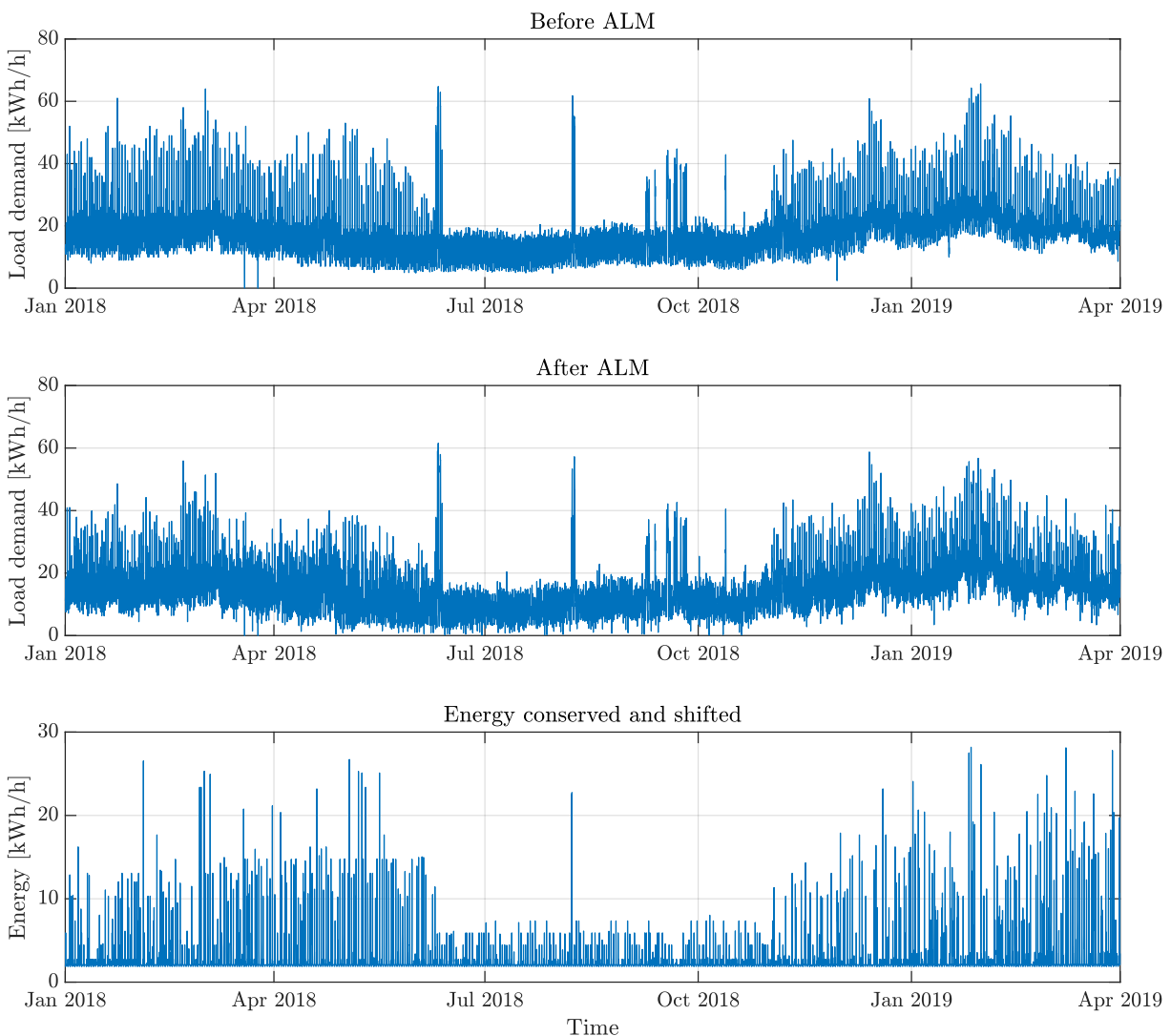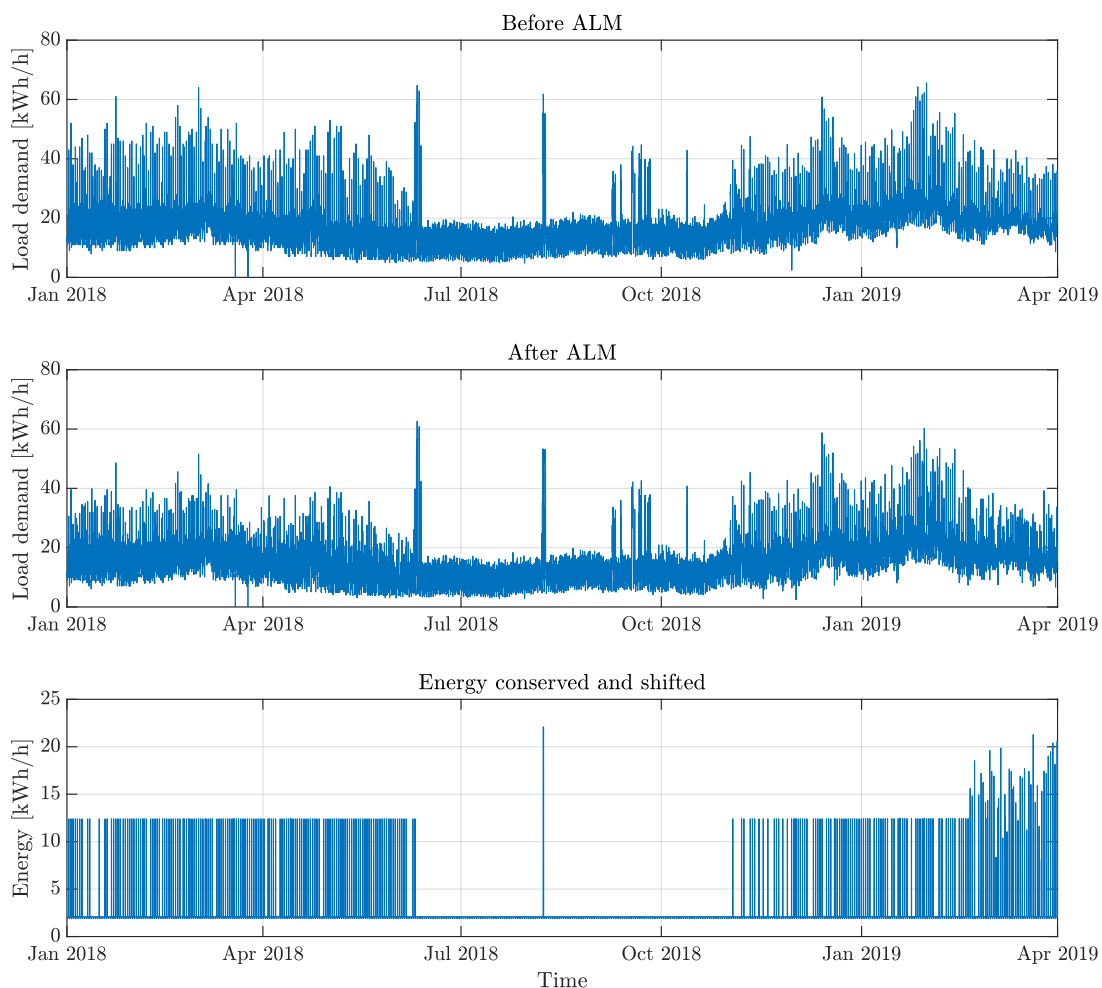

Figure 7.5.1: Plot illustrating the effect of active load management in Case 4, for the time period 1th January 2018 - 1th April 2019. The lowermost plot illustrates the amount of conserved and shifted energy.

The main results from applying ALM in this case are illustrated in table 7.5.1. It can be seen that 2.54 MWh is shifted for 2018. This makes up 1.93 % of the total demand. An energy reduction of 17.8 MWh for 2018 is also presented.

Table 7.5.1: Results from implementing ALM in Case 4.

Period	2018
Total flexible load [MWh]	2.95
Total shifted load [MWh]	2.54
Percentage shifted of total demand [%]	1.93
Energy reduction [MWh]	17.8
Percentage reduced of total demand [%]	13.6

Load factor

Figure 7.5.2 presents the daily development of load factor throughout the regarded time period. It illustrates that the average load factor is 0.490. It can be seen that the load factor is higher during the summer periods, while it is both lower and varies more during the rest of the time period.
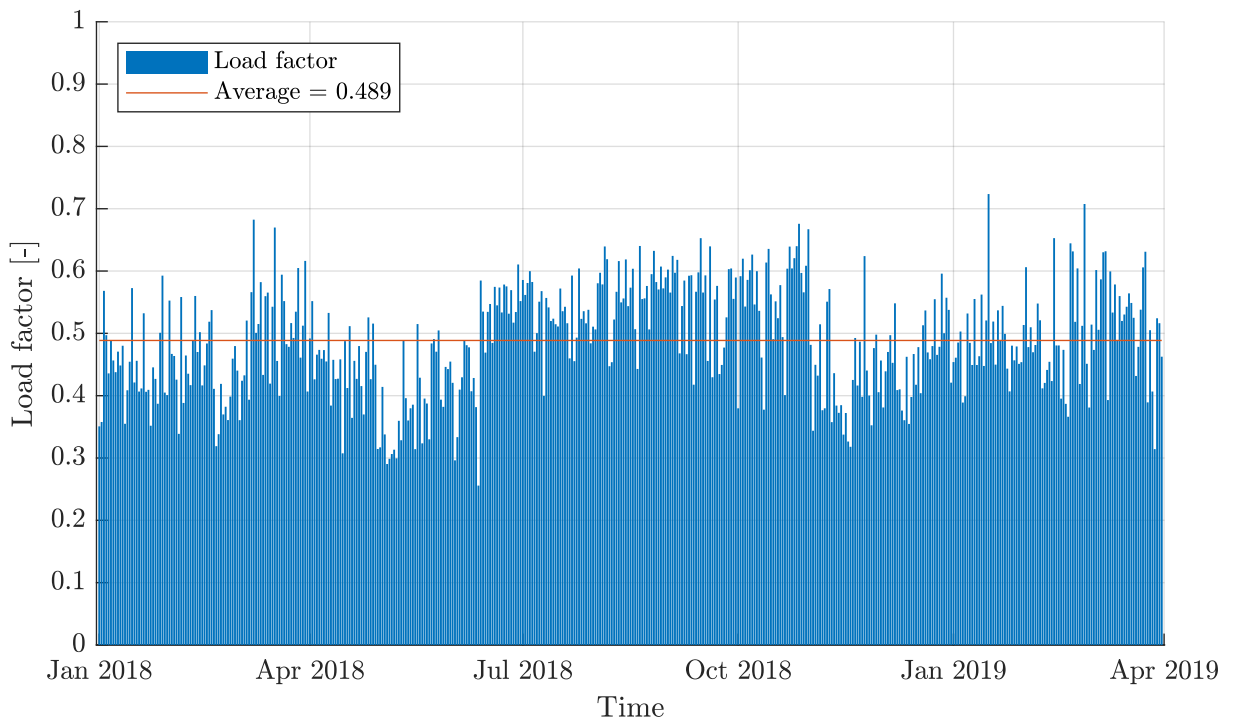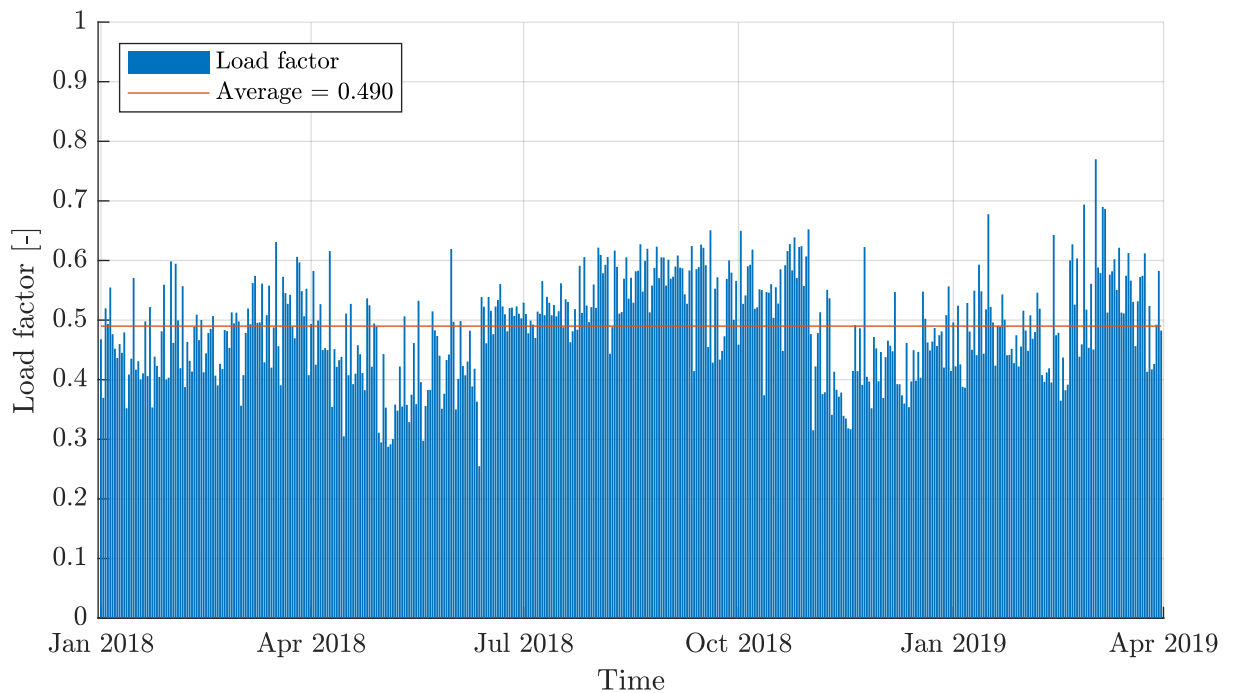

Figure 7.5.2: Illustration of the daily development of the load factor in Case 4 throughout the time period, 1th January 2018 - 1th April 2019. The average load factor is also included.

7.5.2　ESS performance

Compared to the 550 kWh battery in the reference case, the results from this case reveal a possible downsize of the battery capacity to 530 kWh without increasing the energy needed from the main grid for 2018. The results also show that a battery with 550 kWh capacity results in less energy from the main grid than the battery with the same capacity in the reference case. In order to achieve the goal of less than 5.00 % connection to the main grid, a battery capacity of 1.02 MWh would be necessary. The lowest percentage of connection (1.06 %) was achieved with a 5.20 MWh battery.

The effect of load management in this case would lead to a decrease of 5.73 cycles in 2018 with the reference battery. Decreasing the battery capacity to 530 kWh would lead to 11.2 more cycles in 2018.

The throttled energy increases with higher battery capacities. Throttled energy in 2018, applying the reference battery, increased by 0.200 % compared to the reference case. With a battery capacity of 530 kWh, the throttled energy increased by 0.08 %. All results from the ESS performance in this case are listed in table 7.5.2.

Table 7.5.2: Comparing ESS performance results for different battery capacities in Case 4. Results are shown for 2018. Values regarding the reference battery are marked with bold.

2018				
Battery capacity [kWh]	Cycles [-]	Energy from grid [%]	Energy from hydrogen [MWh]	Energy throttled [%]
530	464.2	6.13	47.3	35.1
550	**447.4**	**6.08**	**46.7**	**35.2**
1020	241.2	4.97	36.3	38.2
5200	47.30	1.06	8.60	42.8

Comparing the hydrogen storage status for the 530 kWh and 550 kWh battery it can be observed from figure 7.5.3 that there is a very small difference in energy from hydrogen storage because of the slight difference in capacity. The trend is the same as for the other cases, where there is a lot of unused capacity, especially in the summer months.
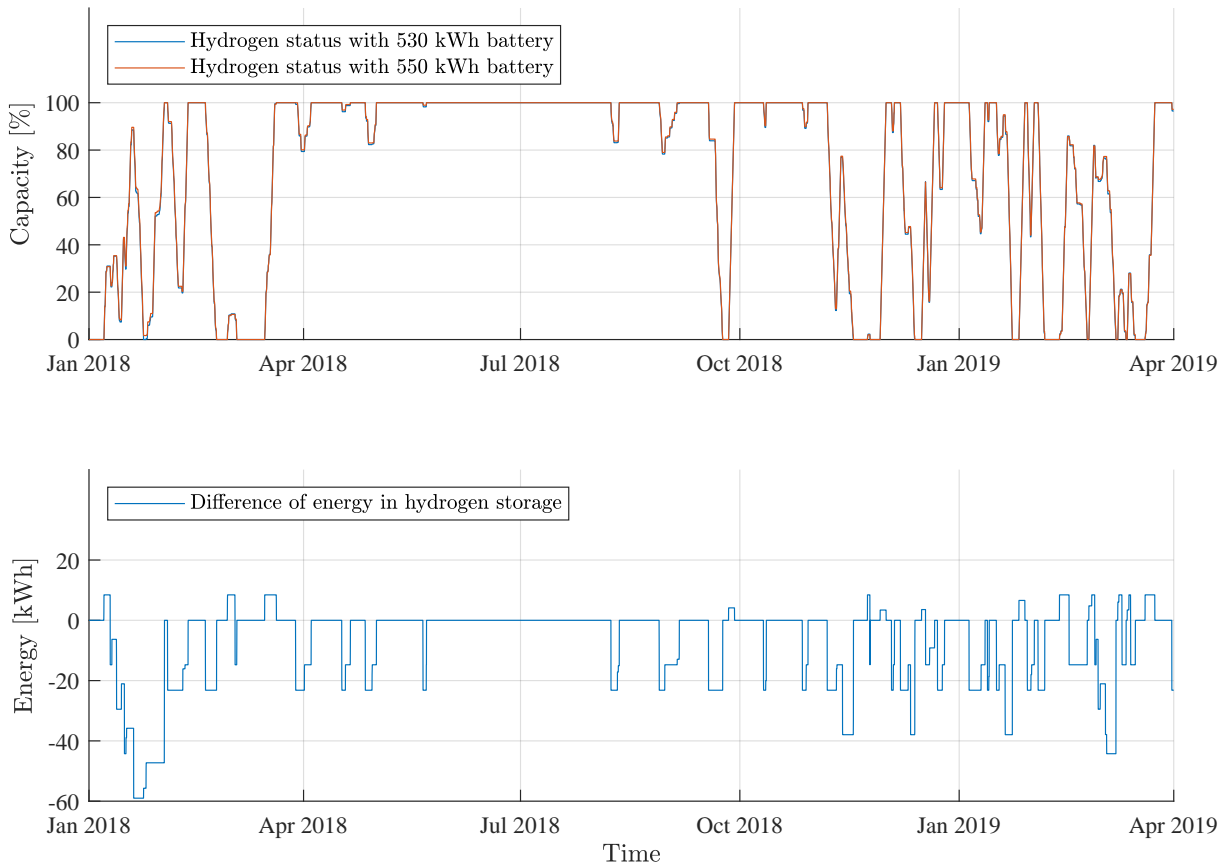
Figure 7.5.3: Comparison of the hydrogen storage capacity status for a battery storage capacity of 530 kWh and 550 kWh, and the difference of utilized energy from hydrogen storage between the two in Case 4. Negative values in the lowermost plot illustrates the extra energy utilized from hydrogen storage with the smaller battery.

Battery lifetime expectancy

The lifetime expectancy for the different battery capacities based on load demand and production data for 2018 is listed in table 7.5.3. It is found that the lifetime expectancy for a 550 kWh battery would be 8.94 years. This is 0.14 years more than the 8.80 years found in the reference case, for the same battery capacity. The lifetime expectancy for the largest battery is found to be 84.57 years, which is not a realistic result as it does not consider other factors.

Table 7.5.3: Lifetime expectancy for different battery capacities based on a expected lifetime of 10 years with 400 annual cycles in Case 4.

Battery capacity [kWh]	530	550	1020	5200
Lifetime expectancy [yr.]	8.62	8.94	16.58	84.57

Chapter 8

Evaluation of procedures & results

This chapter evaluates the procedures and results that are of importance to the objectives of this thesis. First, a case comparison is presented before the reliability & choice of methods are reviewed.

8.1 Case comparison

This section presents a comparison between the different cases, in regards to the effect of active load management, ESS performance and load factor.

Figure 8.1.1 illustrates a comparison of the effect of ALM in the different cases. It can be observed that the amount of reduced load is the same for Case 3 and 4, which is because lights and Telenor are reduced in both cases. Furthermore, it is found that the case with the most shifted load is Case 3 (11.7 %). The case with the least amount shifted is Case 4 (1.9 %), while 3.9 % was shifted in Case 2.
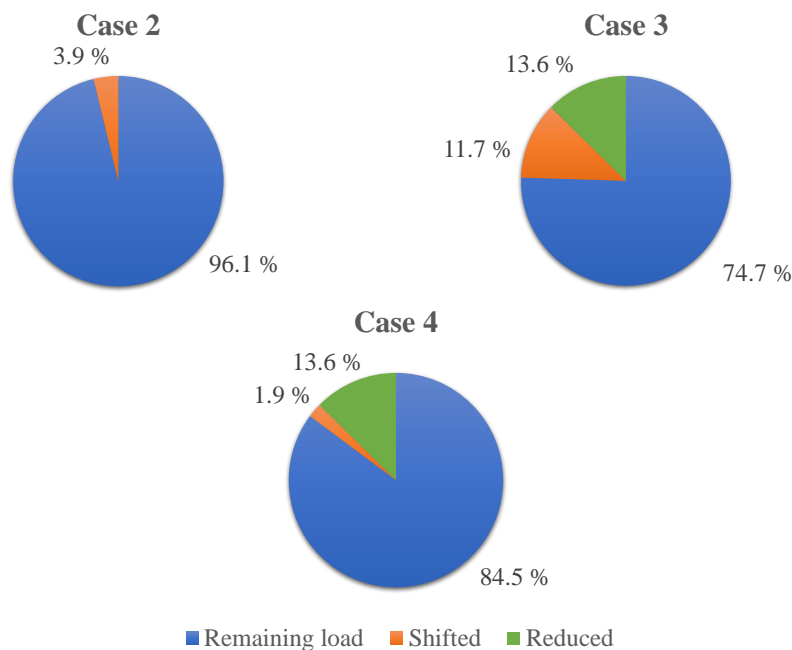
Figure 8.1.1: Comparison of the portion of shifted and reduced load in each respective case for 2018.

A greater amount was shifted in Case 3 than Case 4, which can be seen in figure 8.1.1. This is because of what is regarded as flexible loads in the cases. It is possible that Case 4 represents the minimum amount that could be shifted, while Case 3 may represent the maximum. If the total energy consumption of the flexible loads in the standard is inaccurate, then a more representative result may be somewhere between Cases 3 and 4.

Comparison of ESS performance

In order to observe the effects of active load management in each case, a comparison of the ESS performance based on the reference battery is listed in table 8.1.1. From these results it can be observed that Case 3 has the highest reduction in energy needed from the main grid at 1.96 %, compared to Case 1. Case 4, which is considered as the most conservative case, has a decline of 0.06 % compared to Case 1. Also, it can be observed that the difference between Case 1 and Case 2 is 0.17 %.

Table 8.1.1: Comparing the ESS performance results for each case based on the reference battery.

Results	Case 1	Case 2	Case 3	Case 4
Energy from grid main [%]	6.14	5.97	4.18	6.08
Energy from hydrogen [MWh]	47.18	46.17	35.41	46.73
Throttled energy [%]	35.04	35.50	42.88	35.24
Battery lifetime expectancy [yr.]	8.83	9.10	9.12	8.94

The results from each case reveal that the energy needed from the main grid decreases when implementing ALM. Although, less than 5 % connection to the main grid is only achieved in Case 3. If load measurements on a component level were available, the amount of shifted load could be close to the 12 % obtained in Case 3 in reality. If that is assumed, the effect of ALM would decrease the energy needed from the main grid by more than 2 %, thus achieving the goal of less than 5 % grid connection. It can also be observed that the energy from hydrogen decreases in each case without changing the battery capacity. This is as expected since energy from the main grid is only used when the hydrogen capacity is at 0 %.

The amount of throttled energy increases as the energy from the main grid decreases. This was first not expected, and it is hard to pinpoint the exact reason for this, but less energy is used from the battery and hydrogen storage after the demand has been shifted to more ideal periods. This would mean that less net energy would be needed to keep both the battery and hydrogen at 100 % capacity, which could lead to more energy being throttled. In the case of operating the microgrid in island mode, more throttled energy could just be seen as a waste of resources. On the other hand, if was possible to sell excess energy back to the main grid, this would be ideal. This is because ALM is found to increase the amount of throttled energy and decreases the need for grid connection. Another solution could be to store more of this excess energy in the form of hydrogen gas in a separate storage unit, which could be sold or used for other purposes.

The battery lifetime expectancy does not differ greatly between the cases. It can be observed that implementing ALM increases the expected lifetime for all four cases. By comparing Cases 2 and 3, a difference of 0.02 years can be seen. This is interesting, as the amount of shifted load is significantly greater in Case 3. This indicates that the load shifting does not have a big impact on the lifetime, as the number of cycles do not differ greatly. This is elaborated on Chapter 7. A possible reason for this is the more efficient utilization of the energy production. In other words, every time a load is shifted, this demand may be covered by the production instead of the main grid, battery or hydrogen storage. As a result, the lifetime stays more or less the same, while the energy needed from the main grid decreases.

Effect of energy conservation on ESS performance

Another observation is that the energy reduction in Cases 3 and 4 does not appear to have an impact on the energy needed from the main grid. The same can be seen for the amount of throttled energy. Cases 3 and 4 have the same amount of reduced energy while there is a 1.90 % difference in energy from grid. Comparing Cases 2 and 4, the difference in energy needed from the main grid is only 0.11 %. This is interesting due to the fact that energy conservation is only applied in Case 4. This implies that it is the load shifting that have the most apparent effect on the amount of energy needed from the main grid. Simulations have been performed to back up this assumption.

By intuition, a 13.6 % reduction would have a greater impact on energy needed from the main grid. Although, this is not the case. A reason for this could be that the reduction always leads to a lower load demand, but does not necessarily result in a positive net capacity.

The effect of downsizing battery capacity

The main goal for this thesis is to investigate the possibility of downsizing the battery capacity without exceeding the energy needed from the main grid compared to Case 1. The lowest achieved battery capacity for each case is compared with their respective ESS performance results in table 8.1.2.

Table 8.1.2: Comparing the ESS performance results based on the lowest battery capacities possible without exceeding the 6.14 % energy needed from the main grid simulated in Case 1. For Case 3, the capacity for reaching the goal of the project is also included.

Results	Case 1	Case 2	Case 3	Case 4
Lowest battery capacity [kWh]	550	500	110 / 320	530
Energy from grid [%]	6.14	6.11	6.11 / 4.96	6.13
Energy from hydrogen [MWh]	47.18	47.59	59.87 / 42.02	47.28
Throttled energy [%]	35.04	35.16	36.15 / 41.31	35.12
Battery lifetime expectancy [yr.]	8.83	8.23	1.82 / 5.31	8.62

In Case 2, the simulation revealed that the battery could be downsized to 500 kWh with a 6.11 % connection to the main grid. This would decrease the expected lifetime by 0.6 years compared to the reference battery. Based on Case 3 it was found that the battery capacity could be downsized to 110 kWh, thus drastically reducing the battery lifetime to 1.8 years because of the increased number of annual cycles. It was also found that the project goal of less than 5.00 % connection to the main grid could be achieved with a battery capacity of 320 kWh. This would still have a substantial negative impact on the lifetime expectancy as it is 3.5 years less than what is expected in the reference case. In Case 4, it is found that a 20 kWh reduction could be achieved (530 kWh capacity), with 6.13 % connection to the main grid. With this battery capacity, a reduction of 0.2 years in lifetime expectancy is found, compared to the reference battery.

In every case it is observed that it is possible to downsize the battery, although, the lifetime expectancy is reduced depending on the extent of the capacity reduction. As the battery capacity is reduced, the number of cycles increase which in turn leads to a lower lifetime expectancy. These calculations are based on the assumption that only the number of cycles affect the expected lifetime. It is also worth discussing what effects the simplification of calculating cycles may have had. As mentioned in section 2.6, the maximum capacity of a battery decreases over time. This implies that the number of cycles performed by the battery should not have a linear growth,

which has been assumed. It is unknown how much of an effect this has had on the results, but it is safe to assume that the expected lifetimes are even lower than what is presented. Because of the reduction in lifetime expectancy, an economical evaluation should be performed before considering downsizing the capacity, since the battery storage accounts for a significant investment cost.

The throttled energy for each case decreases when the battery capacity is downsized. With a smaller capacity more of the load demand is provided by the hydrogen storage. Two possible reasons why less energy is throttled is that the there is a lower efficiency in the electrolyzer compared to the battery leading to less excess energy, and the rate limiter set to the power rating of the electrolyzer.

Load factor

When comparing the figures illustrating the daily development of load factors in each case, it can be seen that the load factor improves from Case 1 to all the other cases, with Case 2 increasing the most. The reason for the contrast between Case 2 and the rest is the method applied. As can be seen in figure 7.3.2, the high peaks are often partitioned to other periods, resulting in a generally more smooth load profile than the other cases.

According to these results, ALM increases the load factor. Since flexible loads are mainly shifted to periods with high power production and, then, what remains is shifted to periods with the least consumption, it was partially expected that the load factor would decrease. This seems not to be the case. The reason for this may be because, more often than not, the peaks are shifted to periods with a lower load demand. Another explanation is the shifting of loads to periods with the lowest consumption, which helps to increase the load factor by some degree.

The increase in average load factor may increase the overall stability of the system. This is due to the increased probability of the intermittent energy productions ability to cover the demand. This can be especially important when the microgrid is operating in island mode, to ensure stable system voltage and frequency. On the other hand, the ALM algorithm has decreased the load factor in some periods. However, the energy production is able to cover the new demand in these periods. This indicates that the system stability does not suffer as a consequence of the decreased load factor. In the case of a microgrid at Froan with no possible supply from the main grid, a low load factor could have a negative impact on system stability. Especially if no other backup solution is available.

Validity of Case 2

As previously mentioned, the goal for Case 2 is to investigate the validity of using a statistical method for defining flexible loads. By comparing it to Case 4, which is the most conservative case, it is found that Case 2 shifts about double the amount as Case 4. This can be seen in figure 8.1.1. In reality, all the appliances in Case 3 are flexible and could be shifted with certainty if component level metering was available. In that situation, Case 3 might be the most realistic outcome with regards to the amount of shifted load. The amount of shifted load in Case 2 is far from the two other cases, which indicates that the statistical method is not a good method of classifying flexible loads. It is hard to validate the method of Case 2 in regards to other systems. In this project, the silo is easy to identify and is fortunately also flexible, which works in the favour of Case 2. For other systems, the flexible loads might not be as easy to identify and using this method could risk shifting non-flexible loads.

8.2   Reliability & choice of methods

This section underlines the possible flaws and strengths of the applied methods. It covers the Simulink modeling, PVsyst simulation, and the different approaches in each case. In addition, the choice of starting with an empty ESS is discussed.

Simulink model

In section 6.4 the methods and procedures of modelling Rye microgrid were considered. From this section it can be derived that there are some simplifications in the model that can have an impact on the results. These simplifications are discussed in the following paragraphs.

The placement of transformer 2 allows for the PV production to be reduced as if the energy flow from the PV-site through transformer 2 and then into the battery. In reality, the production flows directly from the PV-site to the battery. This reduces the energy used to charge the battery, which can result in an increase in energy needed from the main grid. This is not considered to have a significant impact, since the transformer efficiency is very high. The model could have been made to account for this simplification, but it would in turn become more complicated.

The model does not consider the no-load losses of any transformer in no-load condition. This means that if there was no wind production for some hours, no-load losses would still occur in transformer 1. These losses are not accounted for. This leads to a lower amount of losses in the system, which in turn yields slightly better results. However, these losses are small, as shown in table 2.4.1, and is not considered to have a significant impact on the results in total.

Mean values for efficiency were calculated for all transformers and implemented in the model. In reality, the losses vary with the load as mentioned in section 2.5. If the load is greater than the mean value, the efficiency would be lower, but where the load is lower than the mean value, the efficiency would be higher. If this simplification have made a significant impact on the results is hard to assess, but its effect is assumed to be negligible.

As mentioned in chapter 6.2 the losses in the transmission line are neglected. This leads to a slight reduction of losses in the results. However, as it was discovered that the maximum losses were only 8.40 W, the losses are regarded as insignificant for the purpose of this thesis.

The simplifications either increase or decrease the amount of losses. Because of this, they are thought to cancel each other out in some degree.

PV production

Meteorological data has a considerable uncertainty factor, as elaborated on in section 3.1. Solar irradiance data has a direct effect on the simulated power output in PVsyst and is something that should be considered when evaluating the production data. The following paragraphs aim to discuss the validity and importance of the simulated power production.

As the PV system at Rye was installed towards the end of the time frame of this thesis, there is only a small amount of data for comparison between the real and simulated power production. As stated in section 7.1.1 the real production was higher in April compared to the simulations. This indicates that Meteonorm uses a conservative method, although the difference could be due to abnormal weather conditions in this period. The comparison between the temperature from the Norwegian Meteorological Institute and the temperature data from Meteonorm, shown in table 7.1.1, indicates that the mean irradiance data over the year might correlate fairly well. Although it was not done for this thesis, performing simulations based on other weather data providers could be interesting to investigate the difference between the providers. Varying data would make it possible to simulate for a worst- and best-case.

The power production has a direct significance on how much load can be shifted. As a result, using meteorological data providers that assume too much irradiance would lead to an inaccurate amount of shiftable load. It could be preferable to use data that is conservative for the objectives of this thesis, in order to get an accurate representation of the effect of active load management.

Starting with or without fully charged ESS

All simulations have been performed based on an empty ESS from start. This is done because the ESS conditions are unknown at the beginning of future years. Therefore, it may be desirable to size the ESS based on a worst-case scenario.

In every case, it was observed that the percent needed from the main grid never reached 0 %, despite increasing the battery capacity substantially. A reason for this can be because it was decided to start with an empty battery (20 % SOC) and hydrogen storage. If there was energy needed from the ESS during the starting period, before the ESS had a chance to be charged, the energy would be needed from the main grid instead. This would result in energy needed from the main grid, no matter how large the ESS is sized.

In reality, it is hard to say if the energy storage would be completely empty or full when a new year starts. The most realistic scenario is probably that the ESS status would be somewhere in between.

Case 2

When defining flexible loads in Case 2, several methods were considered. It was important that the method provided an accurate and realistic upper bound to define flexible loads. Calculating an upper bound for each week was decided, since it supplied an adequate representation of what could be shifted. This made it possible to register days with extreme demand during a week with relatively low demand. The alternatives were to calculate an upper bound for each day or month, but these solutions did not provide accurate results. The reason is that an upper bound for every day does not take the current trend into account, resulting in a day with extremely high demand not being registered as an outlier, even though it was during a time period with relatively low demand. An upper bound for every month, on the other hand, would not consider the natural alteration of demand trends during a month.

Three methods of defining the upper bound were considered. The possibilities were either based on the mean demand, base load or using quartiles. Using a base load as an upper bound would guarantee shifting non-flexible loads. Consequently, this method was discarded. Using the mean load would have the same result, but it would not be as gross of an assumption as using the base load. Using quartiles was assumed to yield the most correct results and was therefore the chosen method for this case. This method locates outliers to a certain extent. This way, only values defined as extremals would be categorized as flexible. This assumption may not be completely accurate, but it takes the trends into account.

What could be regarded as a weakness of the method is the silo's frequent use. Because of this, it is registered as a trend and results in the calculation of a high upper bound. As a consequence, abnormal variations in demand caused by other appliances than the silo are not often detected and therefore not shifted. On the other hand, this method ensures that there are mostly flexible loads that are shifted, since the silo is defined as flexible, and not other non-flexible loads such as heating appliances.

During the winter, it is not realistic to reduce the amount of heating, because it would affect the comfort of the residents. As can be seen in figure 7.3.2, the load shifting does not affect the base load. This may further validate the applied method, because the base load may be the application of heating appliances.

An issue with this method is that the upper bound does not consider if it is dividing loads or not. This means that only parts of loads are moved to other hours. This is unrealistic regarding loads that can not stop if their cycles are started.

Cases 3 & 4

The method applied in Case 3 shares common ground with Case 4. The power demand of Telenor is assumed to be at a fixed value of 1.9 kWh/h, as mentioned in section 5.1. It is not taken into consideration that part of the received compensation from Telenor may also cover the use of space and other possible inconveniences. With these factors in mind, it may be that the applied power consumption is set too high, since the real energy demand is unknown. Another factor to take into consideration is the sources of light in the households. Because of the inaccuracy of the standards, it may also be a source of error in regard to the energy demand of lighting appliances.

The load profile for the silo is developed using statistics in both cases. This method is a source of error, due to the fact that it may not register the use of the silo accurately. Even if it does, the fixed average energy demand is likely to be prone to error. As described in section 5.1, the silo is used on average one time a day, but the specific hour of the day and time period varies in some degree. This results in no straight forward way of obtaining accurate consumption data for the silo. Although, as illustrated in figure 5.1.1, the silo constitutes a great portion of the load demand when in use. This works in the methods favor, since the statistics registers outliers in the data set, but it is, as mentioned above, unlikely that the resulting load profile is a perfect representation of the actual load profile for the silo.

The method in Case 3 consists of sources of error, which is reflected in the results. As can be seen in figure 7.4.1, the demand is occasionally close to, and sometimes is, zero. It is not reasonable to assume that the energy consumption of three households combined is that low. It is therefore safe to assume that a combination of the high load demand of Telenor and the standards contain sources of error. This error can occur because of the fixed hours the standard have defined for water heaters and lights, as this does not necessarily match the user habits for the households. Another factor that is assumed to contribute to this problem is the use of probability to define

the start time of dishwashers and washing machines. This method increases the chances of shifting these loads at the correct times, but in reality, the start times will differ many times over the course of a year. Although the standard proves to be inaccurate, it coincided with the registered power rating of the water heaters in the apartments. This strengthens the validity of the standard. On the other hand, the large area of the cowsheds at both farm sites made the energy consumption of the respective water heaters too high, which again weakens the validity of the standard.

8.3   Flexibility resources

Although components and appliances could be defined as flexible, it also depends on the willingness of the consumer to adapt accordingly. In the case of this thesis, the flexibility of the silo depends on the farmer's willingness to vary his workday according to the energy production. Therefore, it is possible that this component may not be as flexible in reality.

The flexibility of the household appliances defined as flexible in this thesis are also only flexible if they could be set to predefined times or automatically started at the preferred times. It is unlikely that the consumers would do the amount of effort needed to do this manually. Communication-channels to the consumers and smart appliances are thought to be important in order to activate the flexibility potential of the appliances.

The eGauge smart meters installed on the five main circuits at farm site 1 register the load demand in the apartments and cowshed, although, it is not suited for identifying smaller individual loads. As previously elaborated on, measurements on a component level would be needed to get a realistic view on how much of the total load that can be classified as flexible. If measurement equipment with the ability to recognize the usage pattern of different appliances was installed in the apartments, more components might be classified as flexible, thus increasing the amount of shifted load.

For a load shifting algorithm to be implemented, systems for high quality weather forecasting is needed to accurately predict the wind and solar power production. Without such systems in place it is easy to assume that some of the shifted loads could be shifted to times where the capacity is not large enough to cover the new demand. This may prove especially difficult when it comes to components or appliances where the consumer have to stay present under the operation, such as the silo. For the same reasons, reliable load forecasting systems are thought to be an essential element, although, further in-depth investigations in this field would have to be performed.

Chapter 9

Conclusion and further work

9.1 Conclusion

Concerning the main problem, the results from the ESS performance reveal that the battery capacity can be downsized from 550 kWh in each of the cases where ALM is implemented. The potential battery capacities are 500 kWh, 110 kWh and 530 kWh for Cases 2, 3 and 4, respectively. These results are based on not exceeding the connection to the main grid in the reference case. Case 3 was the only case that achieved the goal of under 5 % energy needed from the main grid, with a battery capacity down to 320 kWh. A downsize in battery capacity results in an increase in the number of battery cycles and, as a consequence, reduce the battery lifetime expectancy. An economical evaluation is necessary to asses if a possible downsize is beneficial, although, this is outside the scope of this thesis.

The statistical method applied in Case 2 is found to be an inaccurate method of classifying flexible loads and is not recommended for further use. The amount of shifted load in Case 3 is 11.7% for 2018. This is the most optimistic outcome but is thought to give a good representation of what is realistic, with regards to the amount of shifted loads. Case 4 on the other hand is the most conservative with 1.9 % shifted load for 2018. This is thought to be a minimum of what is theoretically achievable.

The connection to the main grid is reduced in each case where ALM is implemented. This is without changing the battery capacity from the reference battery. Cases 2, 3 and 4 results in 5.97 %, 4.18 % and 6.08 % energy needed from the main grid, respectively.

The model is thought to be a valid representation of the microgrid, despite uncertainties regarding meteorological data and the simplifications applied. Based on results and extensive examinations, the ALM algorithm is also found to function as planned.

The findings in this thesis are only theoretical. In order to implement ALM in a real system, it is imperative to have metering on a component level as a mean to identify the usage pattern of flexible loads and enable their flexibility potential. A reliable forecasting system regarding loads and energy production is also an essential component. In addition the consumers must be willing to adapt in order to reach the maximum effect of ALM.

9.2 Further work

Further extensions to the project could be implemented, if the time frame of the thesis was extended. Given adequate time, the power production from the PV system at Rye could be used to perform new simulations on microgrid performance. This would correct some of the previously mentioned uncertainties. A more accurate model of the microgrid could be implemented if all components were installed. As a consequence, loss simplifications could be rectified. Furthermore, to acquire more reliable results, component level measurements on the flexible and power-shiftable loads would be implemented.

Since the battery capacity could be downsized in all the cases, an economical evaluation would also be performed in each case. Such an evaluation would assess if a battery downsize would be profitable despite the reduced lifetime expectancy. Finding a use for the excess energy could also be investigated. An economical evaluation of the profitability of selling this energy as hydrogen gas, instead of throttling it, would be of interest. This is due to the substantial amount of excess energy. Another possibility would be to sell the energy to the main grid, although this would not be possible for a microgrid operating in island mode.

The demo was originally planned to be stationed at Froan. A natural further work would be to investigate the flexibility potential at Froan and implement ALM to utilize the local energy production more efficiently, if a microgrid was to be installed. This would be performed by applying the methods and recommendations from this thesis.

To be able to implement ALM, a reliable forecasting system would have to be installed. Because of this, researching how these systems operate, and developing one, would be an interesting extension.

Bibliography

[1] Gemini Svein Tønseth. "Denne vindturbinen skal vise hvordan øysamfunn kan bli selvforsynte med fornybar kraft". In: (Feb. 2018). (Accessed on 01/21/2019). URL: https://www.tu.no/artikler/forskning-denne-vindturbinen-skal-vise-hvordan-oysamfunn-kan-bli-selvforsynte-med-fornybar-kraft/430940.

[2] enerWE. "Statnett skal investere 35-45 milliarder i strømnettet frem til 2022 – enerWE". In: (Sept. 2017). (Accessed on 01/21/2019). URL: http://enerwe.no/kraft/statnett-skal-investere-35-45-milliarder-i-stromnettet-frem-til-2022/.

[3] Eirik Iveland. "Microgrid drevet av vindmølle og solceller - Samferdselinfra.no". In: (May 2018). (Accessed on 02/06/2019). URL: https://samferdselinfra.no/artikler/microgrid-drevet-av-vindmolle-og-solceller/435664.

[4] David Wenzhong Gao. *Energy storage for sustainable microgrid.* Academic Press, 2015.

[5] The European Commission. *2030 Energy Strategy.* (Accessed on 05/18/2019). URL: https://ec.europa.eu/energy/en/topics/energy-strategy-and-energy-union/2030-energy-strategy.

[6] TrønderEnergi. *Om TrønderEnergi.* (Accessed on 01/22/2019). URL: https://tronderenergi.no/om-tronderenergi.

[7] SINTEF. *Applied reaserch, technology and innovation.* (Accessed on 05/15/2019). URL: https://www.sintef.no/en/this-is-sintef/.

[8] Eirik Lockertsen. *Solbes AS.* (Accessed on 05/18/2019). URL: https://www.solbes.no/.

[9] Eirik Iveland. "Microgrid drevet av vindmølle og solceller - Samferdselinfra.no". In: (May 2018). (Accessed on 01/21/2019). URL: https://samferdselinfra.no/artikler/microgrid-drevet-av-vindmolle-og-solceller/435664.

[10] REMOTE. *REMOTE project.* (Accessed on 01/21/2019). URL: https://www.remote-euproject.eu/remote-project/.

[11] REMOTE. *Remote area Energy supply with Multiple Options for integrated hydrogen-based TEchnologies.* (Accessed on 01/21/2019). May 2018. URL: https://www.remote-euproject.eu/remote18/rem18-cont/uploads/2018/10/POLITO-remote-brochure-giugno2018-bassa-8print.pdf.

[12] REMOTE. *Bringing clean and innovative energy storage solutions to REMOTE isolated areas.* (Accessed on 01/21/2019). URL: https://www.remote-euproject.eu/remote18/rem18-cont/uploads/2018/10/CS-REMOTEV4_ENG.doc.

[13] Anniken Auke Borgen (Supervisor at TronderEnergi). Personal communication. 08.11.18 - 24.05.19.

[14]   IEC. *Microgrids: Guidelines for microgrid projects planning and specification.* (Accessed on 03/09/2019). May 2017. URL: `https://www.sis.se/api/document/preview/8026626/`.

[15]   International Electrotechnical Commission. *IEC 60050 - International Electrotechnical Vocabulary - Details for IEV number 617-04-22: "microgrid".* (Accessed on 01/24/2019). URL: `http://www.electropedia.org/iev/iev.nsf/display?openform&ievref=617-04-22`.

[16]   International Electrotechnical Commision. *Electropedia: The world's online electrotechnical vocabulary.* (Accessed on 05/21/2019). URL: `http://www.electropedia.org/`.

[17]   Managing director at Solbes Eirik Lockertsen. Personal communication. 2019.

[18]   Massachusetts Institute of Technology (MIT). *A Guide to Understanding Battery Specifications.* (Accessed on 04/29/2019). URL: `http://web.mit.edu/evt/summary_battery_specifications.pdf`.

[19]   REMOTE. *Hydrogen.* (Accessed on 01/21/2019). June 2018. URL: `https://hydrogeneurope.eu/project/remote`.

[20]   Michelle Fung. *Energy Density of Hydrogen - The Physics Factbook.* (Accessed on 03/14/2019). 2005. URL: `https://hypertextbook.com/facts/2005/MichelleFung.shtml`.

[21]   eGauge. *Energy Metering Systems.* (Accessed on 02/19/2019). URL: `https://www.egauge.net/`.

[22]   Nexans Norway AS. *Nexans Kabelboka.* (Accessed on 01/29/2019). 2009. URL: `http://www.nexans.no/Norway/2009/Kabelboka_final_2009.pdf`.

[23]   Theodore Wildi. *Electrical Machines, Drives, and Power systems.* (Accessed on 01/29/2019). PEARSON, 2014.

[24]   Norsk Transformator AS. *Vurdering av transformatortap.* (Accessed on 02/11/2019). URL: `https://www.nortrafo.no/?Mode=Meny&HovedMenyId=81&ThisMenyId=81&InnholdId=469`.

[25]   Store Norske Leksikon (SNL). "Transformatortap". In: (). (Accessed on 04/03/2019). URL: `https://snl.no/transformatortap`.

[26]   Steinar Svarte and Jan H. Sebergsen. *Energiproduksjon og energidistribusjon 1.* Gyldendal, 2016.

[27]   Odne Burheim. *Engineering Energy Storage.* (Accessed on 02/14/2019). Academic Press, 2017. ISBN: 9780128141007.

[28]   National Renewable Energy Laboratory (NREL). *Battery Lifetime Analysis and Simulation Tool Suite.* (Accessed on 05/22/2019). URL: `https://www.nrel.gov/transportation/blast.html`.

[29]   Deutsche Gesellschaft für Sonnenenergie. *Planning and Installing Photovoltaic Systems: A Guide for Installers, Architects and Engineers.* (Accessed on 02/03/2019). United Kingdom: Routledge Ltd, 2013. ISBN: 9781849713436.

[30]   Konrad Mertens. *Photovoltaics : fundamentals, technology and practice.* (Accessed on 02/19/2019). Wiley, 2014. ISBN: 1-118-70336-7.

[31]   NVE. *Solenergi.* (Accessed on 02/25/2019). July 2018. URL: `https://www.nve.no/energiforsyning-og-konsesjon/solenergi/`.

[32] Norsk solenergiforening. *Norske solforhold*. (Accessed on 02/19/2019). URL: `https://www.solenergi.no/norske-solforhold/`.

[33] The World Bank Group. *Global Solar Atlas*. (Accessed on 05/18/2019). URL: `https://globalsolaratlas.info/downloads/world`.

[34] Juan Reca-Cardeña and Rafael López-Luque. *Diffuse Radiation - ScienceDirect*. (Accessed on 03/10/2019). 2018. URL: `https://www.sciencedirect.com/topics/engineering/diffuse-radiation`.

[35] Jeffrey R. S. Brownson. *Collector Orientation, Solar Resource Assessment and Economics*. (Accessed on 04/27/2019). URL: `https://www.e-education.psu.edu/eme810/node/576`.

[36] Jan Kleissl. *Solar Energy Forecasting and Resource Assessment*. Elsevier Science, 2013. ISBN: 0123971772.

[37] Marius Paulescu et al. *Weather Modeling and Forecasting of PV Systems Operation*. Springer London, 2013. ISBN: 978-1-4471-4648-3.

[38] World Radiation Data Centre. *WRDC*. (Accessed on 03/03/2019). URL: `http://wrdc.mgo.rssi.ru/wrdc_en_new.htm`.

[39] PANGAEA. *BSRN Stations*. (Accessed on 03/03/2019). URL: `https://www.pangaea.de/ddi?request=bsrn/BSRNEvent&format=html&title=BSRN+Stations`.

[40] PVsyst. *Logiciel Photovoltaïque*. (Accessed on 02/14/2019). 2019. URL: `https://www.pvsyst.com/`.

[41] Vasilis M. Fthenakis. *Electricity from sunlight: photovoltaic-systems integration and sustainability*. eng. Second edition. Hoboken, New Jersey, 2018. ISBN: 1-118-96377-6.

[42] Kathie Zipp. "How do power optimizers help harvest more energy from solar projects?" In: (Nov. 2015). (Accessed on 03/11/2019). URL: `https://www.solarpowerworldonline.com/2015/11/23495/`.

[43] SolarEdge. *Power Optimizer — SolarEdge — A World Leader in Smart Energy*. (Accessed on 05/18/2019). URL: `https://www.solaredge.com/us/products/power-optimizer#/`.

[44] Next Kraftwerke. "Load management: How TSOs deal with electrical consumption". In: (). URL: `https://www.next-kraftwerke.com/knowledge/load-management`.

[45] Zhaoguang Hu, Xinyang Han, and Quan Wen. *Integrated Resource Strategic Planning and Power Demand-Side Management*. Springer Heidelberg New York Dordrecht London, 2013. ISBN: 978-3-642-37083-0.

[46] Hussein Attia. "Mathematical Formulation of the Demand Side Management Problem and its Optimal Solution". In: (Mar. 2019).

[47] MengChu Zhou. *Energy conservation in residential, Commercial and industrial facilities*. John wiley & sons, Inc, Hoboken, New Jersey, 2018. ISBN: 978-1-119-42206-8.

[48] Satish Saini. "Conservation v. generation: The significance of Demand-Side Management (DSM), its tools and techniques". In: *Refocus* 5 (2004). ISSN: 1471-0846. URL: `http://www.sciencedirect.com/science/article/pii/S1471084604001465`.

[49] Pascal Hategekimana. "Analysis of Electrical Loads and Strategies for Increasing Self-Consumption with BIPV Case study: Skarpnes Zero-Energy House".
(Accessed on 03/14/2019). MA thesis. 2017. URL: `https://uia.brage.unit.no/uia-xmlui/bitstream/handle/11250/2454256/Hategekimana%5C%2c%5C%20Pascal.pdf?sequence=1&isAllowed=y`.

[50]   D. Li, W.-Y. Chiu, and H. Sun. "Demand Side Management in Microgrid Control Systems". In: *Microgrid*. Ed. by Magdi S. Mahmoud. Butterworth-Heinemann, 2017, pp. 203–230. ISBN: 978-0-08-101753-1. URL: `http://www.sciencedirect.com/science/article/pii/B9780081017531000073`.

[51]   Merkebu Zenebe Degafa. "How to estimate flexibility potential of household appliances? (To reduce peak load)". In: (). (Accessed on 04/07/2019). URL: `https://blog.sintef.com/sintefenergy/flexibility-potential-household-appliances/`.

[52]   M. Z. Degefa et al. *Data-driven Household Load Flexibility Modelling: Shiftable Atomic Loads*. (Accessed on 04/08/2019). 2018. URL: `https://sintef.brage.unit.no/sintef-xmlui/bitstream/handle/11250/2582419/DEGEFA2018ddh.pdf?sequence=2&isAllowed=y`.

[53]   Hanne Sæle and Merkebu Zenebe Degefa at SINTEF Energy. Personal communication. 01.04.2019.

[54]   Standard Norge. *Energy performance of buildings - Calculation of energy needs and energy supply*. URL: `https://www.standard.no/no/Nettbutikk/produktkatalogen/Produktpresentasjon/?ProductID=859500`.

[55]   Meteorologisk institutt. Email correspondence. 04.04.2019.

[56]   NVE. "Nettleien øker fra 2018 til 2019, men økningen avdempes av reduksjon i elavgiften". In: (). URL: `https://www.nve.no/nytt-fra-nve/nyheter-reguleringsmyndigheten-for-energi/nettleien-oker-fra-2018-til-2019-men-okningen-avdempes-av-reduksjon-i-elavgiften/`.

[57]   EnergiLOSEN. "Historiske strømpriser". In: (). (Accessed on 04/10/2019). URL: `https://www.los.no/kundeservice/strompris/historiske-strompriser/`.

Appendix A

Load profiles

This appendix presents th e load profiles for all the appliances that are shifted in Case 3 and 4. The load profiles are presented in figure A.1.1. Telenor and lights are not included since these are flat loads. The following load profiles are presented:

- Dishwashers
- Washing machines
- Water heaters
- Silo
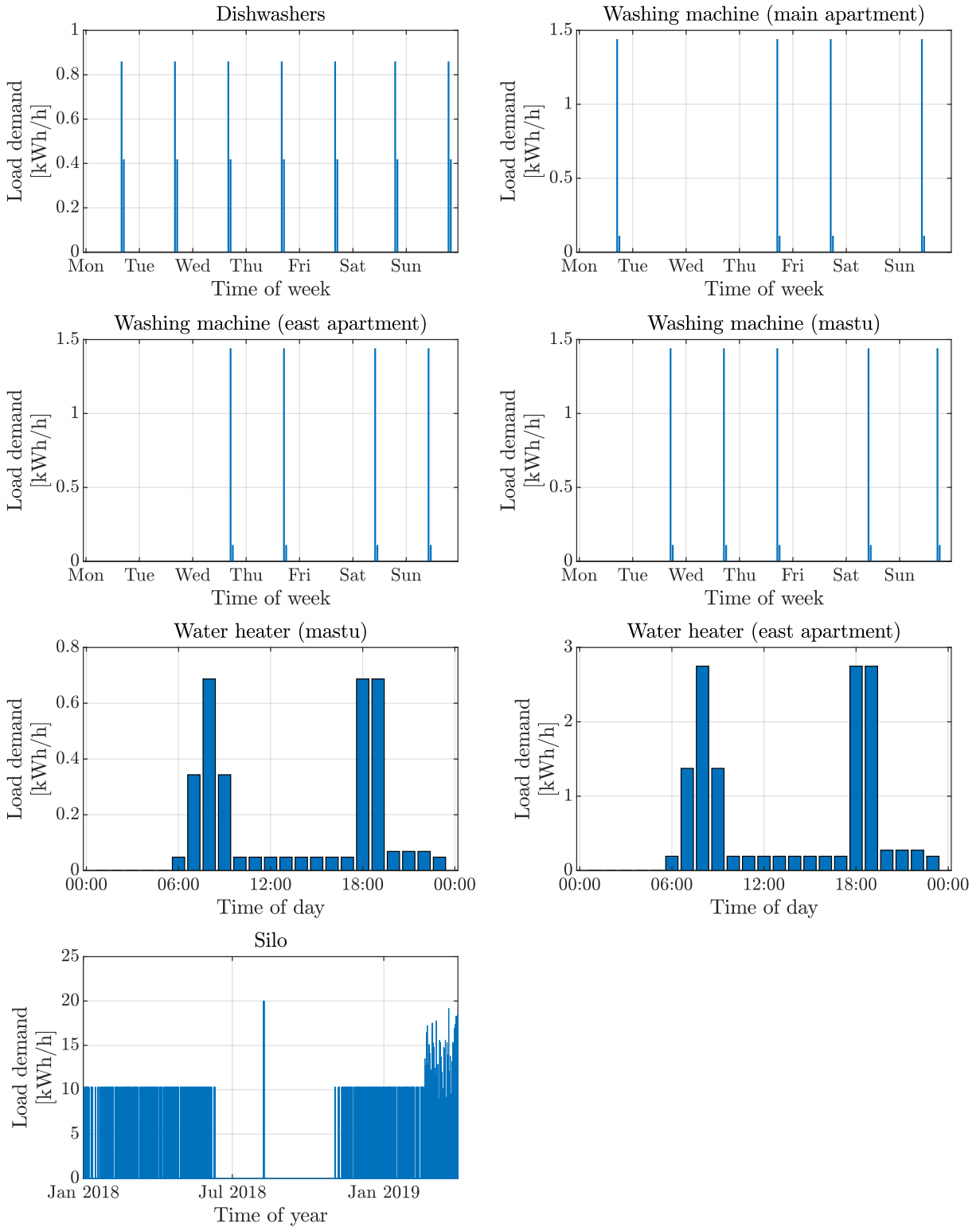
Figure A.1.1: Load profiles for all flexible components that are applied in Case 3 and Case 4. The load profiles for the dishwashers and washing machines are generated based on data from SINTEF Energy, while the water heaters are based on the standard SN/TS 3031. The silo is based on measured data.

Appendix B

PVsyst simulation report

The full report containing results from simulation in PVsyst can be found in this appendix, beginning at the next page. The report contains the following information:

- Simulation parameters
- Near shading definition
- Main results
- Loss diagram

PVSYST V6.78		04/03/19	Page 1/5

Grid-Connected System: Simulation parameters

Project :   **Rye microgrid**

Geographical Site		**Rye**		Country	**Norway**

Situation   Latitude   63.42° N   Longitude   10.12° E
     Time defined as   Legal Time Time zone UT+1   Altitude   79 m
                                    Albedo   0.20
Meteo data: **Rye**   Meteonorm 7.2 (1986-2005) - Synthetic

Simulation variant :   **forste_simulering_RYE**

                                    Simulation date   04/03/19 09h26

Simulation parameters   System type   **Sheds on ground**

Collector Plane Orientation   Tilt   35°   Azimuth   0°

Sheds configuration   Nb. of sheds 6
                                    Sheds spacing 10.2 m   Collector width   3.32 m
Shading limit angle   Limit profile angle 14.4°   Ground cov. Ratio (GCR) 32.7 %

Models used   Transposition Perez   Diffuse   Perez, Meteonorm

Horizon   Free Horizon

Near Shadings   According to strings   Electrical effect 100 %

User's needs :   Unlimited load (grid)

PV Arrays Characteristics   (3 kinds of array defined)

Sub-array "Top row"   Si-mono   Model   **REC 310NP**
   Original PVsyst database   Manufacturer REC

SolarEdge Power Optimizer   Model   **P700 for SE16k+** Unit Nom. Power   730 W
PV modules on one optimizer   in series 2   in parallel   1
Nb. of optimizers   In series 16   In parallel   3 strings
Total number of PV modules   Nb. modules 96   Unit Nom. Power 310 Wp
Array global power   Nominal (STC) **29.76 kWp**   At operating cond. 27.22 kWp (50°C)
Output of optimizers   U oper   750 V   I at Poper   36 A

Sub-array "Mid row"   Si-poly   Model   **REC 295TP2**
   Original PVsyst database   Manufacturer REC

SolarEdge Power Optimizer   Model   **P600 for SE15k+** Unit Nom. Power   600 W
PV modules on one optimizer   in series 2   in parallel   1
Nb. of optimizers   In series 16   In parallel   3 strings
Total number of PV modules   Nb. modules 96   Unit Nom. Power 295 Wp
Array global power   Nominal (STC) **28.32 kWp**   At operating cond. 25.78 kWp (50°C)
Output of optimizers   U oper   750 V   I at Poper   34 A

Sub-array "Bottom row"   Si-poly   Model   **REC 295TP2**
   Original PVsyst database   Manufacturer REC

SolarEdge Power Optimizer   Model   **P600 for SE15k+** Unit Nom. Power   600 W
PV modules on one optimizer   in series 2   in parallel   1
Nb. of optimizers   In series 16   In parallel   3 strings
Total number of PV modules   Nb. modules 96   Unit Nom. Power 295 Wp
Array global power   Nominal (STC) **28.32 kWp**   At operating cond. 25.78 kWp (50°C)
Output of optimizers   U oper   750 V   I at Poper   34 A

PVSYST V6.78			04/03/19	Page 2/5

Grid-Connected System: Simulation parameters

Total Arrays global power	Nominal (STC)	**86 kWp**	Total	288 modules
	Module area	**481 m²**	Cell area	424 m²

Inverter
Original PVsyst database
Characteristics

	Model	**SE27.6K**		
	Manufacturer	SolarEdge		
	Operating Voltage	750 V	Unit Nom. Power	27.6 kWac

Sub-array "Top row"	Nb. of inverters	1 units	Total Power	28 kWac
			Pnom ratio	1.00
Sub-array "Mid row"	Nb. of inverters	1 units	Total Power	28 kWac
			Pnom ratio	0.95
Sub-array "Bottom row"	Nb. of inverters	1 units	Total Power	28 kWac
			Pnom ratio	0.95

Total	Nb. of inverters	3	Total Power	83 kWac

Physical inverters

SE27.6K	1 units, 3 strings	3 strings of 16 optimizers P700 for SE16k+
SE27.6K	1 units, 3 strings	3 strings of 16 optimizers P600 for SE15k+
SE27.6K	1 units, 3 strings	3 strings of 16 optimizers P600 for SE15k+

PV Array loss factors

Array Soiling Losses — Average loss Fraction 19.6 %

Jan.	Feb.	Mar.	Apr.	May	June	July	Aug.	Sep.	Oct.	Nov.	Dec.
80.0%	50.0%	20.0%	5.0%	0.0%	0.0%	0.0%	0.0%	0.0%	0.0%	0.0%	80.0%

Thermal Loss factor	Uc (const)	20.0 W/m²K	Uv (wind)	0.0 W/m²K / m/s
Wiring Ohmic Loss	Array#1	283 mOhm	Loss Fraction	1.5 % at STC
	Array#2	298 mOhm	Loss Fraction	1.5 % at STC
	Array#3	298 mOhm	Loss Fraction	1.5 % at STC
	Global		Loss Fraction	1.5 % at STC
LID - Light Induced Degradation			Loss Fraction	1.0 %
Module Quality Loss		Array#1,	Loss Fraction	-0.4 %
		Array#2,	Loss Fraction	-0.5 %
		Array#3,	Loss Fraction	-0.5 %
Module Mismatch Losses			Loss Fraction	0.0 % (fixed voltage)

Incidence effect (IAM): Fresnel AR coating, n(glass)=1.526, n(AR)=1.290

0°	30°	50°	60°	70°	75°	80°	85°	90°
1.000	0.999	0.987	0.962	0.892	0.816	0.681	0.440	0.000

PVsyst Evaluation mode

PVSYST V6.78		04/03/19	Page 3/5

Grid-Connected System: Near shading definition

Project :   **Rye microgrid**

Simulation variant :   **forste_simulering_RYE**

Main system parameters	System type	**Sheds on ground**		
Near Shadings	According to strings		Electrical effect	100 %
PV Field Orientation	tilt	35°	azimuth	0°
PV modules	Model	REC 310NP	Pnom	310 Wp
PV modules	Model	REC 295TP2	Pnom	295 Wp
PV Array	Nb. of modules	288	Pnom total	**86.4 kWp**
Inverter	Model	SE27.6K	Pnom	27.60 kW ac
Inverter pack	Nb. of units	3.0	Pnom total	**82.8 kW ac**
User's needs	Unlimited load (grid)			

Perspective of the PV-field and surrounding shading scene

Iso-shadings diagram

Rye microgrid

Beam shading factor (according to strings) : Iso-shadings curves

Shading loss: 1 %
Shading loss: 5 %
Shading loss: 10 %
Shading loss: 20 %
Shading loss: 40 %

Attenuation for diffuse: 0.023 and albedo: 0.443

1: 22 june
2: 22 may - 23 july
3: 20 apr - 23 aug
4: 20 mar - 23 sep
5: 21 feb - 23 oct
6: 19 jan - 22 nov
7: 22 december

PVsyst Evaluation mode

PVSYST V6.78		04/03/19	Page 4/5

Grid-Connected System: Main results

Project :	**Rye microgrid**
Simulation variant :	**forste_simulering_RYE**

Main system parameters	System type	**Sheds on ground**		
Near Shadings	According to strings		Electrical effect	100 %
PV Field Orientation	tilt	35°	azimuth	0°
PV modules	Model	REC 310NP	Pnom	310 Wp
PV modules	Model	REC 295TP2	Pnom	295 Wp
PV Array	Nb. of modules	288	Pnom total	**86.4 kWp**
Inverter	Model	SE27.6K	Pnom	27.60 kW ac
Inverter pack	Nb. of units	3.0	Pnom total	**82.8 kW ac**
User's needs	Unlimited load (grid)			

Main simulation results

System Production	**Produced Energy**	**80.04 MWh/year**	Specific prod.	926 kWh/kWp/year
	Performance Ratio PR	80.50 %		

Normalized productions (per installed kWp): Nominal power 86.4 kWp

Lc : Collection Loss (PV-array losses) 0.56 kWh/kWp/day
Ls : System Loss (inverter, ...) 0.05 kWh/kWp/day
Yf : Produced useful energy (inverter output) 2.54 kWh/kWp/day

Performance Ratio PR

PR : Performance Ratio (Yf / Yr) : 0.805

forste_simulering_RYE

Balances and main results

	GlobHor	DiffHor	T_Amb	GlobInc	GlobEff	EArray	E_Grid	PR
	kWh/m²	kWh/m²	°C	kWh/m²	kWh/m²	MWh	MWh	
January	5.8	4.12	0.25	18.6	2.8	0.17	0.15	0.095
February	22.7	11.24	-0.60	55.5	25.6	1.98	1.93	0.402
March	64.2	26.43	1.03	114.5	88.0	7.48	7.34	0.742
April	110.5	48.37	5.76	147.4	133.9	11.07	10.86	0.853
May	152.9	67.09	9.33	170.5	162.9	13.15	12.88	0.875
June	158.3	76.60	12.05	161.5	153.7	12.31	12.06	0.865
July	153.7	76.46	15.21	161.7	153.9	12.20	11.96	0.856
August	112.3	64.59	14.62	132.5	126.1	10.09	9.89	0.864
September	66.5	29.79	10.88	98.5	94.3	7.58	7.43	0.872
October	29.5	17.92	6.57	57.5	53.9	4.29	4.20	0.847
November	7.9	5.48	2.91	22.0	17.4	1.30	1.27	0.669
December	2.7	2.02	0.30	10.6	1.4	0.08	0.07	0.076
Year	887.1	430.12	6.57	1150.8	1014.0	81.70	80.04	0.805

Legends:	GlobHor	Horizontal global irradiation		GlobEff	Effective Global, corr. for IAM and shadings
	DiffHor	Horizontal diffuse irradiation		EArray	Effective energy at the output of the array
	T_Amb	Ambient Temperature		E_Grid	Energy injected into grid
	GlobInc	Global incident in coll. plane		PR	Performance Ratio

PVsyst Evaluation mode

PVSYST V6.78		04/03/19	Page 5/5

Grid-Connected System: Loss diagram

Project : **Rye microgrid**

Simulation variant : **forste_simulering_RYE**

Main system parameters	System type	**Sheds on ground**		
Near Shadings	According to strings		Electrical effect	100 %
PV Field Orientation	tilt	35°	azimuth	0°
PV modules	Model	REC 310NP	Pnom	310 Wp
PV modules	Model	REC 295TP2	Pnom	295 Wp
PV Array	Nb. of modules	288	Pnom total	**86.4 kWp**
Inverter	Model	SE27.6K	Pnom	27.60 kW ac
Inverter pack	Nb. of units	3.0	Pnom total	**82.8 kW ac**
User's needs	Unlimited load (grid)			

Loss diagram over the whole year

887 kWh/m² **Horizontal global irradiation**

+29.7% **Global incident in coll. plane**

-0.2% Global incident below threshold

-2.7% Near Shadings: irradiance loss

-2.8% IAM factor on global

-6.6% Soiling loss factor

1014 kWh/m² * 481 m² coll. **Effective irradiation on collectors**

efficiency at STC = 17.99% PV conversion

87.8 MWh **Array nominal energy (at STC effic.)**

-2.4% PV loss due to irradiance level

-2.0% PV loss due to temperature

-0.7% Shadings: Electrical Loss acc. to strings

-0.7% Optimizer efficiency loss

+0.4% Module quality loss

-1.0% LID - Light induced degradation

0.0% Module array mismatch loss

-0.7% Ohmic wiring loss

81.7 MWh **Array virtual energy at MPP**

-2.0% Inverter Loss during operation (efficiency)

0.0% Inverter Loss over nominal inv. power

0.0% Inverter Loss due to max. input current

0.0% Inverter Loss over nominal inv. voltage

0.0% Inverter Loss due to power threshold

0.0% Inverter Loss due to voltage threshold

80.0 MWh **Available Energy at Inverter Output**

80.0 MWh **Energy injected into grid**

PVsyst Evaluation mode

Appendix C

Simulink modeling

This appendix presents a more detailed description of how the Simulink model works. First, it is described how the used blocks in Simulink work, and how they are used in the model. Then an algorithm for calculating energy needed from the main grid and energy throttled is presented.

Block based programming

Simulink uses blocks to communicate within a model, and between MATLAB and Simulink. Figure C.1.1 illustrates the different blocks used to model the microgrid.
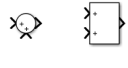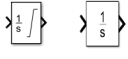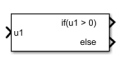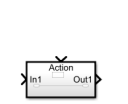
Block symbols	Block name	Block function
	Sum	Sum or subtract values for two or more inputs
	Integrator	Integrates input signal. Can be used as accumulator
Windproduction	From workspace	Imports data from MATLAB workspace
simout	To workspace	Exports input signal to MATLAB workspace
if(u1 > 0) else	IF	The IF block gives a "true" or "false" signal. 1 is true and 0 is false. Elseif conditions can be applied.
Action In1 Out1	IF action	The IF action block recieves a true or false signal from the IF block. If signal is "true", the action is executed
-K-	Gain	Multiplies the input with a function or constant value
	Rate limiter	Limits the rising and falling slew rate of input
1 1	In / out port	Creates in / out port for subsystems

Figure C.1.1: List of the blocks used in Simulink for making a model of the microgrid.

The sum blocks are used either to sum all the loads to get total load or as a block to subtract values.

The integrator block is used to accumulate values. It can limit outputs for upper and lower values, which is used to set the limits for the battery and hydrogen units.

Exporting and importing values or functions between MATLAB and Simulink is executed with the "From workspace" and "To workspace" blocks.

The "IF" and "IF action" blocks are used together to make an if or else statement, and execute an action.

To implement efficiencies, the "Gain" block is used. This block can be set to a constant value or as a function that is multiplied with the input signal.

The "Rate limiter" block is used to limit how fast the components in the energy storage system can be charged and discharged, by limiting the rising and falling slew rate (slope of the curve). This means setting a limit for charge or discharge, based on the respective components power rating, which are presented in section 2.2.

"In" and "Out" ports blocks are applied to create interaction between systems and subsystems.

Algorithm for calculating energy needed from the main grid and throttled energy

Figure C.1.2 displays a flowchart of the algorithm applied to calculate the energy needed from the main grid and throttled energy. The algorithm calculates the energy needed from main grid by first checking if the ESS is empty. If the ESS is empty and the net energy is negative, then the net energy is needed from the main grid. Throttled energy is calculated by checking if the ESS is full. If full, and the net energy is positive, then the positive net energy is throttled. In addition, the algorithm checks the rate limiter from hydrogen. If the value is positive, the energy is throttled. A negative value would lead to more energy needed from the main grid.
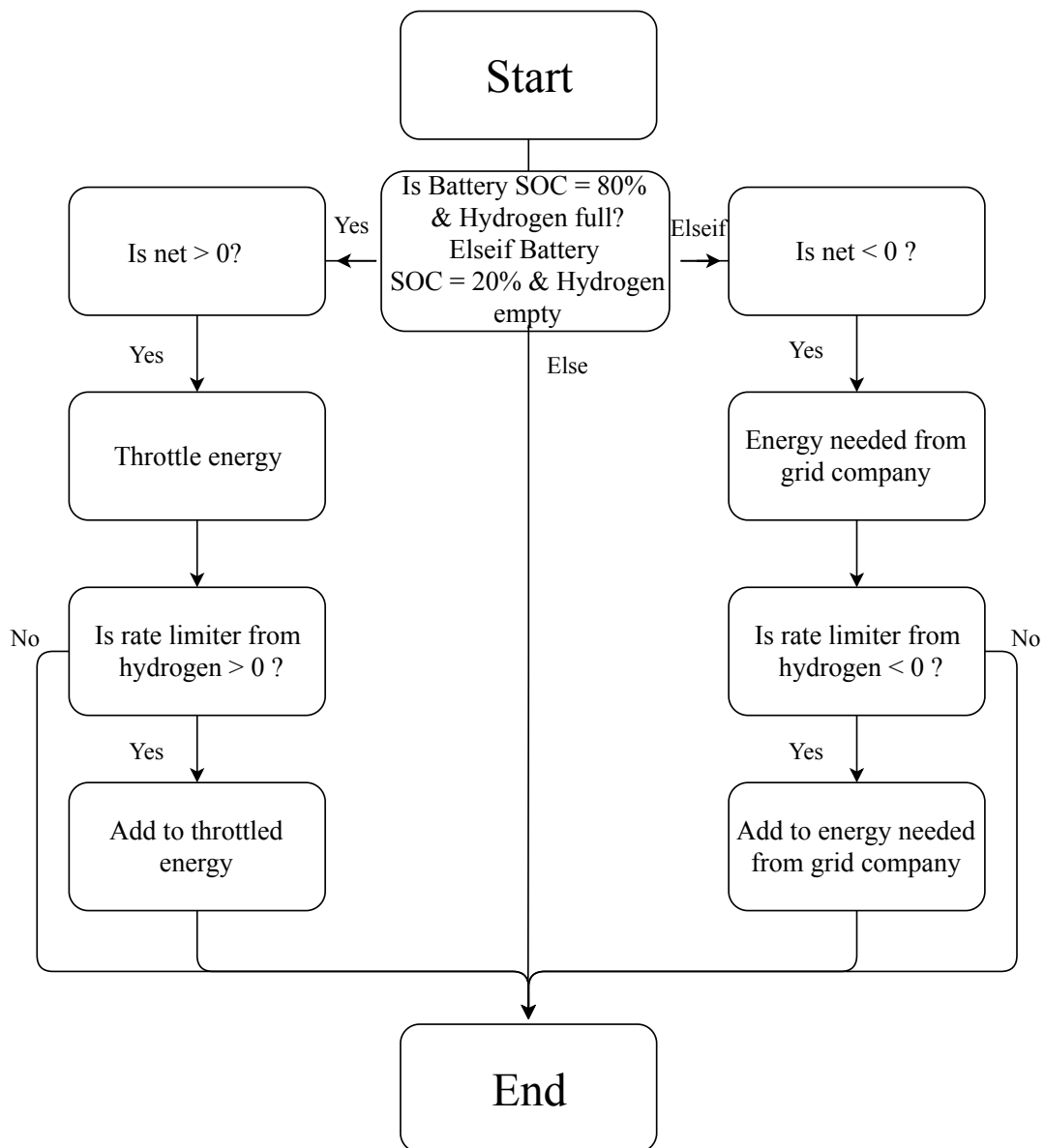
Figure C.1.2: Algorithm used for calculating energy throttled and energy needed from the main grid in Simulink. First ESS status is checked, before net energy between production and total demand is checked. Depending on the statements, energy needed from main grid or throttled energy is calculated. In addition, the rate limiter from hydrogen is considered.

XII

Appendix D

Example from MATLAB-code

This appendix presents an excerpt of the implemented MATLAB script performing ALM. An example illustrating detailed results after performing ALM is also included.

The following script from MATLAB is part of the code used to execute the energy reduction strategy and load shift algorithm in Case 4. Variations of this is applied in the other cases.

```matlab
%% Generating categories for shifting

% Category: Days
Categories=discretize(Table.Timestamp,'day','categorical');
Table.Days=Categories;

Days=findgroups(Table.Days);

Table.D=Days;

clear Days Categories

% Category: 12 hr.
a = [1];

for i = 12:12:length(Table.Timestamp)

    a = [a i];

end

b = [1];

for i = 1:length(a)-1

    for n = a(i)+1:a(i+1)

    b(n) = i;

    end
end
```

```matlab
32
33  b = transpose(b);
34
35  Table.Limit_12h = b;
36
37  Kat12 = [0];
38
39  for i=1:length(Table.Timestamp)-1
40      if b(i)~=b(i+1)
41          Kat12 = [Kat12 i];
42      end
43  end
44
45  Kat12 = [Kat12 length(Table.D)];
46
47  % Category: Silo
48    for i = 2:length(Table.Limit_silo)
49      a(1)=1;
50      if Table.Limit_silo(i) == Table.Limit_silo(i-1)
51
52          a(i) = a(i-1);
53
54      else
55
56          a(i) = a(i-1)+1;
57      end
58    end
59
60  a = transpose(a);
61
62  Table.Limit_silo = a;
63
64  Kat_silo = [0];
65
66  for i=1:length(Table.Timestamp)-1
67      if a(i)~=a(i+1)
68          Kat_silo = [Kat_silo i];
69      end
70  end
71
72  Kat_silo = [Kat_silo length(Table.D)];
73
74  %% Applying energy conservation strategy
75
76  for i = 1:length(Table.Timestamp)
77
78          Table.Totalforbruk(i) = Table.Totalforbruk(i) - Table.
                Limit_lights_main(i) - Table.Limit_lights_east(i) + Table.
                Limit_lights_mastu(i);
79          Table.Totalforbruk(i) = Table.Totalforbruk(i) - Table.Telenor
                (i);
```

```matlab
80   end
81
82   % Calculates updated capacity
83
84   for i=1:length(Table.Timestamp)
85       Table.Kapasitet(i) = Table.Totalproduksjon(i) - Table.
             Totalforbruk(i);
86   end
87
88   %% Shifting Silo with regard to high capacity
89
90   for i=1:length(Table.Timestamp)
91
92       Table.Silo_shifted(i) = 0;
93   end
94
95   for i=1:length(Kat_silo)-1
96       for j=Kat_silo(i)+1:Kat_silo(i+1)
97           max_flytt = max(Table.Silo(Kat_silo(i)+1:Kat_silo(i+1)));
98           max_kap = max(Table.Kapasitet(Kat_silo(i)+1:Kat_silo(i+1)));
99
100              for k=Kat_silo(i)+1:Kat_silo(i+1)
101                  if Table.Kapasitet(k) == max_kap
102                      pos_maxkap = k;
103                  end
104
105                  if Table.Silo(k) == max_flytt
106                      pos_maxflytt = k;
107                  end
108
109              end
110
111              if max_kap >= max_flytt && pos_maxkap~=pos_maxflytt
112                  Table.Silo(pos_maxflytt) = Table.Silo(pos_maxflytt) -
                         max_flytt;
113                  Table.Silo_shifted(pos_maxkap) = Table.Silo_shifted(
                         pos_maxkap) + max_flytt;
114                  Table.Totalforbruk(pos_maxflytt) = Table.Totalforbruk
                         (pos_maxflytt) - max_flytt;
115                  Table.Totalforbruk(pos_maxkap) = Table.Totalforbruk(
                         pos_maxkap) + max_flytt;
116                  Table.Kapasitet(pos_maxflytt) = Table.Kapasitet(
                         pos_maxflytt) + max_flytt;
117                  Table.Kapasitet(pos_maxkap) = Table.Kapasitet(
                         pos_maxkap) - max_flytt;
118              end
119      end
120   end
121
122   %% Shifting silo with regard to minimum consumption
123
```

```matlab
124  for i=1:length(Kat_silo)-1
125      for j=Kat_silo(i)+1:Kat_silo(i+1)
126          max_flytt = max(Table.Flyttbar(Kat_silo(i)+1:Kat_silo(i+1)));
127          max_kap = max(Table.Kapasitet(Kat_silo(i)+1:Kat_silo(i+1)));
128          min_forb=min(Table.Totalforbruk(Kat_silo(i)+1:Kat_silo(i+1)))
                 ;
129
130          for k=Kat_silo(i)+1:Kat_silo(i+1)
131              if Table.Kapasitet(k) == max_kap
132                      pos_maxkap = k;
133              end
134
135              if Table.Flyttbar(k) == max_flytt
136                      pos_maxflytt = k;
137              end
138
139              if Table.Totalforbruk(k) == min_forb
140                      pos_minforb = k;
141              end
142          end
143
144          if      max_flytt > 0 ...
145                  && Table.Totalproduksjon(pos_minforb) - Table.
                         Totalforbruk(pos_minforb) - max_flytt ...
146                  > Table.Totalproduksjon(pos_maxflytt) - Table.
                         Totalforbruk(pos_maxflytt) ...
147                  && pos_minforb~=pos_maxflytt
148
149                  Table.Flyttbar(pos_maxflytt) = Table.Flyttbar(
                         pos_maxflytt) - max_flytt;
150                  Table.Silo_shifted(pos_minforb) = Table.Silo_shifted(
                         pos_minforb) + max_flytt;
151                  Table.Totalforbruk(pos_maxflytt) = Table.Totalforbruk(
                         pos_maxflytt) - max_flytt;
152                  Table.Totalforbruk(pos_minforb) = Table.Totalforbruk(
                         pos_minforb) + max_flytt;
153                  Table.Kapasitet(pos_minforb) = Table.Kapasitet(
                         pos_minforb) - max_flytt;
154                  Table.Kapasitet(pos_maxflytt) = Table.Kapasitet(
                         pos_maxflytt) + max_flytt;
155          end
156      end
157  end
```

Example of detailed results from ALM

Table D.1.1 illustrates an extract of results achieved by implementing ALM in Case 4. By studying the table, it can be seen that the silo is shifted to an hour where the capacity is sufficiently large to cover the entire load demand. It is only shifted within the category, which is made in the attached MATLAB script.

Delving into the table, it can be observed that the silo is not shifted within category 10, because of the lack of capacity. During category 12, on the other hand, the algorithm locates 06.01.2018 13:00 due to its high capacity and shifts 10.31 kWh of the silo to that hour, while updating the demand and capacity after the shift is accomplished. The next iteration locates 06.01.2018 15:00 and shifts the other part of the silo to that location and updates the correlating values. The hours and values of interest are marked with bold in the table.

This has been executed throughout the time period, with variations to accommodate the time limit and properties of each respective appliance.

Table D.1.1: Extract of table from MATLAB, illustrating detailed result from implementing the ALM algorithm.

Timestamp	Demand prior [kWh]	Demand after [kWh]	Capacity prior [kWh]	Capacity after [kWh]	Reduction [kWh]	Silo prior [kWh]	Silo after [kWh]	Shifted Silo [kWh]	Category [-]
05.01.2018 08:00	23.0	20.9	0.0	2.1	2.1	0.0	0.0	0.0	10.0
05.01.2018 09:00	32.0	29.9	-10.0	-7.9	2.1	**10.3**	**10.3**	0.0	10.0
05.01.2018 10:00	29.0	26.9	-18.0	-15.9	2.1	0.0	0.0	0.0	10.0
05.01.2018 11:00	21.0	18.9	-15.6	-13.5	2.1	0.0	0.0	0.0	10.0
05.01.2018 12:00	19.0	16.9	-15.0	-12.9	2.1	0.0	0.0	0.0	10.0
05.01.2018 13:00	15.0	12.9	-10.0	-7.9	2.1	0.0	0.0	0.0	10.0
05.01.2018 14:00	14.0	11.9	-14.0	-11.9	2.1	0.0	0.0	0.0	10.0
05.01.2018 15:00	13.0	10.9	-13.0	-10.9	2.1	0.0	0.0	0.0	10.0
05.01.2018 16:00	18.0	15.9	-18.0	-15.9	2.1	0.0	0.0	0.0	10.0
05.01.2018 17:00	15.0	12.9	-15.0	-12.9	2.1	0.0	0.0	0.0	10.0
05.01.2018 18:00	16.0	13.9	-16.0	-13.9	2.1	0.0	0.0	0.0	10.0
05.01.2018 19:00	35.0	32.9	-35.0	-32.9	2.1	**10.3**	**10.3**	0.0	10.0
05.01.2018 20:00	40.0	37.9	-40.0	-37.9	2.1	**10.3**	**10.3**	0.0	10.0
05.01.2018 21:00	20.0	17.9	-20.0	-17.9	2.1	0.0	0.0	0.0	10.0
05.01.2018 22:00	19.0	16.9	-19.0	-16.9	2.1	0.0	0.0	0.0	10.0
05.01.2018 23:00	16.0	13.9	-16.0	-13.9	2.1	0.0	0.0	0.0	10.0
06.01.2018 00:00	12.0	10.1	-12.0	-10.1	1.9	0.0	0.0	0.0	11.0
06.01.2018 01:00	18.0	16.1	-18.0	-16.1	1.9	0.0	0.0	0.0	11.0
06.01.2018 02:00	15.0	13.1	-13.0	-11.1	1.9	0.0	0.0	0.0	11.0
06.01.2018 03:00	11.0	9.1	-11.0	-9.1	1.9	0.0	0.0	0.0	11.0
06.01.2018 04:00	12.0	10.1	-12.0	-10.1	1.9	0.0	0.0	0.0	11.0
06.01.2018 05:00	13.0	11.1	-13.0	-11.1	1.9	0.0	0.0	0.0	11.0
06.01.2018 06:00	12.0	10.1	-12.0	-10.1	1.9	0.0	0.0	0.0	11.0
06.01.2018 07:00	13.0	10.9	-6.0	-3.9	2.1	0.0	0.0	0.0	12.0
06.01.2018 08:00	12.0	9.9	-4.0	-1.9	2.1	0.0	0.0	0.0	12.0
06.01.2018 09:00	16.0	13.9	-5.0	-2.9	2.1	0.0	0.0	0.0	12.0
06.01.2018 10:00	24.0	21.9	-20.0	-17.9	2.1	0.0	0.0	0.0	12.0
06.01.2018 11:00	21.0	18.9	-6.1	-4.0	2.1	0.0	0.0	0.0	12.0
06.01.2018 12:00	20.0	17.9	-9.5	-7.4	2.1	0.0	0.0	0.0	12.0
06.01.2018 13:00	17.0	25.2	61.6	53.4	2.1	0.0	**10.3**	**10.3**	12.0
06.01.2018 14:00	12.0	9.9	28.0	30.1	2.1	0.0	0.0	0.0	12.0
06.01.2018 15:00	13.0	21.2	56.0	47.8	2.1	0.0	**10.3**	**10.3**	12.0
06.01.2018 16:00	14.0	11.9	21.0	23.1	2.1	0.0	0.0	0.0	12.0
06.01.2018 17:00	16.0	13.9	23.0	25.1	2.1	0.0	0.0	0.0	12.0
06.01.2018 18:00	13.0	10.9	19.0	21.1	2.1	0.0	0.0	0.0	12.0
06.01.2018 19:00	14.0	11.9	46.0	48.1	2.1	0.0	0.0	0.0	12.0
06.01.2018 20:00	44.0	31.6	-17.0	-4.6	2.1	**10.3**	0.0	0.0	12.0
06.01.2018 21:00	34.0	21.6	-11.0	1.4	2.1	**10.3**	0.0	0.0	12.0
06.01.2018 22:00	18.0	15.9	13.0	15.1	2.1	0.0	0.0	0.0	12.0
06.01.2018 23:00	16.0	13.9	46.0	48.1	2.1	0.0	0.0	0.0	12.0

K. Lyngved, T. Mickelborg and A. Teigmoen

Active load management in microgrids

NTNU
Kunnskap for en bedre verden

TrønderEnergi®